REFINED FOURIER ANALYSIS: PROCEDURES, ERROR ESTIMATES AND APPLICATIONS

G. GÓMEZ[a], J.M. MONDELO[b] and C. SIMÓ[a]
[a] *Departament de Matemàtica Aplicada i Anàlisi, Universitat de Barcelona*
Gran Via 585, 08007 Barcelona, Spain
[b] *Departament de Matemàtica Aplicada I, Universitat Politècnica de Catalunya*
Diagonal 647, 08028 Barcelona, Spain

Abstract

The purpose of this paper is to develop and analyze Fourier analysis procedures that allow an accurate determination of the frequencies and the amplitudes when the analyzed function is quasi–periodic or close to it. The procedures and theoretical results are illustrated with examples and applications.
Key words: Fourier analysis, Fast Fourier Transform, quasi–periodic functions.

Contents

1 Introduction

We are faced to the following problem: given the samples $\{f(t_l)\}_{l\in J}$ of a real-valued function $f(t)$, which are assumed to be distributed on an interval $[0,T]$, we want to determine a trigonometric polynomial

$$Q_f(t) = A_0^c + \sum_{l=1}^{N_f} \left(A_l^c \cos(\frac{2\pi\nu_l t}{T}) + A_l^s \sin(\frac{2\pi\nu_l t}{T})\right)$$

being a good approximation of $f(t)$. This means the computation of the dominant frequencies $\{\nu_l\}_{l=1}^{N_f}$ and amplitudes $\{A_l^c\}_{l=0}^{N_f}$, $\{A_l^s\}_{l=1}^{N_f}$ with high accuracy.

Within the framework of the almost–periodic functions, this problem can be solved theoretically by means of the Bohr Transform, which is defined as

$$B_f(\alpha) = \lim_{T\to\infty} \frac{1}{T}\int_0^T f(t)e^{-2\pi i\alpha t}dt, \qquad \alpha \in \mathbb{R}. \tag{1}$$

It is known (see [2],[18]) that, for an almost-periodic function $f(t)$, $B_f(\alpha)$ exists $\forall\alpha \in \mathbb{R}$ and the set $\{\alpha : B_f(\alpha) \neq 0\}$ is at most countable. Let $\{\alpha_n\}_{n\in\mathbb{N}}$ be an enumeration, then

$$f(t) \sim \sum_{n\in\mathbb{N}} B_f(\alpha_n)e^{2\pi i\alpha_n t},$$

where the $\sim$ sign is an equality if the series is uniformly convergent. Of course this property is not useful from a numerical point of view, since we only have a sample of finite size of the function $f(t)$.

A first reduction is to drop the lim in (1), that is to replace the Bohr Transform by a *Truncated Continuous Fourier Transform* (TCFT) in the interval $[0,T]$:

$$\phi_{f,T}(\alpha) = \frac{1}{T}\int_0^T f(t)e^{-2\pi i\alpha t}dt.$$

In this case, the values at which the Bohr Transform is different from zero are approximated by local maxima of $|\phi_{f,T}(\alpha)|$. This gives a method to compute the frequencies which is discussed in Section 3.1. The fact that the maxima of $|\phi_{f,T}(\alpha)|$ are not the true frequencies but approximations is due to an effect called *leakage*, which we discuss in Section 2.2, together with strategies to reduce it. Note that some of the maxima can disappear if they correspond to small values of $B_f(\alpha)$ and there are other α_n very close with $B_f(\alpha_n)$ large enough. This depends also on T.

Once we have approximations for the frequencies $\{\nu_l\}_{l=1}^{N_f}$, we can compute the related amplitudes by asking the TCFT of the function $f(t)$ given by the samples and the TCFT of the approximating trigonometric polynomial Q_f to be equal, this is

$$\phi_{f,T}(\alpha) = A_0^c\phi_{1,T}(\alpha) + \sum_{l=1}^{N_f}\left(A_l^c\phi_{\cos(2\pi\nu_l t/T),T}(\alpha) + A_l^s\phi_{\sin(2\pi\nu_l t/T),T}(\alpha)\right), \quad \alpha \in \mathbb{R}.$$

The $\phi_{f,T}(\alpha)$ term above can be found for arbitrary values of α using numerical quadrature formulae. Moreover, analytic expressions for $\phi_{\cos(2\pi\nu_l t/T),T}(\alpha)$ and $\phi_{\sin(2\pi\nu_l t/T),T}(\alpha)$ can be found. If we further select a finite set of values of α, $\{\alpha_j\}_{j\in E}$, then the above equation becomes a linear system of equations in the unknowns $\{A_l^c\}_{l=0}^{N_f}$, $\{A_l^s\}_{l=1}^{N_f}$, namely

$$\phi_{f,T}(\alpha_j) = A_0^c\phi_{1,T}(\alpha_j) + \sum_{l=1}^{N_f}\left(A_l^c\phi_{\cos(2\pi\nu_l t/T),T}(\alpha_j) + A_l^s\phi_{\sin(2\pi\nu_l t/T),T}(\alpha_j)\right), \quad j \in E. \tag{2}$$

The $\{\alpha_j\}_{j\in E}$ should be selected such that the above system is well conditioned.

An analogous scheme can be used to iteratively improve initial approximations of both frequencies and amplitudes: select some values of α, $\{\alpha_j\}_{j\in F}$, and then solve for $\{\nu_l\}_{l=1}^{N_f}$, $\{A_l^c\}_{l=0}^{N_f}$, $\{A_l^s\}_{l=1}^{N_f}$

$$\phi_{f,T}(\alpha_j) = A_0^c\phi_{1,T}(\alpha_j) + \sum_{l=1}^{N_f}\left(A_l^c\phi_{\cos(2\pi\nu_l t/T),T}(\alpha_j) + A_l^s\phi_{\sin(2\pi\nu_l t/T),T}(\alpha_j)\right), \quad j \in F, \tag{3}$$

which is again a finite system of equations, but no longer linear.

The use of the TCFT in (2) and (3) implies in practice the computation of many integrals by numerical quadrature. In order to avoid these computations and make use of the efficiency of the FFT algorithm, in our implementation of the procedures (2) and (3) we have used the *Discrete Fourier Transform* (DFT) instead of the TCFT. This introduces new restrictions:

- In addition to the leakage produced by the TCFT, the use of the DFT introduces a new effect called *aliasing*, which reduces the range of frequencies that we are able to detect. Frequencies outside this range and having relevant amplitude are also dangerous.
- The sampling points $\{t_l\}_{l\in J}$ are required to be equally spaced over the sampling interval $[0,T]$.
- Standard FFT implementations require N to be an integer power of two.

For the reader's convenience the basic notions are introduced first. The DFT and related notation is introduced in Section 2.1. Leakage and aliasing effects for the DFT are discussed in Sections 2.2 and 2.3 respectively. In Sections 3.2 and 3.3 we give the details of the procedures (2) and (3) using DFT. Section 4 is devoted to the implementation details of the proposed algorithm.

Next step (Section 5) is to obtain error estimates on the results (frequencies and amplitudes) produced by the algorithm. The assumptions are natural: we ask the function to be analyzed to be analytic quasi–periodic and the basic frequencies to satisfy a Diophantine condition. The theoretical result (theorem 5.1) gives computable bounds and ensures convergence of the approximation to the function when the time interval, T, and the size of the sample, N, are large enough and are related in a suitable way.

In Section 6.1 we provide some illustrations. First we want to recover frequencies from a given function. Different values of T and N are used. The results are compared to the theoretical bounds. Furthermore, the robustness of the procedure is tested when the data is affected of random noise.

An application is made to detect regular and chaotic motions in a family of symplectic 2D maps. Both the initial actions and a large range of the parameter (where the main bifurcations occur) are scanned. The results are compared with other methods to detect the character of the motion. Several other applications in progress are mentioned.

2 The Discrete Fourier Transform (DFT)

2.1 Preliminaries and notation

Let D be the space of real valued functions defined on a discrete set of N equally spaced points $t_0,\dots,t_{N-1}$ over the interval $[0,T]$, i.e. $t_l = l\cdot\Delta t$, with $\Delta t = T/N$. The equality of the spacing is only a technical requirement, since the DFT could be adapted to a non equally spaced set of samples. Nevertheless, all what follows has been written assuming Δt constant. From now on N is assumed to be even. If $f,\ g\in D$, we define their discrete scalar product as

$$\langle f,g\rangle = \sum_{l=0}^{N-1} f(t_l)g(t_l).$$

The set of functions $\left\{\{\varphi_j\}_{j=0}^{N/2},\{\psi_j\}_{j=1}^{N/2-1}\right\}\subset D$, being

$$\varphi_j(t)=\cos(\frac{2\pi jt}{T}),\quad \psi_j(t)=\sin(\frac{2\pi jt}{T}),$$

is an orthogonal basis of D. Therefore, every function $f\in D$ can be written as

$$f(t_l)=P_{f,T,N}(t_l),\qquad l=0,\dots,N-1,$$

where

$$\begin{aligned} P_{f,T,N}(t) &= \frac{1}{2}\Big(c_{f,T,N}(0)+c_{f,T,N}(\frac{N}{2})\cos(\frac{2\pi\frac{N}{2}t}{T})\Big)\\ &\quad+\sum_{j=1}^{N/2-1}\Big(c_{f,T,N}(j)\cos(\frac{2\pi jt}{T})+s_{f,T,N}(j)\sin(\frac{2\pi jt}{T})\Big). \end{aligned} \tag{4}$$

with

$$c_{f,T,N}(j) = \delta_j \frac{\langle f, \varphi_j \rangle}{\langle \varphi_j, \varphi_j \rangle}, \quad j = 0, \dots, \frac{N}{2}, \qquad s_{f,T,N}(j) = \frac{\langle f, \psi_j \rangle}{\langle \psi_j, \psi_j \rangle}, \quad j = 1, \dots, \frac{N}{2} - 1,$$

with

$$\delta_j = \begin{cases} 2, & j = 0, \\ 1, & j = 1, ..., N/2 - 1, \\ 2, & j = N/2, \end{cases}$$

Equation (4) defines the *Discrete Fourier Transform in sines and cosines* (DFT) of $f \in D$ as a function of the discrete set of frequencies j/T, $j = 0, \dots, N/2$. The values $c_{f,T,N}(j)$ and $s_{f,T,N}(j)$ are the coefficients related to the j/T frequency of the trigonometric interpolating polynomial $P_{f,T,N}(t)$ of the function f at the nodes $\{t_l\}_{l=0}^{N-1}$. All the frequencies of $P_{f,T,N}(t)$ are multiples of $1/T$. The DFT coefficients can be explicitly written as

$$\begin{aligned} c_{f,T,N}(j) &= \frac{2}{N} \sum_{l=0}^{N-1} f(t_l) \cos(2\pi \frac{j}{N} l), \quad j = 0, ..., N/2, \\ s_{f,T,N}(j) &= \frac{2}{N} \sum_{l=0}^{N-1} f(t_l) \sin(2\pi \frac{j}{N} l), \quad j = 1, ..., N/2 - 1. \end{aligned} \tag{5}$$

For a general complex–valued function f, using the discrete scalar product $\langle f, g \rangle = \sum_{l=0}^{N-1} f(t_l) \overline{g(t_l)}$ and the orthogonal basis $\{e^{2\pi i \frac{j}{T} t}\}_{j=0}^{N-1}$, we can define the DFT as

$$F_{f,T,N}(j) = \frac{1}{N} \sum_{l=0}^{N-1} f(t_l) e^{-2\pi i \frac{j}{T} t_l}, \quad j = 0, ..., N - 1. \tag{6}$$

If f takes real values, $F_{N-j}(f) = \overline{F_j(f)}$, the $F_{f,T,N}(j)$, $c_{f,T,N}(j)$, $s_{f,T,N}(j)$ coefficients are related by

$$F_{f,T,N}(j) = \frac{1}{2}(c_{f,T,N}(j) - i s_{f,T,N}(j)) \quad j = 0, \dots, \frac{N}{2},$$

where we assume $s_{f,T,N}(0) = s_{f,T,N}(N/2) = 0$. This allows to compute efficiently the $c_{f,T,N}(j)$, $s_{f,T,N}(j)$ coefficients using a standard Fast Fourier Transform (FFT) algorithm (see, for instance, [5], [4] or [20]).

The complex–valued function

$$\phi_{f,T}(\alpha) = \frac{1}{T} \int_0^T f(t) e^{-i2\pi\alpha t} dt$$

will be called *Truncated Continuous Fourier Transform* (TCFT) of f. Note that $\phi_{f,T,N}(\frac{j}{T})$, $j \in \mathbb{Z}$, are the coefficients of the Fourier series of f on the interval $[0, T]$. Note also that the DFT can be seen as a Riemann sum of the TCFT, more concretely

$$\phi_{f,T}\left(\frac{k}{T}\right) = \frac{1}{T} \int_0^T f(t) e^{-2\pi i \frac{k}{T} t} dt \approx \frac{1}{T} \sum_{l=0}^{N-1} f(t_l) e^{-2\pi i \frac{k}{T} t_l} \frac{T}{N} = F_{f,T,N}(k). \tag{7}$$

Consequently, we can obtain the TCFT as the limit when $N \to \infty$ of the DFT. This justifies the use of the DFT instead of the TCFT in the procedures (2) and (3) outlined in the introduction. In section 5, Lemma 5.4, we will give an explicit bound of the difference between the DFT and the TCFT of a complex exponential term $e^{i2\pi\omega t}$.

2.2 Leakage effect and filtering

For periodic functions, when the length T of the time interval spanned by the samples is not an integer multiple of the period of the function (or equivalently, when the frequency of the function is not an integer multiple of the "basic frequency" $1/T$ associated to the sample interval $[0, T]$), there appear in the DFT spurious frequencies, that is, the DFT is different from zero at frequencies not being multiple of the frequency of the function. This is a phenomenon known as *leakage*, for which we give a graphical example in figure 1. Leakage also affects the TCFT.

For the procedures that will be described later, we are interested in reducing leakage for functions of the form $e^{2\pi i\omega t}$. The way to do this is to use a filter or window function.

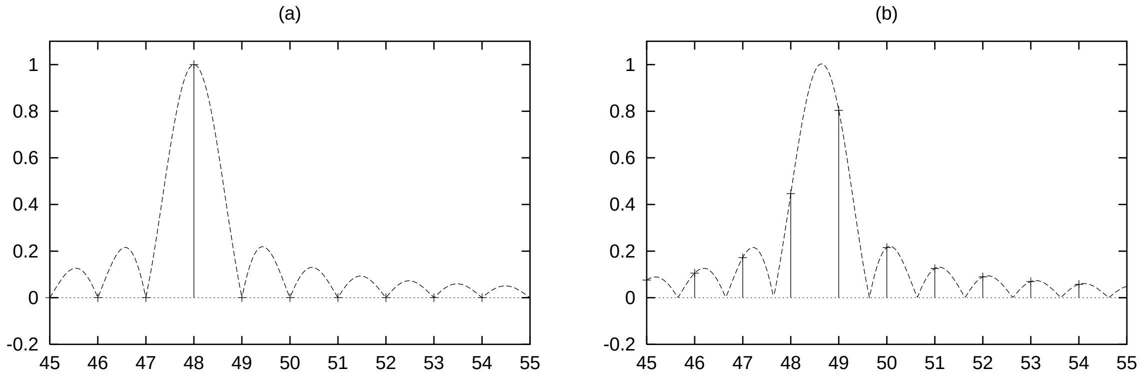

Figure 1: Plot of $\left[\left(c_{f,T,N}(j)\right)^2 + \left(s_{f,T,N}(j)\right)^2\right]^{1/2}$ as a function of j (dashed line) and for $j = 45, \ldots, 55$ (solid vertical lines), with $f(t) = \cos(2\pi\omega t)$, $T = 64$ and $N = 256$. In (a) $\omega = 0.75$, so $48 \cdot (0.75)^{-1} = 64 = T$ and there is no leakage. This is not the case for (b), where $\omega = 0.76$.

Definition 2.1 *$H(t)$ is said to be a* filter function of degree $r \geq 0$ for the interval $[0,T]$ *if it is a positive function of class C^{r-1} with $H^{(j)}(0) = H^{(j)}(T) = 0$ for $j = 0, \ldots, r-1$, such that $H^{(r)}$ is continuous except for a finite set of jump discontinuities, and has bounded variation. We also assume that*

$$\frac{1}{T}\int_0^T H(t)dt = 1. \tag{8}$$

It is enough to focus on the TCFT, since it is the limit of the DFT when $N \to \infty$ (equation (7)). The reduction of leakage for the TCFT of $H(t)e^{2\pi i\omega t}$, which depends directly on the regularity of the filter function, is given by corollary 2.1.

Proposition 2.1 If g is a filter function of degree r for the interval $[0, 2\pi]$, then

$$\left|\int_0^{2\pi} g(t)e^{i\alpha t}dt\right| \leq \frac{2B(g^{(r)}) + V(g^{(r)})}{|\alpha|^{r+1}},$$

where $B(g^{(r)})$ is a bound for $g^{(r)}$ in $[0, 2\pi]$ and $V(g^{(r)})$ is the variation of $g^{(r)}$ in the same interval. Moreover, if we assume $g^{(r)}(0) = g^{(r)}(2\pi) = 0$, then

$$\left|\int_0^{2\pi} g(t)e^{i\alpha t}dt\right| \leq \frac{V(g^{(r)})}{|\alpha|^{r+1}}.$$

Proof: Let $t_1, \ldots t_{m-1}$ be the jump discontinuities of $g^{(r)}$ in $(0, 2\pi)$, and let $t_0 = 0$, $t_m = 2\pi$ (which may be jump discontinuities or not). Successive integrations by parts yield

$$\begin{aligned}
\int_0^{2\pi} g(t)e^{i\alpha t}dt &= \left[g(t)\frac{e^{i\alpha t}}{i\alpha}\right]_{t=0}^{t=2\pi} - \frac{1}{i\alpha}\int_0^{2\pi} g'(t)e^{i\alpha t}dt \\
&= \ldots = \left(\frac{-1}{i\alpha}\right)^{r-1}\sum_{j=0}^{m-1}\int_{t_j}^{t_{j+1}} g^{(r-1)}(t)e^{i\alpha t}dt \\
&= \left(\frac{-1}{i\alpha}\right)^{r-1}\left(\sum_{j=0}^{m-1}\left[g^{(r-1)}(t)\frac{e^{i\alpha t}}{i\alpha}\right]_{t=t_j}^{t=t_{j+1}} + \frac{-1}{i\alpha}\sum_{j=0}^{m-1}\int_{t_j}^{t_{j+1}} g^{(r)}(t)e^{i\alpha t}dt\right).
\end{aligned}$$

The first sum vanishes because it is a telescopic sum and $g^{(r-1)}(0) = g^{(r-1)}(2\pi) = 0$.

Given $\varepsilon > 0$, let δ_j be such that, for $t^*, t^{**} \in [t_j, t_{j+1}]$, if $|t^* - t^{**}| < \delta_j$ then $|g^{(r)}(t^*) - g^{(r)}(t^{**})| < \varepsilon$ ($j = 0 \div m-1$). These δ_j exist because $g^{(r)}$ is uniformly continuous in each interval $[t_j, t_{j+1}]$. Reducing δ_j if necessary, we can assume $t_{j+1} - t_j = n_j\delta_j$ for $n_j \in \mathbb{N}$. Define $M = n_0 + \ldots + n_{m-1}$ and

$$\begin{gathered}
s_0 = t_0,\ s_1 = t_0 + \delta_0,\ \ldots,\ s_{n_0-1} = t_0 + (n_0-1)\delta_0,\ s_{n_0} = t_0 + n_0\delta_0 = t_1, \\
s_{n_0+1} = t_1 + \delta_1,\ \ldots,\ s_{n_0+\ldots+n_{m-1}-1} = t_{m-1} + (n_{m-1}-1)\delta_{m-1},\ s_M = t_m.
\end{gathered}$$

Denoting by $\xi_j = \frac{1}{2}(s_j + s_{j+1})$,

$$\begin{aligned}
\int_0^{2\pi} g(t)e^{i\alpha t}dt &= \Big(\frac{-1}{i\alpha}\Big)^r \sum_{j=0}^{M-1} \int_{s_j}^{s_{j+1}} \big(g^{(r)}(\xi_j) + g^{(r)}(t) - g^{(r)}(\xi_j)\big)e^{i\alpha t}dt \\
&= \Big(\frac{-1}{i\alpha}\Big)^r \sum_{j=0}^{M-1} \Big(g^{(r)}(\xi_j)\frac{e^{i\alpha s_{j+1}} - e^{i\alpha s_j}}{i\alpha} + \int_{s_j}^{s_{j+1}} \big(g^{(r)}(t) - g^{(r)}(\xi_j)\big)e^{i\alpha t}dt\Big) \\
&= \Big(\frac{-1}{i\alpha}\Big)^r \Bigg[\frac{1}{i\alpha}\Big(-g^{(r)}(\xi_0)e^{i\alpha s_0} + g^{(r)}(\xi_{M-1})e^{i\alpha s_M} \\
&\qquad + \sum_{j=1}^{M-1} \big(g^{(r)}(\xi_{j-1}) - g^{(r)}(\xi_j)\big)e^{i\alpha s_j}\Big) \\
&\qquad + \sum_{j=0}^{M-1} \int_{s_j}^{s_{j+1}} \big(g^{(r)}(t) - g^{(r)}(\xi_j)\big)e^{i\alpha t}dt\Bigg],
\end{aligned}$$

and hence

$$\Big|\int_0^{2\pi} g(t)e^{i\alpha t}dt\Big| \le \frac{1}{|\alpha|^r}\Big[\frac{1}{|\alpha|}\big(2B(g^{(r)}) + V(g^{(r)})\big) + 2\pi\varepsilon\Big].$$

Since $\varepsilon > 0$ is arbitrary, doing $\varepsilon \to 0$ we get the first equality of the proposition. The second bound follows from a slight modification of the above computations. □

For $\alpha = j/T$, the above Proposition is a standard result about the decaying of the Fourier coefficients (see, e.g., [4] and references therein). The above proof covers the case $\alpha \neq j/T$.

Corollary 2.1 If H is a filter function of degree r for $[0, T]$, then

$$\phi_{H(t)e^{2\pi i\nu t/T},T}(\alpha/T) = O\Big(\frac{1}{|\nu - \alpha|^{r+1}}\Big).$$

Proof: We have

$$\phi_{H(t)e^{2\pi i\nu t/T},T}(\alpha/T) = \frac{1}{T}\int_0^T H(t)e^{2\pi i(\nu-\alpha)t/T}dt = \frac{1}{2\pi}\int_0^{2\pi} H\big(\frac{T}{2\pi}s\big)e^{i(\nu-\alpha)s}ds,$$

and hence

$$|\phi_{H(t)e^{2\pi i\nu t/T},T}(\alpha/T)| \le \frac{2B(H^{(r)}) + V(H^{(r)})}{2\pi|\nu - \alpha|^{r+1}}.$$

□

We will use as a filter function the *Hanning window function*, which is defined as

$$H_T(t) = 1 - \cos\left(2\pi\frac{1}{T}t\right).$$

and has degree 2. To increase the degree of the filter, the Hanning function can be iterated and we can consider *Hanning functions of order* $n_h \in \mathbb{N}$, defined as

$$H_T^{n_h}(t) = q_{n_h}\left(1 - \cos\left(2\pi\frac{1}{T}t\right)\right)^{n_h},$$

where the constants q_{n_h} are computed in order to fulfill (8), so

$$q_{n_h} = \left[\frac{1}{T}\int_0^T \left(1 - \cos\left(2\pi\frac{1}{T}t\right)\right)^{n_h} dt\right]^{-1} = \frac{n_h!}{(2n_h-1)!!}.$$

The advantage of the Hanning function with respect to other well–known window functions (see [5]) is its degree of differentiability. For instance, $H^{n_h}(t)$ has degree $2n_h$, whereas a general "triangle window function" $T^{n_t}(t)$ defined as

$$T^{n_t}(t) = (n_t+1)\Big(1-\Big|\frac{2}{T}t-1\Big|\Big)^{n_t}.$$

has degree just n_t. The *Bartlett window* and the *Parzen window* are the particular cases $n_t = 1$ and $n_t = 3$ of $T^{n_t}(t)$ respectively. The Hanning function has its simplicity as an additional advantage. The properties of trigonometric functions allow to obtain relations like Lemma 2.1.

The DFT coefficients with Hanning order n_h of $f(t)$ are defined as the DFT coefficients of $H_T^{n_h}(t)f(t)$, and will be denoted by

$$\begin{aligned} F^{n_h}_{f,T,N}(j) &= F_{H^{n_h}f,T,N}(j), \\ c^{n_h}_{f,T,N}(j) &= c_{H^{n_h}f,T,N}(j), \\ s^{n_h}_{f,T,N}(j) &= s_{H^{n_h}f,T,N}(j). \end{aligned}$$

Analogously, for the TCFT we will have

$$\phi^{n_h}_{f,T,N}(\alpha) = \frac{1}{T}\int_0^T H^{n_h}(t)f(t)e^{-2\pi i\alpha t}dt.$$

The following lemma relates the coefficients of filtered and non–filtered transforms of a function $f(t)$:

Lemma 2.1 The following relations hold:

(a) $$F^{n_h}_{f,T,N}(j) = \frac{q_{n_h}}{2^{n_h}}\sum_{l=-n_h}^{n_h}(-1)^l\binom{2n_h}{n_h+l}F_{f,T,N}(j+l) = \sum_{l=-n_h}^{n_h}\frac{(-1)^l(n_h!)^2F_{f,T,N}(j+l)}{(n_h+l)!(n_h-l)!}.$$

(b) $$\phi^{n_h}_{f,T,N}(\alpha) = \frac{q_{n_h}}{2^{n_h}}\sum_{l=-n_h}^{n_h}(-1)^l\binom{2n_h}{n_h+l}\phi_{f,T,N}(\alpha+\frac{l}{T}) = \sum_{l=-n_h}^{n_h}\frac{(-1)^l(n_h!)^2\phi_{f,T,N}(\alpha+l/T)}{(n_h+l)!(n_h-l)!}.$$

Proof: We only prove (a). Similar calculations are valid for (b). Using that $1-\cos x = 2\sin^2\frac{x}{2}$, we have

$$\begin{aligned} F^{n_h}_{f,T,N}(j) &= \sum_{k=0}^{N-1} q_{n_h}\Big(1-\cos(2\pi\frac{1}{T}t_k)\Big)^{n_h} f(t_k)e^{-2\pi i\frac{j}{T}t_k} \\ &= \sum_{k=0}^{N-1} q_{n_h}2^{n_h}\sin^{2n_h}(\pi\frac{1}{T}t_k)f(t_k)e^{-2\pi i\frac{j}{T}t_k} \\ &= \sum_{k=0}^{N-1} q_{n_h}2^{n_h}\frac{(e^{\pi i\frac{1}{T}t_k}-e^{-\pi i\frac{1}{T}t_k})^{2n_h}}{(2i)^{2n_h}}f(t_k)e^{-2\pi i\frac{j}{T}t_k} \\ &= \sum_{k=0}^{N-1}\frac{q_{n_h}}{(-2)^{n_h}}\sum_{l=0}^{2n_h}\binom{2n_h}{l}e^{\pi i\frac{2n_h-l}{T}t_k}(-1)^l e^{-\pi i\frac{l}{T}t_k}f(t_k)e^{-2\pi i\frac{j}{T}t_k} \\ &= \frac{q_{n_h}}{2^{n_h}}\sum_{l=0}^{2n_h}(-1)^{l-n_h}\binom{2n_h}{l}\sum_{k=0}^{N-1}f(t_k)e^{-2\pi i\frac{j+(l-n_h)}{T}t_k}. \end{aligned}$$

Shifting the index by n_h units, and using that

$$\frac{q_{n_h}}{2^{n_h}}\binom{2n_h}{n_h+l} = \frac{(n_h!)(n_h!)(2n_h)!}{(n_h!)2^{n_h}(2n_h-1)!!(n_h+l)!(n_h-l)!} = \frac{(n_h!)^2(2n_h)!}{(2n_h)!(n_h+l)!(n_h-l)!},$$

we get (a). □

For $c^{n_h}_{f,T,N}(j)$ and $s^{n_h}_{f,T,N}(j)$ relations similar to those of Lemma 2.1(a) hold. For instance, for $n_h = 1,2$ we get

$$\begin{aligned} F^1_{f,T,N}(j) &= -\frac{1}{2}F_{f,T,N}(j-1)+F_{f,T,N}(j)-\frac{1}{2}F_{f,T,N}(j+1), \\ F^2_{f,T,N}(j) &= \frac{1}{6}F_{f,T,N}(j-2)-\frac{2}{3}F_{f,T,N}(j-1)+F_{f,T,N}(j)-\frac{2}{3}F_{f,T,N}(j+1)+\frac{1}{6}F_{f,T,N}(j+2). \end{aligned}$$

As H^{n_h} is a filter function of degree $2n_h$, according to Corollary 2.1 we have

$$\phi^{n_h}_{e^{2\pi i\nu t/T},T}(\alpha/T) = O\Big(\frac{1}{(|\nu-\alpha|)^{2n_h+1}}\Big).$$

In fact, it can be explicitly calculated that

$$\phi^{n_h}_{e^{2\pi i\nu t/T},T}(\alpha/T) = \frac{(-1)^{n_h}(n_h!)^2(e^{2\pi i(\nu-\alpha)}-1)}{2\pi i\psi_{n_h}(\nu-\alpha)} \tag{9}$$

being

$$\psi_{n_h}(x) = \prod_{l=-n_h}^{n_h}(x+l). \tag{10}$$

2.3 Aliasing effect

Apart from leakage, another common effect when performing DFT is *aliasing.* It consists in the fact that any frequency greater than half the frequency associated to the sampling width, i.e. any frequency greater than $\omega_c := \frac{N}{2T}$, is *aliased* in a frequency less than ω_c. This is due to the following fact. Denoting $p^{n_h}_{f,T,N}(j) = \big((c^{n_h}_{f,T,N}(j))^2 + (s^{n_h}_{f,T,N}(j))^2\big)^{1/2}$, we have that

$$\begin{aligned} p^{n_h}_{\mathrm{cs}(2\pi(\omega+\frac{N}{T})t),T,N}(j) &= p^{n_h}_{\mathrm{cs}(2\pi\omega t),T,N}(j), \\ p^{n_h}_{\mathrm{cs}(2\pi(-\omega)t),T,N}(j) &= p^{n_h}_{\mathrm{cs}(2\pi\omega t)}(j), \end{aligned}$$

where cs stands for any of the functions cos or sin. If $\omega > \frac{N}{2T}$ and $m \in \mathbb{Z}$ is such that $\widetilde{\omega} := \omega - m\frac{N}{T} \in [-\frac{N}{2T}, \frac{N}{2T}]$, then the frequencies ω and $|\widetilde{\omega}|$ are undistinguisheable from a DFT point of view when using the p function. The frequency ω_c is called the *Nyquist critical frequency* in the literature.

Indeed, when all the frequency components of the continuous Fourier Transform are confined to the interval $[-\omega_c, \omega_c]$, the function is called *band-width limited.* More concretely, this means

$$\int_{-\infty}^{\infty} f(t)e^{-2\pi i\omega t}dt = 0, \qquad \text{for} \qquad |\omega| > \omega_c.$$

In this case, assuming that we have a sampling of infinite size $\{j\cdot\Delta t\}_{j\in\mathbb{Z}}$, the *Shannon sampling theorem* (see [4], [20]) allows to reconstruct the function $f(t)$ from its samples, namely

$$f(t) = \Delta t\sum_{j=-\infty}^{\infty} f(t_j)\frac{\sin\big(2\pi\omega_c(t-t_j)\big)}{\pi(t-t_j)}.$$

Note that quasi–periodic functions are not band–width limited.

3 Procedures for the refined Fourier analysis

Given N values, $\{f(t_l)\}_{l=0}^{N-1}$, $t_l = lT/N \in [0,T]$ of a certain function f, which is assumed to be quasi–periodic, we want to find a polynomial trigonometric approximation with a fixed number of frequencies N_f,

$$Q_f(t) = A_0^c + \sum_{l=1}^{N_f}\big(A_l^c\cos(\frac{2\pi\nu_l t}{T}) + A_l^s\sin(\frac{2\pi\nu_l t}{T})\big). \tag{11}$$

Of course, the number of frequencies may not be known a priori. See Section 4.1 for the iterative increase of the number of frequencies taken.

A standard approach to detect the frequencies of a given signal is to look for "peaks" of the modulus of its DFT, $p^{n_h}_{f,T,N}(j)$, which is also known as *power spectral density* in the literature. J. Laskar ([15], [17], [16]) introduced a refinement of this procedure, which consists in looking for maxima of $|\phi^{n_h}_{f,T,N}(j/T)|$, assuming that j takes real values. An alternative methodology for frequency determination was introduced in [12],[10]. It is the starting point for the methodology that will be developed here.

Our procedure is based entirely on the DFT for reasons that will be given below. The basic idea is to ask for the equality between the DFT of the sampled initial function and the DFT of its quasi–periodic approximation. It has three main steps: to get first approximations of the frequencies (either following the standard approach or using the method of Laskar), to compute the related approximated amplitudes and, finally, to perform a simultaneous improvement of frequencies and amplitudes.

3.1 First approximation of frequencies

If f has only one complex exponential term $f(t) = ae^{2\pi i \frac{\nu}{T} t}$, it follows from (9) that the modulus of its TCFT is

$$|\phi^{n_h}_{f,T}(\alpha/T)| = \frac{(n_h!)^2|a||1 - e^{i2\pi(\nu-\alpha)}|}{2\pi|\psi_{n_h}(\nu-\alpha)|}.$$

This function has a maximum at $\alpha = \nu$ (see Fig. 2). So, the problem of finding ν can be reduced to maximize the previous function with respect to α.

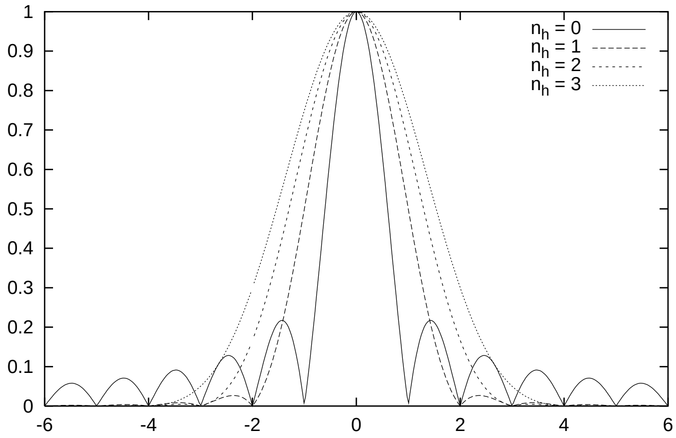

Figure 2: Plot of $|\phi^{n_h}_{e^{2\pi i \nu t/T},T}(\alpha/T)|$ as a function of $(\nu - \alpha)$ for $n_h = 0, 1, 2, 3$.

In a more general case, if $f(t)$ has m different frequencies,

$$f(t) = \sum_{l=1}^{m} a_l e^{2\pi i \frac{\nu_l}{T} t},$$

then $|\phi^{n_h}_{f,T}(\alpha/T)|$ does not have its maxima exactly at $\nu_1, \ldots, \nu_m$, but we can write

$$|\phi^{n_h}_{f,T}(\alpha/T) - \phi^{n_h}_{a_j e^{i2\pi\nu_j t/T},T}(\alpha/T)| \leq \sum_{\substack{l=1\\ l\neq j}}^{m} |\phi^{n_h}_{a_l e^{i2\pi\nu_l t/T},T}(\alpha/T)|.$$

If α is close to ν_j, then $\sum_{l\neq j} |\phi^{n_h}_{a_l e^{i2\pi\nu_l t/T},T}(\alpha/T)|$ (that is, leakage from the other frequencies) will be relatively small, so $|\phi^{n_h}_{f,T}(\alpha/T)|$ will be close to $|\phi^{n_h}_{a_j e^{i2\pi\nu_j t/T},T}(\alpha/T)|$, and therefore will have a maximum near ν_j. Here we are assuming implicitly that the frequencies we want to determine do not have too small amplitudes when compared to the amplitudes of other frequencies. In this way, looking to the local maxima of the function $|\phi^{n_h}_{f,T}(\alpha/T)|^2$, we get a first procedure for computing an estimate of the frequencies. This is the method used by Laskar ([15], [17], [16]). In his procedure, used for the computation and analysis of *frequency maps* related to observables of dynamical systems defined by the function $f(t)$, he looks for the local maxima of the function $|\phi^{n_h}_{f,T}(\alpha/T)|^2$ using some numerical quadrature formula for the evaluation of the TCFT at a discrete set of values of the argument α. Once some values of α near the maxima have been computed, the values of the maxima are refined by interpolation.

Since leakage is responsible for the maxima of $|\phi^{n_h}_{f,T}(\alpha/T)|$ not being the true frequencies, the use of filtering improves this procedure, since it reduces leakage. However, it is not advisable to take n_h too large, since as we increase n_h the "peaks" of the TCFT become wider and may shade nearby frequencies (see Fig. 2).

In our procedure, we maximize (directly, see later) the modulus of the filtered DFT of the initial function, $|F^{n_h}_{f,T,N}(j)|$ (where j may take real values), instead of approximating the TCFT using a numerical quadrature formula and maximizing this approximation. The reasons for this are:

- Although the DFT suffers from aliasing, whereas the TCFT does not, numerical quadrature formulae suffer aliasing at least as much as the DFT does. For instance, using a Newton-Côtes formula with all the sampling points as nodes, which is assumed to be written as $\int_0^T f(t)dt \approx \sum_{l=0}^{N-1} A_l f(lT/N)$, we have

$$
\begin{aligned}
\phi^{n_h}_{f,T}\Big(\frac{\alpha+N}{T}\Big) &= \frac{1}{T}\int_0^T H^{n_h}_T(t)f(t)e^{\frac{-i2\pi(\alpha+N)t}{T}}dt \\
&\approx \frac{1}{T}\sum_{l=0}^{N-1} A_l H^{n_h}_T(l\tfrac{T}{N})f(l\tfrac{T}{N})e^{\frac{-i2\pi(\alpha+N)}{T}l\frac{T}{N}} \\
&= \frac{1}{T}\sum_{l=0}^{N-1} A_l H^{n_h}_T(l\tfrac{T}{N})f(l\tfrac{T}{N})e^{\frac{-i2\pi\alpha}{T}l\frac{T}{N}} \approx \phi^{n_h}_{f,T}(\frac{\alpha}{T})
\end{aligned}
$$

- The use of a numerical quadrature formula does not guarantee the accuracy of the theoretical TCFT, since the error formulas include a power of the integration step, which in our case is the sampling width, and it does not need to be small. However, the DFT is close to the TCFT when there is no aliasing, as it will be shown in Lemma 5.4.

We use Newton's method to maximize $|F^{n_h}_{f,T,N}(j)|$. For that, we need to evaluate $\frac{\partial}{\partial j}|F^{n_h}_{f,T,N}(j)|$, and $\frac{\partial^2}{\partial j^2}|F^{n_h}_{f,T,N}(j/T)|$. Expressions for these functions can be obtained from (6). We take the "peaks" of the DFT as initial approximations for Newton's method. That is, given j_0 such that $p_{j_0-1} < p_{j_0} > p_{j_0+1}$, we use $\alpha = j_0$ as initial approximation.

3.2 Computation of the amplitudes assuming known frequencies

Once we know the frequencies $\{\nu_l\}_{l=1}^{N_f}$ in (11), we can compute the related amplitudes $\{A^c_l\}_{l=0}^{N_f}$, $\{A^s_l\}_{l=1}^{N_f}$ by asking the DFT of the current quasi–periodic approximation Q_f of f to be equal to the DFT of the sampled data $\{f(t_l)\}_{l=0}^{N-1}$. That is,

$$
F^{n_h}_{Q_f,T,N}(j) = F^{n_h}_{f,T,N}(j), \tag{12}
$$

for suitable values of j. Since we are interested in real functions, we will use the sines–cosines form of the DFT (5) instead of the complex one. In order to get a square system for the $1+2N_f$ unknowns, we select values of j in (12) in such a manner that we get

$$
\begin{aligned}
A^c_0 + \sum_{l=1}^{N_f}\big(A^c_l\overline{c}^{n_h}_{\nu_l,N}(0) + A^s_l\widetilde{c}^{n_h}_{\nu_l,N}(0)\big) &= c^{n_h}_{f,T,N}(0), \\
A^c_0 c^{n_h}_1(j_i) + \sum_{l=1}^{N_f}\big(A^c_l\overline{c}^{n_h}_{\nu_l,N}(j_i) + A^s_l\widetilde{c}^{n_h}_{\nu_l,N}(j_i)\big) &= c^{n_h}_{f,T,N}(j_i), \\
\sum_{l=1}^{N_f}\big(A^c_l\overline{s}^{n_h}_{\nu_l,N}(j_i) + A^s_l\widetilde{s}^{n_h}_{\nu_l,N}(j_i)\big) &= s^{n_h}_{f,T,N}(j_i),
\end{aligned} \tag{13}
$$

where

$$
\begin{aligned}
c^{n_h}_1(j) &= c^{n_h}_{1,T,N}(j), \\
\overline{c}^{n_h}_{\nu,N}(j) &= c^{n_h}_{\cos(\frac{2\pi\nu t}{T}),T,N}(j), \qquad \overline{s}^{n_h}_{\nu,N}(j) = s^{n_h}_{\cos(\frac{2\pi\nu t}{T}),T,N}(j), \\
\widetilde{c}^{n_h}_{\nu,N}(j) &= c^{n_h}_{\sin(\frac{2\pi\nu t}{T}),T,N}(j), \qquad \widetilde{s}^{n_h}_{\nu,N}(j) = s^{n_h}_{\sin(\frac{2\pi\nu t}{T}),T,N}(j),
\end{aligned} \tag{14}
$$

and the j_i are chosen as the closest integers to ν_i, that is, such that $|j_i - \nu_i| \le 1/2$ for $i = 1 \div N_f$. Note that $c^{n_h}_1(j)$ is independent of T and N. The fact that $\overline{c}^{n_h}_{\nu,N}(j)$, $\overline{s}^{n_h}_{\nu,N}(j)$, $\widetilde{c}^{n_h}_{\nu,N}(j)$ and $\widetilde{s}^{n_h}_{\nu,N}(j)$ do not depend on T will be shown in Section 4.3.

In this way we get a $(1+2N_f)\times(1+2N_f)$ linear system, which, assuming that $j_i \geq 1+n_h$ for $i=1\div N_f$, can be written in compact block form as

$$\begin{pmatrix} 2 & u_1 & \dots & u_{N_f} \\ 0 & B_{1,1} & \dots & B_{1,N_f} \\ \vdots & \vdots & \ddots & \vdots \\ 0 & B_{N_f,1} & \dots & B_{N_f,N_f} \end{pmatrix} \begin{pmatrix} A_0^c \\ v_1 \\ \vdots \\ v_{N_f} \end{pmatrix} = \begin{pmatrix} c_{f,T,N}^{n_h}(0) \\ w_1 \\ \vdots \\ w_{N_f} \end{pmatrix}, \tag{15}$$

where

$$\begin{aligned} u_l &= \begin{pmatrix} \overline{c}_{\nu_l,N}^{n_h}(0) & \widetilde{c}_{\nu_l,N}^{n_h}(0) \end{pmatrix}, & B_{i,l} &= \begin{pmatrix} \overline{c}_{\nu_l,N}^{n_h}(j_i) & \widetilde{c}_{\nu_l,N}^{n_h}(j_i) \\ \overline{s}_{\nu_l,N}^{n_h}(j_i) & \widetilde{s}_{\nu_l,N}^{n_h}(j_i) \end{pmatrix}, \\ v_i &= \begin{pmatrix} A_i^c \\ A_i^s \end{pmatrix}, & w_i &= \begin{pmatrix} c_{f,T,N}^{n_h}(j_i) \\ s_{f,T,N}^{n_h}(j_i) \end{pmatrix}. \end{aligned} \tag{16}$$

Since the DFT decreases as $|\nu-j|$ goes away from zero, this system is near to block–diagonal if N is large enough and therefore it is well conditioned. In theorem 5.1 we give a bound of the inverse of its coefficient matrix. Moreover, because of its structure, it is very well suited for a 2×2 block Jacobi method, which can be written, if we remove the first equation of (15), as

$$v_i^{(n+1)} = B_{i,i}^{-1}\Big(-\sum_{\substack{j=1\\ j\neq i}}^{N_f} B_{i,j}v_j^{(n)} + w_i\Big), \qquad i=1\div N_f. \tag{17}$$

Once we have values for $\{A_l^c, A_l^s\}_{l=1}^{N_f}$, we can compute A_0^c from the first equation of (15). In corollary 5.1 we give a result about the convergence of this Jacobi procedure. In practice, the results have shown that the convergence is very fast when starting from the values given directly by the DFT. Usually 3 or 4 iterates of the block Jacobi method are enough for Hanning level $n_h=2$ and a tolerance of 10^{-15} for the maximum difference between two consecutive iterates (these values correspond to the analysis of a trigonometric polynomial with three frequencies).

3.3 Simultaneous improvement of frequencies and amplitudes

Given approximations of frequencies and amplitudes, we can improve them simultaneously by solving a system of equations similar to the one used in the previous section. With respect to that system, we need now an additional equation for each frequency, since frequencies are now unknown. We therefore solve iteratively the system

$$\begin{aligned} A_0^c &+ \sum_{l=1}^{N_f}\left(A_l^c\overline{c}_{\nu_l,N}^{n_h}(0) + A_l^s\widetilde{c}_{\nu_l,N}^{n_h}(0)\right) = c_{f,T,N}^{n_h}(0), \\ A_0^c c_1^{n_h}(j_i) &+ \sum_{l=1}^{N_f}\left(A_l^c\overline{c}_{\nu_l,N}^{n_h}(j_i) + A_l^s\widetilde{c}_{\nu_l,N}^{n_h}(j_i)\right) = c_{f,T,N}^{n_h}(j_i), \\ & \sum_{l=1}^{N_f}\left(A_l^c\overline{s}_{\nu_l,N}^{n_h}(j_i) + A_l^s\widetilde{s}_{\nu_l,N}^{n_h}(j_i)\right) = s_{f,T,N}^{n_h}(j_i), \\ A_0^c cs_1^{n_h}(j_i^+) &+ \sum_{l=1}^{N_f}\left(A_l^c\overline{cs}_{\nu_l,N}^{n_h}(j_i^+) + A_l^s\widetilde{cs}_{\nu_l,N}^{n_h}(j_i^+)\right) = cs_{f,T,N}^{n_h}(j_i^+), \end{aligned} \tag{18}$$

for $\{\nu_l\}_{l=1}^{N_f}$, $\{A_l^c\}_{l=0}^{N_f}$, $\{A_l^s\}_{l=1}^{N_f}$, where j_i and j_i^+ are defined as

$$\begin{array}{ll} j_i=[\nu_i],\ j_i^+=[\nu_i]+1 & \text{if } \nu_i-[\nu_i]\leq 1/2, \\ j_i=[\nu_i]+1,\ j_i^+=[\nu_i] & \text{otherwise,} \end{array}$$

for $i=1\div N_f$. In the last equation of (18), cs denotes either c or s; the criterium to choose one or the other is given bellow.

If $j_i \geq 1 + n_h$ for $i = 1 \div N_f$, the differential of (18) with respect to the unknowns

$$\left(\begin{array}{cccccccc} A_0^c & \nu_1 & A_1^c & A_1^s & \dots & \nu_{N_f} & A_{N_f}^c & A_{N_f}^s \end{array} \right),$$

which is needed in order to apply Newton's method, can be written as

$$M = \begin{pmatrix} 2 & v_1 & \dots & v_{N_f} \\ 0 & B_{1,1} & \dots & B_{1,N_f} \\ \vdots & \vdots & \ddots & \vdots \\ 0 & B_{N_f,1} & \dots & B_{N_f,N_f} \end{pmatrix},$$

being

$$\begin{array}{rcl} v_l & = & \left(\begin{array}{ccc} A_l^c \partial \overline{c}_{\nu_l,N}^{n_h}(0) + A_l^s \partial \widetilde{c}_{\nu_l,N}^{n_h}(0) & \overline{c}_{\nu_l,N}^{n_h}(0) & \widetilde{c}_{\nu_l,N}^{n_h}(0) \end{array} \right), \\ B_{i,l} & = & \begin{pmatrix} A_l^c \partial \overline{c}_{\nu_l,N}^{n_h}(j_i) + A_l^s \partial \widetilde{c}_{\nu_l,N}^{n_h}(j_i) & \overline{c}_{\nu_l,N}^{n_h}(j_i) & \widetilde{c}_{\nu_l,N}^{n_h}(j_i) \\ A_l^c \partial \overline{s}_{\nu_l,N}^{n_h}(j_i) + A_l^s \partial \widetilde{s}_{\nu_l,N}^{n_h}(j_i) & \overline{s}_{\nu_l,N}^{n_h}(j_i) & \widetilde{s}_{\nu_l,N}^{n_h}(j_i) \\ A_l^c \partial \overline{cs}_{\nu_l,N}^{n_h}(j_i^+) + A_l^s \partial \widetilde{cs}_{\nu_l,N}^{n_h}(j_i^+) & \overline{cs}_{\nu_l,N}^{n_h}(j_i^+) & \widetilde{cs}_{\nu_l,N}^{n_h}(j_i^+) \end{pmatrix}, \end{array} \tag{19}$$

where ∂ denotes derivative with respect to ν. As in the preceding section, this matrix is close to block–diagonal and, therefore, the system to be solved at each Newton iteration is well conditioned.

For each block $B_{i,l}$, the criterium to choose cs from c and s is to set it equal to the one that minimizes $\|B_{i,i}^{-1}\|_\infty$. This further improves the well–conditioning of the system, and is theoretically justified in Section 5 (Lemma 5.9).

With the exception of rounding errors, the only source of error in this procedure is the leakage from frequencies that we are skipping, as will be shown in Section 5. In particular, this method is exact for trigonometric polynomials (the combination of the procedures of Sections 3.1 and 3.2 is not).

As a final remark note that, because of the use of the DFT, both this procedure and the one of the previous section suffer from the aliasing effect introduced in Section 2.3.

4 Implementation details

In this section we give some details for the implementation of the procedures described in the previous section.

4.1 Algorithm for the procedure

Starting from the sampling $\{f(t_l)\}_{l=0}^{N-1}$ of a function which is known to have a quasi–periodic behavior, we carry out its Fourier analysis by finding initial approximations for the frequencies using the procedure of Section 3.1, obtaining the related amplitudes using Section 3.2 and iteratively refining the approximations of frequencies and amplitudes through Section 3.3.

In order to prevent some frequencies to "hide" nearby frequencies of lower amplitude, it is advisable to proceed iteratively, in such a way that at each iteration we only consider those frequencies whose amplitude is greater than a given tolerance.

Concretely, the algorithm used for the numerical examples of the last section is the following.

Algorithm 4.1 *Provided a minimum amplitude b_{min} for the frequencies to be computed, and a number of iterations n for the procedure, first define*

$$p_{max} = \max_{j=1\div\frac{N}{2}} p_{f,T,N}^{n_h}(j), \qquad db = (b_{min}/p_{max})^{1/n},$$

where $p_{f,T,N}^{n_h}(j) = \left((c_{f,T,N}^{n_h}(j))^2 + (s_{f,T,N}^{n_h}(j))^2\right)^{1/2}$, and set

$$Q_f(t) \leftarrow 0, \qquad b \leftarrow p_{max}, \qquad N_f \leftarrow 0.$$

$Q_f(t)$ will be the current quasi–periodic approximation of f, b the minimum amplitude of the frequencies to be detected in the current iteration, and N_f the number of frequencies computed. Then, while $b > b_{min}$, proceed as:

1. *Set $b \leftarrow b{\cdot}db$. Let $k_{N_f+1}, \ldots, k_{N_f+m}$ be the peaks of the modulus of the DFT of $f - Q_f$ with minimum amplitude b, that is, $\{k_{N_f+1}, \ldots k_{N_f+m}\} = \{j \in \mathbb{Z} : n_h + 2 \le j \le \frac{N}{2} - n_h - 2,\ p^{n_h}_{f-Q_f,T,N}(j) \ge b,\ p^{n_h}_{f-Q_f,T,N}(j-1) \le p^{n_h}_{f-Q_f,T,N}(j) \ge p^{n_h}_{f-Q_f,T,N}(j+1)\}$. For each k_l, apply the procedure of Section 3.1 to obtain ν_l.*
2. *Solve (13), according to Section 3.2, to get $\{A^c_l\}_{l=0}^{N_f+m}$ and $\{A^s_l\}_{l=1}^{N_f+m}$ from $\{\nu_l\}_{l=1}^{N_f+m}$.*
3. *Solve (18), according to Section 3.3 to iteratively refine $\{\nu_l\}_{l=1}^{N_f+m}$, $\{A^c_l\}_{l=0}^{N_f+m}$ and $\{A^s_l\}_{l=1}^{N_f+m}$.*
4. *Update the number of frequencies and the current quasi–periodic approximation,*

$$N_f \leftarrow N_f + m, \qquad Q_f(t) \leftarrow A^c_0 + \sum_{l=1}^{N_f} \left(A^c_l \cos(\frac{2\pi\nu_l t}{T}) + A^s_l \sin(\frac{2\pi\nu_l t}{T})\right)$$

and go to step 1.

We stop the algorithm if

- *N_f reaches a given maximum number of frequencies, or if*
- *$\max_{l=0\div N-1} |f(t_l) - Q_f(t_l)|$ is under a given tolerance, or if*
- *$\max_{j=0\div N/2} p^{n_h}_{f-Q_f,T,N}(j)$ is under a given tolerance, or if*
- *there appear two frequencies too close. We usually consider ν_{l_1}, ν_{l_2} to be too close if $|\nu_{l_1} - \nu_{l_2}| < 2 + n_h$.*

In all the examples tested (see Section 6.1 and [19]), the DFT approximation is good enough for Newton's method in step 3 to converge, provided the initial data is close enough to a sample of a quasi–periodic function. That is, for the examples for which the procedure of Section 3.3 is divergent, we have also obtained divergence when the preliminary estimates of frequencies (given by the DFT) have been refined by any other method. Hence, we can skip the preliminary determination of the frequencies of Section 3.1 by setting $\nu_l = k_l$ in step 1, and then compute the amplitudes related to these frequencies following step 2. It may be useful to use the procedure of Section 3.1 anyway when N_f is very large and we want to save some Newton iterates in step 3, since we have to solve a $(1 + 3N_f) \times (1 + 3N_f)$ linear system at each Newton iterate.

4.2 Use of trigonometric recurrences

Large amounts of computing time can be saved if we avoid the evaluation of the sin and cos functions when we have to evaluate the DFT using its definition in the procedure of Section 3.1, or when we have to compute $\{f(t_l) - Q_f(t_l)\}_{l=0}^{N-1}$ in step 1 of the algorithm given above. This can be accomplished through the use of trigonometric recurrences for the evaluation of $\cos(lx)$ and $\sin(lx)$ for $l \in \mathbb{N}$ and $x \in \mathbb{R}$. One has to be careful in choosing such recurrences, in order to avoid numerical instability (see [24] for a discussion). The recurrence we have used is given in [24], p. 24: first set

$$dc_1 := -2\sin^2\frac{x}{2}, \quad t := 2dc_1, \quad ds_1 := \sqrt{-dc_1(2 + dc_1)}, \quad s_0 := 0, \quad c_0 := 1,$$

and then compute, for $m := 1, 2, \ldots$,

$$\begin{aligned} c_m &:= c_{m-1} + dc_m, & dc_{m+1} &:= t \cdot c_m + dc_m, \\ s_m &:= s_{m-1} + ds_m, & ds_{m+1} &:= t \cdot s_m + ds_m. \end{aligned}$$

Just for illustrating purposes, we compare in Fig. 3 the errors produced by the trigonometric recurrence previously given with the following one: first set

$$cc_0 = 1, \quad cc_1 = \cos x, \quad ss_0 = 0, \quad ss_1 = \sin x,$$

and then compute, for $m := 2, 3, \ldots$,

$$\begin{aligned} cc_{m+1} &= (2\cos x)cc_m - cc_{m-1}, \\ ss_{m+1} &= (2\cos x)ss_m - ss_{m-1}. \end{aligned}$$

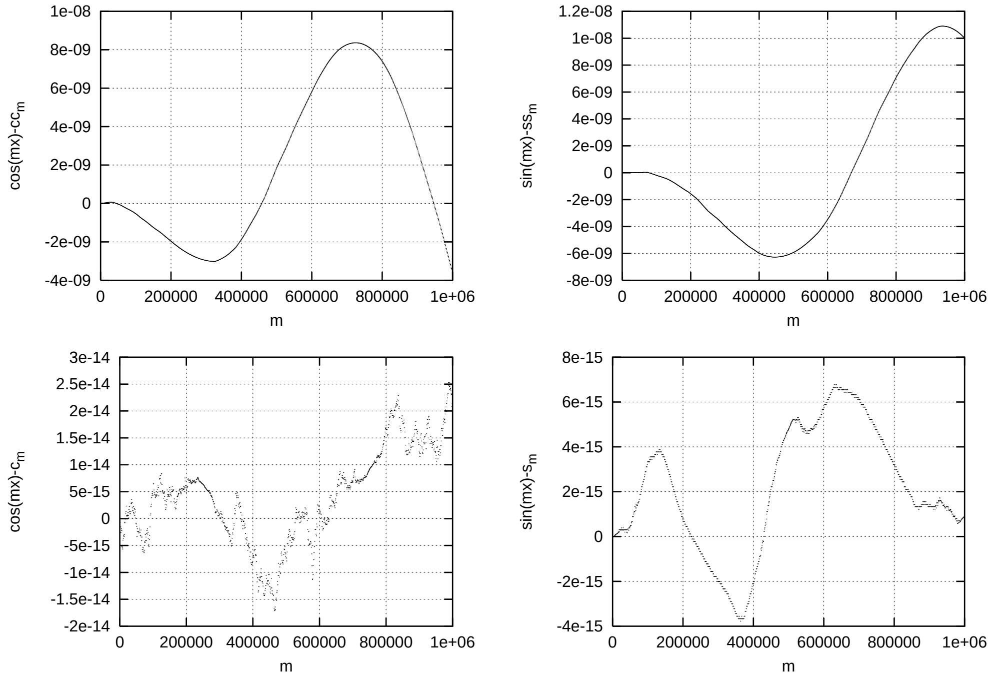

Figure 3: Illustration of the numerical instability of trigonometric recurrences. For $x = 2\pi \times 10^{-6}$ and $n = 10^6$, we have evaluated $\{\cos(mx), \sin(mx)\}_{m=0}^{n}$ and the values $\{c_m, s_m\}_{m=0}^{n}$ and $\{cc_m, ss_m\}_{m=0}^{n}$ using the recurrences detailed in the text. In the left–hand plots we show the differences $\cos(mx) - cc_m$ (top) and $\cos(mx) - c_m$ (bottom). In the right–hand ones, we show the differences $\sin(mx) - ss_m$ (top) and $\sin(mx) - s_m$. These values are machine and compiler–dependent. The program that has computed these plots has been compiled with GNU gcc 2.95.2 with the optimization option '–O3' on an Intel Pentium II processor.

4.3 Evaluation of the DFT of sines and cosines

Special care must be taken in the evaluation of the DFT of sines and cosines, in order to avoid cancellations and singularities. In this section we describe some of the strategies followed in our implementation, especially those related to small values of $\nu - j$.

The DFT of sines and cosines can be evaluated from the complex DFT of a complex exponential term through the following formulae:

$$\begin{aligned}
\overline{c}^{n_h}_{\nu,N}(j) &= \operatorname{Re} F^{n_h}_{e^{i2\pi\nu t/T},T,N}(j) + \operatorname{Re} F^{n_h}_{e^{i2\pi(-\nu)t/T},T,N}(j), \\
\overline{s}^{n_h}_{\nu,N}(j) &= -\operatorname{Im} F^{n_h}_{e^{i2\pi\nu t/T},T,N}(j) - \operatorname{Im} F^{n_h}_{e^{i2\pi(-\nu)t/T},T,N}(j), \\
\widetilde{c}^{n_h}_{\nu,N}(j) &= \operatorname{Im} F^{n_h}_{e^{i2\pi\nu t/T},T,N}(j) - \operatorname{Im} F^{n_h}_{e^{i2\pi(-\nu)t/T},T,N}(j), \\
\widetilde{s}^{n_h}_{\nu,N}(j) &= \operatorname{Re} F^{n_h}_{e^{i2\pi\nu t/T},T,N}(j) - \operatorname{Re} F^{n_h}_{e^{i2\pi(-\nu)t/T},T,N}(j).
\end{aligned}$$

By derivating with respect to ν, we get similar relations that allow to obtain $\partial\overline{c}^{n_h}_{\nu,N}(j)$, $\partial\widetilde{c}^{n_h}_{\nu,N}(j)$, $\partial\overline{s}^{n_h}_{\nu,N}(j)$, $\partial\widetilde{s}^{n_h}_{\nu,N}(j)$ from $\partial F^{n_h}_{e^{i2\pi(-\nu)t/T},T,N}(j)$. As before, ∂ denotes derivative with respect to ν.

The non-filtered complex DFT of a complex exponential term is a geometric progression,

$$F_{e^{i2\pi\nu t/T},T,N}(j) = \frac{1}{N}\sum_{l=0}^{N-1} e^{i2\pi(\nu-j)l/N} = \frac{1-e^{i2\pi(\nu-j)}}{N(1-e^{i2\pi(\nu-j)/N})},$$

and its derivative with respect to ν is

$$\partial F^{n_h}_{e^{i2\pi\nu t/T},T,N}(j) = \frac{i2\pi}{N}\cdot\frac{\frac{1}{N}e^{i2\pi(\nu-j)/N} - e^{i2\pi(\nu-j)} + \frac{N-1}{N}e^{i2\pi(N+1)(\nu-j)/N}}{(1-e^{i2\pi(\nu-j)/N})^2}.$$

Using the relations of Lemma 2.1 and its derivatives, we can get the filtered complex DFT of $e^{i2\pi\nu t/T}$, as well as its derivatives with respect to ν, from the non–filtered values.

The computation of $F_{e^{i2\pi\nu t/T},T,N}(j)$ is organized as follows:

$$F_{e^{i2\pi\nu t/T},T,N}(j) = \frac{1}{N}\Big(\frac{ac+bd}{c^2+d^2} + i\frac{bc-ad}{c^2+d^2}\Big),$$

being

$$\begin{array}{rclcllcl} a &=& 1-\cos(2\pi(\nu-j)) &=& 2\sin^2(\pi(\nu-j)), & b &=& -\sin(2\pi(\nu-j)), \\ c &=& 1-\cos(2\pi(\nu-j)/N) &=& 2\sin^2(\pi(\nu-j)/N), & d &=& -\sin(2\pi(\nu-j)/N). \end{array}$$

For a and c, we use the second expressions in order to avoid cancellations.

Concerning to $\partial F_{e^{i2\pi\nu t/T},T,N}(j)$, we compute it as

$$\partial F_{e^{i2\pi\nu t/T},T,N}(j) = \frac{2\pi}{N}\Big(\frac{ad-bc}{c^2+d^2} + i\frac{ac+bd}{c^2+d^2}\Big),$$

being

$$\begin{array}{rcl} a &=& \frac{1}{N}\cos\Big(\frac{2\pi(\nu-j)}{N}\Big) - \cos\big(2\pi(\nu-j)\big) + \frac{N-1}{N}\cos\Big(\frac{2\pi(N+1)(\nu-j)}{N}\Big) \\ &=& \frac{2}{N}\sin\Big(\frac{\pi(2+N)(\nu-j)}{N}\Big)\sin\big(\pi(\nu-j)\big) - 2\sin\Big(\frac{\pi(2N+1)(\nu-j)}{N}\Big)\sin\Big(\frac{\pi(\nu-j)}{N}\Big), \\ b &=& \frac{1}{N}\sin\Big(\frac{2\pi(\nu-j)}{N}\Big) - \sin\big(2\pi(\nu-j)\big) + \frac{N-1}{N}\sin\Big(\frac{2\pi(N+1)(\nu-j)}{N}\Big) \\ &=& -\frac{2}{N}\cos\Big(\frac{\pi(2+N)(\nu-j)}{N}\Big)\sin\big(\pi(\nu-j)\big) + 2\cos\Big(\frac{\pi(2N+1)(\nu-j)}{N}\Big)\sin\Big(\frac{\pi(\nu-j)}{N}\Big), \\ e &=& 1-\cos\Big(\frac{2\pi(\nu-j)}{N}\Big) = 2\sin^2\Big(\frac{\pi(\nu-j)}{N}\Big), \\ f &=& -\sin\Big(\frac{2\pi(\nu-j)}{N}\Big), \\ c &=& e^2-f^2, \\ d &=& 2ef. \end{array}$$

As before, for a, b, and e we use the second form in order to avoid cancellations, although the second expression of b does not remove cancellations completely.

Since $F_{e^{i2\pi\nu t/T},T,N}(j) = h(\nu-j)$, being

$$h(\alpha) = \frac{1}{N}\sum_{l=0}^{N-1} e^{i2\pi\alpha l/N} = \frac{1-e^{i2\pi\alpha}}{N(1-e^{i2\pi\alpha/N})},$$

we can use the Taylor expansion of h to evaluate $F_{e^{i2\pi\nu t/T},T,N}(j)$ and $\partial F_{e^{i2\pi\nu t/T},T,N}(j)$ for $|\nu-j|$ small. Indeed, we could use this Taylor expansion for any $|\nu-j|$, because h is an entire function (it is a finite sum of exponentials), but the convergence of the expansion is slow for large $|\nu-j|$. We have set a threshold δ in such a way that for $|\nu-j|\geq\delta$ we use the previous formulation and for $|\nu-j|<\delta$ we use the Taylor expansion. The value of δ is chosen in order to have fast convergence of the Taylor expansion and a small error due to the cancellation in the second expression of b. We have taken $\delta = 0.1$, since

$$\lim_{N\to\infty}\Big|\frac{\gamma-\beta}{\beta}\Big| = 0.1352,$$

being

$$\beta = \frac{2}{N}\cos\Big(\frac{\pi(2+N)\delta}{N}\Big)\sin(\pi\delta), \qquad \gamma = 2\cos\Big(\frac{\pi(2N+1)\delta}{N}\Big)\sin\Big(\frac{\pi\delta}{N}\Big),$$

and, in this way, the loss of precision due to the cancellation of the second expression of b is at most one order of magnitude. Moreover, since

$$\Big|\frac{h^{(k)}(0)}{k!}\delta^k\Big| \leq \frac{(2\pi)^k}{(k+1)!}|\delta|^k,$$

the convergence of the Taylor expansion is fast for $|\nu - j| < \delta$.

For the evaluation of the Taylor expansion of h, we have used that

$$h^{(k)}(0) = \frac{(i2\pi)^k}{N^{k+1}} \sum_{l=0}^{N-1} l^k,$$

and, for $k \geq 1$,

$$\sum_{l=1}^{N-1} l^k = \frac{(N-1)^{k+1}}{k+1} + \frac{(N-1)^k}{2} + \sum_{j=1}^{[k/2]} \frac{1}{2j}\binom{k}{2j-1} B_{2j}(N-1)^{k-2j+1},$$

where the B_i are the Bernoulli numbers.

5 Error estimates

In order to derive error bounds, we will assume through this section that the function f to be analyzed is real analytic and quasi–periodic, that is

$$f(t) = \sum_{k\in\mathbb{Z}^m} a_k e^{i2\pi k\omega t} = A_0^c + \sum_{\substack{k\in\mathbb{Z}^m\\ k\omega>0}} \left(A_k^c \cos(2\pi k\omega t) + A_k^s \sin(2\pi k\omega t)\right) \tag{20}$$

where $k\omega = k_1\omega_1 + \ldots + k_m\omega_m$, $A_k = 2\,\mathrm{Re}\, a_k$, $B_k = -2\,\mathrm{Im}\, a_k$, the frequency vector $\omega = (\omega_1, \ldots, \omega_m)$ is assumed to satisfy a Diophantine condition of the form

$$|k\omega| \geq \frac{D}{|k|^\tau}, \tag{21}$$

for all $k \in \mathbb{Z}^m \setminus \{0\}$ with $D, \tau > 0$ and $|k| = ||k||_1 = \sum_{i=1}^m |k_i|$, and the Fourier coefficients of f satisfy the *Cauchy estimates*,

$$|a_k| \leq Ce^{-\delta|k|}, \quad \forall k \in \mathbb{Z}^m \tag{22}$$

for some $C > 0$, $\delta > 0$. We will also assume that we want to compute the frequencies of f up to order $|k| \leq r_0 - 1$ as well as its related amplitudes. That is, we want to approximate f by a trigonometric polynomial

$$p(t) = A_0^c + \sum_{l=1}^{N_f} \left(A_l^c \cos(\frac{2\pi\nu_l}{T}t) + A_l^s \sin(\frac{2\pi\nu_l}{T}t)\right),$$

being

$$\{\nu_1, \ldots, \nu_{N_f}\} = \{Tk\omega : k \in \mathbb{Z}^m, 1 \leq |k| \leq r_0 - 1, Tk\omega > 0\}. \tag{23}$$

We will give error bounds for two cases: the case in which we want to compute the amplitudes from known frequencies (Section 3.2) and the case in which both frequencies and amplitudes are unknown (Section 3.3). In order to perform error analysis for the second case, we split the right–hand side of (18) and rewrite it as

$$\begin{aligned}
A_0^c + \sum_{l=1}^{N_f} \left(A_l^c \overline{c}_{\nu_l,N}^{n_h}(0) + A_l^s \widetilde{c}_{\nu_l,N}^{n_h}(0)\right) &= c_{p,T,N}^{n_h}(0) + c_{f-p,T,N}^{n_h}(0) \\
A_0^c c_1^{n_h}(j_i) + \sum_{l=1}^{N_f} \left(A_l^c \overline{c}_{\nu_l,N}^{n_h}(j_i) + A_l^s \widetilde{c}_{\nu_l,N}^{n_h}(j_i)\right) &= c_{p,T,N}^{n_h}(j_i) + c_{f-p,T,N}^{n_h}(j_i) \\
\sum_{l=1}^{N_f} \left(A_l^c \overline{s}_{\nu_l,N}^{n_h}(j_i) + A_l^s \widetilde{s}_{\nu_l,N}^{n_h}(j_i)\right) &= s_{p,T,N}^{n_h}(j_i) + s_{f-p,T,N}^{n_h}(j_i) \\
\underbrace{A_0^c cs_1^{n_h}(j_i^+) + \sum_{l=1}^{N_f} \left(A_l^c \overline{cs}_{\nu_l,N}^{n_h}(j_i^+) + A_l^s \widetilde{cs}_{\nu_l,N}^{n_h}(j_i^+)\right)}_{g(y+\Delta y)} &= \underbrace{cs_{p,T,N}^{n_h}(j_i^+)}_{b} + \underbrace{cs_{f-p,T,N}^{n_h}(j_i^+)}_{\Delta b}.
\end{aligned} \tag{24}$$

If we denote collectively the exact frequencies and amplitudes as y for brevity, we would obtain them by solving $g(y) = b$. But the system to be solved is $g(y + \Delta y) = b + \Delta b$, and therefore the error we have (assuming no rounding errors) can be bounded (in the first order approximation) by

$$\|\Delta y\|_\infty \lesssim \|Dg(y)^{-1}\|_\infty \|\Delta b\|_\infty$$

A similar argument is applied to the case in which the frequencies are known and we want to compute the amplitudes. We have again an equation of the form

$$g(y + \Delta y) = b + \Delta b, \tag{25}$$

but in this case, g, y, Δy, b and Δb are defined as in (24) just skipping the last line.

This section is devoted to the computation of bounds for $\|Dg(y)^{-1}\|_\infty$ and $\|\Delta b\|_\infty$ in terms of T, N, n_h and the properties of the analyzed function f. From now on, and unless otherwise stated, we will use the supremum norm.

5.1 Error bounds for $\|Dg(y)^{-1}\|_\infty$

In order to simplify the expressions to be manipulated, we will bound the TCFT instead of the DFT. That is, we will use $\mathcal{C}^{n_h}_{f,T}$ and $\mathcal{S}^{n_h}_{f,T}$ defined by

$$\phi^{n_h}_{f,T}\left(\frac{j}{T}\right) = \frac{1}{2}\left(\mathcal{C}^{n_h}_{f,T}(j) - i\mathcal{S}^{n_h}_{f,T}(j)\right), \tag{26}$$

(here $i = \sqrt{-1}$). As in the discrete case (14), we will note

$$\begin{array}{rclrcl}
\mathcal{C}^{n_h}_1(j) & = & \mathcal{C}^{n_h}_{1,T,N}(j), & & & \\
\overline{\mathcal{C}}^{n_h}_\nu(j) & = & \mathcal{C}^{n_h}_{\cos(\frac{2\pi\nu t}{T}),T}(j), & \overline{\mathcal{S}}^{n_h}_\nu(j) & = & \mathcal{S}^{n_h}_{\cos(\frac{2\pi\nu t}{T}),T}(j), \\
\widetilde{\mathcal{C}}^{n_h}_\nu(j) & = & \mathcal{C}^{n_h}_{\sin(\frac{2\pi\nu t}{T}),T}(j), & \widetilde{\mathcal{S}}^{n_h}_\nu(j) & = & \mathcal{S}^{n_h}_{\sin(\frac{2\pi\nu t}{T}),T}(j),
\end{array}$$

and the derivatives of $\overline{\mathcal{C}}^{n_h}_\nu(j)$, $\overline{\mathcal{S}}^{n_h}_\nu(j)$, $\widetilde{\mathcal{C}}^{n_h}_\nu(j)$ and $\widetilde{\mathcal{S}}^{n_h}_\nu(j)$ with respect to ν will be denoted as $\partial\overline{\mathcal{C}}^{n_h}_\nu(j)$, $\partial\overline{\mathcal{S}}^{n_h}_\nu(j)$, $\partial\widetilde{\mathcal{C}}^{n_h}_\nu(j)$ and $\partial\widetilde{\mathcal{S}}^{n_h}_\nu(j)$, respectively. We give expressions for these transforms in the following

Lemma 5.1 *Denote $\psi_{n_h}(x) = \prod_{l=-n_h}^{n_h}(x+l)$. We have*

$$\begin{array}{rcl}
\overline{\mathcal{C}}^{n_h}_\nu(j) & = & \dfrac{(-1)^{n_h}(n_h!)^2}{2\pi}\Big(\dfrac{\sin\big(2\pi(\nu-j)\big)}{\psi_{n_h}(\nu-j)} + \dfrac{\sin\big(2\pi(-\nu-j)\big)}{\psi_{n_h}(-\nu-j)}\Big), \\
\widetilde{\mathcal{C}}^{n_h}_\nu(j) & = & \dfrac{(-1)^{n_h}(n_h!)^2}{2\pi}\Big(\dfrac{1-\cos\big(2\pi(\nu-j)\big)}{\psi_{n_h}(\nu-j)} - \dfrac{1-\cos\big(2\pi(-\nu-j)\big)}{\psi_{n_h}(-\nu-j)}\Big), \\
\overline{\mathcal{S}}^{n_h}_\nu(j) & = & \dfrac{(-1)^{n_h}(n_h!)^2}{2\pi}\Big(-\dfrac{1-\cos\big(2\pi(\nu-j)\big)}{\psi_{n_h}(\nu-j)} - \dfrac{1-\cos\big(2\pi(-\nu-j)\big)}{\psi_{n_h}(-\nu-j)}\Big), \\
\widetilde{\mathcal{S}}^{n_h}_\nu(j) & = & \dfrac{(-1)^{n_h}(n_h!)^2}{2\pi}\Big(\dfrac{\sin\big(2\pi(\nu-j)\big)}{\psi_{n_h}(\nu-j)} - \dfrac{\sin\big(2\pi(-\nu-j)\big)}{\psi_{n_h}(-\nu-j)}\Big), \\
\partial\overline{\mathcal{C}}^{n_h}_\nu(j) & = & \dfrac{(-1)^{n_h}(n_h!)^2}{2\pi}\Big(\dfrac{h_r(\nu-j)}{\psi_{n_h}(\nu-j)} - \dfrac{h_r(-\nu-j)}{\psi_{n_h}(-\nu-j)}\Big), \\
\partial\widetilde{\mathcal{C}}^{n_h}_\nu(j) & = & \dfrac{(-1)^{n_h}(n_h!)^2}{2\pi}\Big(\dfrac{h_i(\nu-j)}{\psi_{n_h}(\nu-j)} + \dfrac{h_i(-\nu-j)}{\psi_{n_h}(-\nu-j)}\Big), \\
\partial\overline{\mathcal{S}}^{n_h}_\nu(j) & = & \dfrac{(-1)^{n_h}(n_h!)^2}{2\pi}\Big(-\dfrac{h_i(\nu-j)}{\psi_{n_h}(\nu-j)} + \dfrac{h_i(-\nu-j)}{\psi_{n_h}(-\nu-j)}\Big), \\
\partial\widetilde{\mathcal{S}}^{n_h}_\nu(j) & = & \dfrac{(-1)^{n_h}(n_h!)^2}{2\pi}\Big(\dfrac{h_r(\nu-j)}{\psi_{n_h}(\nu-j)} + \dfrac{h_r(-\nu-j)}{\psi_{n_h}(-\nu-j)}\Big),
\end{array}$$

where

$$\begin{array}{rcl}
h_r(x) & = & 2\pi\cos(2\pi x) - r_{n_h}(x)\sin(2\pi x), \\
h_i(x) & = & 2\pi\sin(2\pi x) - r_{n_h}(x)\big(1-\cos(2\pi x)\big), \\
r_{n_h}(x) & = & \displaystyle\sum_{l=-n_h}^{n_h}\frac{1}{x+l} = \frac{\psi'_{n_h}(x)}{\psi_{n_h}(x)}.
\end{array}$$

Proof: We have

$$
\begin{aligned}
\overline{\mathcal{C}}_\nu^{n_h}(j) &= \mathcal{C}^{n_h}_{\cos(2\pi\nu t/T),T}(j) \overset{(26)}{=} 2\,\mathrm{Re}\,\phi^{n_h}_{\cos(2\pi\nu t/T),T}(j/T) \\
&= 2\,\mathrm{Re}\,\phi^{n_h}_{(e^{i2\pi\nu t/T}+e^{i2\pi(-\nu)t/T})/2,T}(j/T) \\
&= \mathrm{Re}\,\phi^{n_h}_{e^{i2\pi\nu t/T},T}(j/T) + \mathrm{Re}\,\phi^{n_h}_{e^{i2\pi(-\nu)t/T},T}(j/T), \\
\widetilde{\mathcal{C}}_\nu^{n_h}(j) &= \mathrm{Im}\,\phi^{n_h}_{e^{i2\pi\nu t/T},T}(j/T) - \mathrm{Im}\,\phi^{n_h}_{e^{i2\pi(-\nu)t/T},T}(j/T), \\
\overline{\mathcal{S}}_\nu^{n_h}(j) &= -\mathrm{Im}\,\phi^{n_h}_{e^{i2\pi\nu t/T},T}(j/T) - \mathrm{Im}\,\phi^{n_h}_{e^{i2\pi(-\nu)t/T},T}(j/T), \\
\widetilde{\mathcal{S}}_\nu^{n_h}(j) &= \mathrm{Re}\,\phi^{n_h}_{e^{i2\pi\nu t/T},T}(j/T) - \mathrm{Re}\,\phi^{n_h}_{e^{i2\pi(-\nu)t/T},T}(j/T).
\end{aligned}
$$

Then, the lemma follows from (9) and

$$
\frac{d}{d\nu}\phi^{n_h}_{e^{i2\pi\nu t/T},T}(j/T) = \frac{(-1)^{n_h}(n_h!)^2}{2\pi\psi_{n_h}(\nu-j)}\Big(2\pi e^{i2\pi(\nu-j)} - i(1-e^{i2\pi(\nu-j)})\sum_{l=-n_h}^{n_h}\frac{1}{\nu-j+l}\Big).
$$

□

In order to bound the error due to the approximation of the DFT by the TCFT, we need the following lemmas.

Lemma 5.2 *(Discrete Poisson summation formula) If $n_h \geq 1$, we have*

$$
F^{n_h}_{f,T,N}(j) = \sum_{l=-\infty}^{\infty}\phi^{n_h}_{f,T}\Big(\frac{j+lN}{T}\Big).
$$

In particular, $\overline{c}^{n_h}_{\nu,N}(j) = \sum_{l=-\infty}^{\infty}\overline{c}^{n_h}_\nu(j+lN)$, and analogous identities hold for $\widetilde{c}^{n_h}_{\nu,N}(j)$, $\overline{s}^{n_h}_{\nu,N}(j)$, $\widetilde{s}^{n_h}_{\nu,N}(j)$, and their derivatives with respect to ν.

Proof: This is a known result (see, for instance, [4]). We give a proof here for completeness, and also to clarify the need for the hypothesis $n_h \geq 1$.

We first note that, by definition of the TCFT, the Fourier expansion of $H^{n_h}_T(t)f(t)$ with respect to the interval $[0,T]$ is

$$
\sum_{k=-\infty}^{\infty}\phi^{n_h}_{f,T}\big(\frac{k}{T}\big)e^{\frac{i2\pi kt}{T}}.
$$

The function $H^{n_h}_T(t)f(t)$ coincides with its Fourier expansion for all $t \in [0,T]$ because, since $n_h \geq 1$, we have $H^{n_h}_T(0)f(0) = H^{n_h}_T(T)f(T) = 0$.

Then, using the definition (6) of the complex DFT and the above Fourier expansion,

$$
\begin{aligned}
F^{n_h}_{f,T,N}(j) &= \frac{1}{N}\sum_{l=0}^{N-1}\Big(\sum_{k=-\infty}^{\infty}\phi^{n_h}_{f,T}\big(\frac{k}{T}\big)e^{\frac{i2\pi k}{T}l\frac{T}{N}}\Big)e^{-\frac{i2\pi j}{T}l\frac{T}{N}} \\
&= \frac{1}{N}\sum_{k=-\infty}^{\infty}\phi^{n_h}_{f,T}\big(\frac{k}{T}\big)\sum_{l=0}^{N-1}e^{\frac{i2\pi(k-j)l}{N}},
\end{aligned}
$$

and the lemma follows from the fact that the inner sum above is equal to N if $k-j$ is an integer multiple of N and zero otherwise. □

Lemma 5.3 *For $|x| \geq n_h + 2$ we have*

$$
\begin{aligned}
|r_{n_h}(x)| &\leq \ln(|x|+n_h) - \ln(|x|-n_h-1), \\
|h_r(x)|, |h_i(x)| &\leq 2\pi + 2\big(\ln(|x|+n_h) - \ln(|x|-n_h-1)\big).
\end{aligned}
$$

Proof: For the first inequality, we have

$$|r_{n_h}(x)| = \sum_{l=-n_h}^{n_h} \frac{1}{|x|+l} \leq \int_{|x|-n_h}^{|x|+n_h+1} \frac{1}{z-1} dz = \ln(|x|+n_h) - \ln(|x|-n_h-1).$$

The bounds for $|h_r(x)|, |h_i(x)|$ follow from this one. □

Lemma 5.4 *Assume $n_h \geq 1$. For $j \geq 0$, $N - j - |\nu| - n_h > 0$, we have*

$$|F^{n_h}_{e^{i2\pi\nu t/T},T,N}(j) - \phi^{n_h}_{e^{i2\pi\nu t/T},T,N}(\frac{j}{T})| \leq \frac{2(n_h!)^2(1+\frac{1}{2n_h})}{\pi(N-j-|\nu|-n_h)^{1+2n_h}},$$

for $j, \nu \geq 0$, $N - j - \nu - n_h > 0$,

$$|\widetilde{\overline{cs}}^{n_h}_{\nu,N}(j) - \widetilde{\overline{\mathcal{CS}}}^{n_h}_{\nu}(j)| \leq \frac{4(n_h!)^2(1+\frac{1}{2n_h})}{\pi(N-j-\nu-n_h)^{1+2n_h}},$$

and for $j, \nu \geq 0$, $N - j - \nu - n_h \geq 2$,

$$|\partial\widetilde{\overline{cs}}^{n_h}_{\nu,N}(j) - \partial\widetilde{\overline{\mathcal{CS}}}^{n_h}_{\nu}(j)| \leq \frac{4(n_h!)^2(1+\frac{1}{2n_h})\big(\pi + \ln(N-j-\nu+n_h) - \ln(N-j-\nu-n_h-1)\big)}{\pi(N-j-\nu-n_h)^{1+2n_h}}.$$

In the previous expressions, $\widetilde{\overline{cs}}$ denotes one of $\overline{c}$, $\widetilde{c}$, $\overline{s}$, $\widetilde{s}$, and $\widetilde{\overline{\mathcal{CS}}}$ denotes one of $\overline{\mathcal{C}}$, $\widetilde{\mathcal{C}}$, $\overline{\mathcal{S}}$, $\widetilde{\mathcal{S}}$.

Proof: For the first inequality, using the Discrete Poisson summation formula (Lemma 5.2),

$$\begin{aligned}
|F^{n_h}_{e^{i2\pi\nu t/T},T,N}(j) - \phi^{n_h}_{e^{i2\pi\frac{\nu}{T}t},T}(\frac{j}{T})| &\leq \sum_{l=1}^{\infty}\Big(|\phi^{n_h}_{e^{i2\pi\frac{\nu}{T}t},T}(\frac{j+lN}{T})| + |\phi^{n_h}_{e^{i2\pi\frac{\nu}{T}t},T}(\frac{j-lN}{T})|\Big) \\
&\stackrel{(9)}{\leq} \sum_{l=1}^{\infty}\Big(\frac{(n_h!)^2}{\pi\psi_{n_h}(|\nu-j-lN|)} + \frac{(n_h!)^2}{\pi\psi_{n_h}(|\nu-j+lN|)}\Big).
\end{aligned}$$

Now, if $N - j - |\nu| > n_h$, we have $|\nu - j \pm lN| \geq |j \pm lN| - |\nu| \geq lN - j - |\nu|$, and we can bound the previous series by

$$\begin{aligned}
&\sum_{l=1}^{\infty} \frac{2(n_h!)^2}{\pi(lN-j-|\nu|-n_h)^{1+2n_h}} \\
&\qquad \leq \frac{2(n_h)^2}{N\pi}\Big(\frac{N}{(N-j-|\nu|-n_h)^{1+2n_h}} + \int_{2N-j-|\nu|-n_h}^{\infty} \frac{1}{(y-N)^{1+2n_h}} dy\Big) \\
&\qquad \leq \frac{2(n_h)^2}{N\pi}\Big(\frac{N}{(N-j-|\nu|-n_h)^{1+2n_h}} + \frac{1/(2n_h)}{(N-j-|\nu|-n_h)^{2n_h}}\Big) \\
&\qquad \leq \frac{2(n_h!)^2(1+\frac{1}{2n_h})}{\pi(N-j-|\nu|-n_h)^{1+2n_h}}.
\end{aligned}$$

Regarding to the other two inequalities, if we take into account that

$$\begin{aligned}
|\widetilde{\overline{\mathcal{CS}}}^{n_h}_{\nu}(j)| &\leq \frac{2(n_h!)^2}{\pi\psi_{n_h}(|\nu-j|)}, \\
|\partial\widetilde{\overline{\mathcal{CS}}}^{n_h}_{\nu}(j)| &\leq \frac{2(n_h!)^2\big(\pi + \ln(|\nu-j|+n_h) - \ln(|\nu-j|-n_h-1)\big)}{\pi\psi_{n_h}(|\nu-j|)},
\end{aligned}$$

we can easily adapt the previous sequence of inequalities to both cases. Note that, for the second inequality above, we need the hypothesis $N - j - \nu - n_h \geq 2$ in order to apply Lemma 5.3. □

In order to bound $\|Dg(y)^{-1}\|$, we will further simplify $\overline{\mathcal{C}}^{n_h}_{\nu}(j)$, $\widetilde{\mathcal{C}}^{n_h}_{\nu}(j)$, etc., by eliminating the second term in the sums given by Lemma 5.1. For this we introduce $\overline{\mathfrak{c}}$, $\widetilde{\mathfrak{c}}$, …, according to the following

Definition 5.1 *We define*

$$\begin{aligned}
\overline{\mathfrak{c}}_\nu^{n_h}(j) &= \frac{(-1)^{n_h}(n_h!)^2}{2\pi}\cdot\frac{\sin\big(2\pi(\nu-j)\big)}{\psi_{n_h}(\nu-j)}, & \overline{\mathfrak{s}}_\nu^{n_h}(j) &= -\widetilde{\mathfrak{c}}_\nu^{n_h}(j),\\
\widetilde{\mathfrak{c}}_\nu^{n_h}(j) &= \frac{(-1)^{n_h}(n_h!)^2}{2\pi}\cdot\frac{1-\cos\big(2\pi(\nu-j)\big)}{\psi_{n_h}(\nu-j)}, & \widetilde{\mathfrak{s}}_\nu^{n_h}(j) &= \overline{\mathfrak{c}}_\nu^{n_h}(j),\\
\partial\overline{\mathfrak{c}}_\nu^{n_h}(j) &= \frac{(-1)^{n_h}(n_h!)^2}{2\pi}\cdot\frac{h_r(\nu-j)}{\psi_{n_h}(\nu-j)}, & \partial\overline{\mathfrak{s}}_\nu^{n_h}(j) &= -\partial\widetilde{\mathfrak{c}}_\nu^{n_h}(j),\\
\partial\widetilde{\mathfrak{c}}_\nu^{n_h}(j) &= \frac{(-1)^{n_h}(n_h!)^2}{2\pi}\cdot\frac{h_i(\nu-j)}{\psi_{n_h}(\nu-j)}, & \partial\widetilde{\mathfrak{s}}_\nu^{n_h}(j) &= \partial\overline{\mathfrak{c}}_\nu^{n_h}(j).
\end{aligned}$$

In the following lemma, we bound the error after this simplification.

Lemma 5.5 *If* $|\nu+j|>n_h+2$, *we have*

$$|\partial\overline{\mathfrak{c}}_\nu^{n_h}(j)-\partial\overline{\mathcal{C}}_\nu^{n_h}(j)|\le\frac{(n_h!)^2\big(\pi+\ln(|-\nu-j|+n_h)-\ln(|-\nu-j|-n_h-1)\big)}{\pi(|-\nu-j|-n_h)^{1+2n_h}},$$

and the same bound holds for $|\partial\widetilde{\mathfrak{c}}_\nu^{n_h}(j)-\partial\widetilde{\mathcal{C}}_\nu^{n_h}(j)|$, $|\partial\overline{\mathfrak{s}}_\nu^{n_h}(j)-\partial\overline{\mathcal{S}}_\nu^{n_h}(j)|$, $|\partial\widetilde{\mathfrak{s}}_\nu^{n_h}(j)-\partial\widetilde{\mathcal{S}}_\nu^{n_h}(j)|$. *We also have*

$$|\overline{\mathfrak{c}}_\nu^{n_h}(j)-\overline{\mathcal{C}}_\nu^{n_h}(j)|\le\frac{(n_h!)^2}{\pi(|-\nu-j|-n_h)^{1+2n_h}},$$

and the same bound holds for $|\widetilde{\mathfrak{c}}_\nu^{n_h}(j)-\widetilde{\mathcal{C}}_\nu^{n_h}(j)|$, $|\overline{\mathfrak{s}}_\nu^{n_h}(j)-\overline{\mathcal{S}}_\nu^{n_h}(j)|$, $|\widetilde{\mathfrak{s}}_\nu^{n_h}(j)-\widetilde{\mathcal{S}}_\nu^{n_h}(j)|$.

Proof: It is a direct application of Definition 5.1 and Lemma 5.3. □

5.1.1 Error estimation for known frequencies

If we assume in (25) that $j_i\ge n_h+1$ for $i=1\div N_f$, then $c_1^{n_h}(j_i)=0$ for $i=1\div N_f$ and the first equation of system (25) is uncoupled with the other ones. Therefore, we can write $Dg(y)$ as

$$M=\begin{pmatrix}2 & B_{0,1} & \dots & B_{0,N_f}\\ 0 & B_{1,1} & \dots & B_{1,N_f}\\ \vdots & \vdots & \ddots & \vdots\\ 0 & B_{N_f,1} & \dots & B_{N_f,N_f}\end{pmatrix},$$

where $B_{0,l}=u_l$ are 1×2 blocks, being u_l as defined in (16), and $B_{i,l}$, $i,l=1\div N_f$, are 2×2 blocks defined as in (16). Let us split M in its block–diagonal and block–off–diagonal parts, that is $M=M_D+M_O$, being

$$M_D=\begin{pmatrix}2 & 0 & \dots & 0\\ 0 & B_{1,1} & \dots & 0\\ \vdots & \vdots & \ddots & \vdots\\ 0 & 0 & \dots & B_{N_f,N_f}\end{pmatrix},\quad M_O=\begin{pmatrix}0 & B_{0,1} & \dots & B_{0,N_f}\\ 0 & 0 & \dots & B_{1,N_f}\\ \vdots & \vdots & \ddots & \vdots\\ 0 & B_{N_f,1} & \dots & 0\end{pmatrix}.$$

From Definition 5.1 and lemmas 5.5 and 5.4, under suitable hypothesis, $\overline{cs}_{\nu,N}^{n_h}(j)$ and $\widetilde{cs}_{\nu,N}^{n_h}(j)$ decrease as ν goes away from j, and therefore M is close to its diagonal part. What we will do is to obtain bounds for $\|M_D^{-1}\|$ and $\|M_O\|$ and then use them to bound $\|M^{-1}\|$ using the following

Lemma 5.6 *If M and ΔM are $n\times n$ matrices satisfying that M is invertible and* $\|M^{-1}\|\|\Delta M\|<1$, *then $M+\Delta M$ is inversible and satisfies*

$$\|(M+\Delta M)^{-1}\|\le\frac{\|M^{-1}\|}{1-\|M^{-1}\|\|\Delta M\|}$$

Proof: See [24], p. 188. □

To simplify notation, we introduce the following

Definition 5.2 *We will denote by $\mathcal{M}$, $\mathcal{M}_D$, $\mathcal{M}_O$ and $\mathcal{B}_{i,l}$ the equivalents of M, M_D, M_O and $B_{i,l}$, respectively, but replacing $\overline{c}_\nu^{n_h}$, $\widetilde{c}_\nu^{n_h}$, etc. by $\overline{\mathcal{C}}_\nu^{n_h}$, $\widetilde{\mathcal{C}}_\nu^{n_h}$, etc. That is, by replacing the DFT by the TCFT. We will also denote by $\mathfrak{M}$, $\mathfrak{M}_D$, $\mathfrak{M}_O$ and $\mathfrak{B}_{i,l}$ the equivalents of M, M_D, M_O and $B_{i,l}$, respectively, but replacing $\overline{c}_\nu^{n_h}$, $\widetilde{c}_\nu^{n_h}$, etc. by $\overline{\mathfrak{c}}_\nu^{n_h}$, $\widetilde{\mathfrak{c}}_\nu^{n_h}$, etc. In this way, for instance,*

$$\mathfrak{B}_{i,l} = \begin{pmatrix} \overline{\mathfrak{c}}_{\nu_l}^{n_h}(j_i) & \widetilde{\mathfrak{c}}_{\nu_l}^{n_h}(j_i) \\ \overline{\mathfrak{s}}_{\nu_l}^{n_h}(j_i) & \widetilde{\mathfrak{s}}_{\nu_l}^{n_h}(j_i) \end{pmatrix}$$

In the following proposition, we give bounds for $\|\mathfrak{M}_D^{-1}\|$ and $\|\mathfrak{M}_O\|$.

Proposition 5.1 *If $\frac{TD}{(2r_0-2)^\tau} > \frac{1}{2} + n_h$, where D, τ are given by (21) and r_0 is given by (23), then*

$$\|\mathfrak{M}_D^{-1}\| \leq \frac{5}{3}, \qquad \|\mathfrak{M}_O\| \leq \frac{\sqrt{2}N_f(n_h!)^2}{\pi\left(\frac{TD}{(2r_0-1)^\tau} - \frac{1}{2} - n_h\right)^{1+2n_h}}.$$

Proof: From the definitions of $\mathfrak{M}_D$ and $\mathfrak{M}_O$, we have

$$\|\mathfrak{M}_D^{-1}\| \leq \max\left(\max_{i=1,\ldots,N_f} \|(\mathfrak{B}_{i,i})^{-1}\|, \frac{1}{2}\right), \qquad \|\mathfrak{M}_O\| \leq \max_{i=0,\ldots,N_f} \sum_{l=1}^{N_f} \|\mathfrak{B}_{i,l}\| \tag{27}$$

Denoting $\rho_{i,l} = \nu_l - j_i$ and using the trigonometric identities $\sin(2\varepsilon)/2 = \sin(\varepsilon)\cos(\varepsilon)$, $(1-\cos(2\varepsilon))/2 = \sin^2(\varepsilon)$, we can write

$$\mathfrak{B}_{i,l} = \frac{(-1)^{n_h}(n_h!)^2 \sin(\pi\rho_{i,l})}{\pi\psi_{n_h}(\rho_{i,l})} \begin{pmatrix} \cos(\pi\rho_{i,l}) & \sin(\pi\rho_{i,l}) \\ -\sin(\pi\rho_{i,l}) & \cos(\pi\rho_{i,l}) \end{pmatrix}.$$

Therefore

$$(\mathfrak{B}_{i,l})^{-1} = \frac{\pi\psi_{n_h}(\rho_{i,l})}{(-1)^{n_h}(n_h!)^2 \sin(\pi\rho_{i,l})} \begin{pmatrix} \cos(\pi\rho_{i,l}) & -\sin(\pi\rho_{i,l}) \\ \sin(\pi\rho_{i,l}) & \cos(\pi\rho_{i,l}) \end{pmatrix}$$

and

$$\begin{aligned} \|\mathfrak{B}_{i,l}\| &= \left|\frac{(n_h!)^2 \sin(\pi\rho_{i,l})}{\pi\psi_{n_h}(\rho_{i,l})}\right| \big(|\cos(\pi\rho_{i,l})| + |\sin(\pi\rho_{i,l})|\big), \\ \|(\mathfrak{B}_{i,i})^{-1}\| &= \left|\frac{\pi\psi_{n_h}(\rho_{i,i})}{(n_h!)^2 \sin(\pi\rho_{i,i})}\right| \big(|\cos(\pi\rho_{i,i})| + |\sin(\pi\rho_{i,i})|\big). \end{aligned} \tag{28}$$

Let us define

$$F_1(\rho_{i,i}) = \left|\frac{\pi\psi_{n_h}(\rho_{i,i})}{(n_h!)^2 \sin(\pi\rho_{i,i})}\right|$$

Recalling that the j_i, $i = 1 \div N_f$, were chosen such that $|\nu_i - j_i| < 0.5$, we only have to bound (28) for $-0.5 \leq \rho_{i,i} \leq 0.5$. From the definition (10) of ψ_{n_h}, we can write $F_1(\rho_{i,i})$ as

$$F_1(\rho_{i,i}) = \left|\frac{\pi\rho_{i,i}}{\sin(\pi\rho_{i,i})}\right| \prod_{l=1}^{n_h} \frac{l^2 - \rho_{i,i}^2}{l^2},$$

and it is readily checked that if $-0.5 \leq \rho_{i,i} \leq 0.5$ then $F_1(\rho_{i,i})$ decreases as $n_h \to \infty$. The limit is a positive value because of the Weierstrass factorization formula for the sine (see, for instance, [25]):

$$\sin(\pi z) = \pi z \prod_{n=1}^{\infty}\left(1 - \frac{z^2}{n^2}\right) \qquad \text{for } z \in \mathbb{C}.$$

Therefore, $\mathfrak{B}_{i,i}$ is invertible and we can bound $\|(\mathfrak{B}_{i,i})^{-1}\|$ for $n_h \in \mathbb{N}$ by the bound for $n_h = 0$, which is

$$\|(\mathfrak{B}_{i,i})^{-1}\| \leq \left|\frac{\pi\rho_{i,i}}{\sin(\pi\rho_{i,i})}\right| \big(|\cos(\pi\rho_{i,i})| + |\sin(\pi\rho_{i,i})|\big) \leq \frac{5}{3} \qquad \text{for } -0.5 \leq \rho_{i,i} \leq 0.5. \tag{29}$$

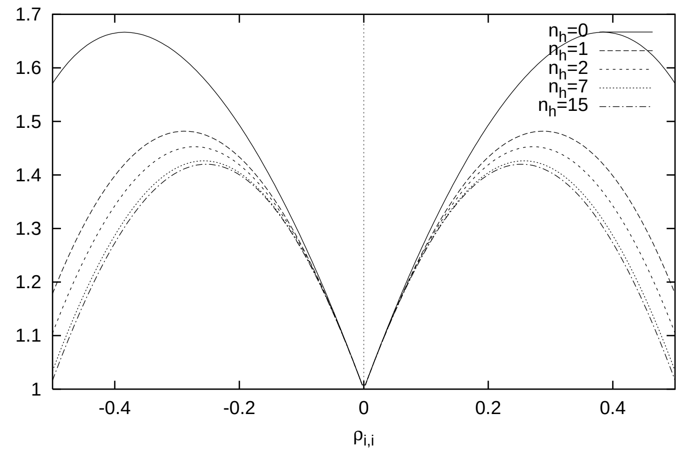

Figure 4: Graph of $\|\mathfrak{B}_{i,i}^{-1}\|_\infty$ for $-0.5 \le \rho_{i,i} \le 0.5$ and $n_h = 0, 1, 3, 5, 15$.

For the actual behavior of $\|\mathfrak{B}_{i,i}^{-1}\|$ in terms of $\rho_{i,i}$, see Fig. 4.

Concerning $\|\mathfrak{B}_{i,l}\|$, for $\rho_{i,l} \in \mathbb{R}$ and $n_h \in \mathbb{N}$, we have

$$\|\mathfrak{B}_{i,l}\| \le \frac{(n_h!)^2}{\pi|\psi_{n_h}(\rho_{i,l})|} \max_{x\in\mathbb{R}}\big(|\cos(\pi x)| + |\sin(\pi x)|\big) = \frac{\sqrt{2}(n_h!)^2}{\pi|\psi_{n_h}(\rho_{i,l})|}. \tag{30}$$

If we define $j_0 = 0$, the previous bound is also valid for $\|\mathfrak{B}_{0,l}\|$. For the actual behavior of $\|\mathfrak{B}_{i,l}\|$ in terms of $\rho_{i,l}$, see Fig. 5.

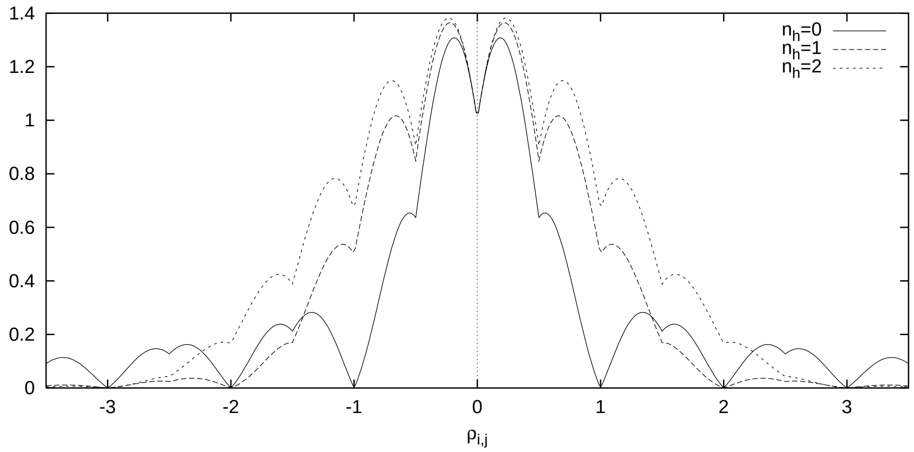

Figure 5: Graph of $\|\mathfrak{B}_{i,l}(\rho_{i,l})\|_\infty$ for $n_h = 0, 1, 2$.

Now from (27), (29) and (30),

$$\|\mathfrak{M}_D^{-1}\| \le 5/3, \qquad \|\mathfrak{M}_O\| \le \max_{i=0\div N_f} \sum_{l=1}^{N_f} \frac{\sqrt{2}(n_h!)^2}{\pi|\psi_{n_h}(\nu_l - j_i)|}.$$

Since by definition $|\nu_i - j_i| \le 1/2$, we have $|\nu_l - j_i| \ge |\nu_l - \nu_i| - 1/2 = T|(k_l - k_i)\omega| - 1/2$. Using the Diophantine condition (21),

$$T|(k_l - k_i)\omega| - \frac{1}{2} \ge \frac{TD}{|k_l - k_i|^\tau} - \frac{1}{2} \ge \frac{TD}{(2r_0 - 2)^\tau} - \frac{1}{2}.$$

This bound is also valid for $i = 0$:

$$|\nu_l - j_0| = |\nu_l| = T|k_l\omega| \ge \frac{TD}{(r_0 - 1)^\tau} \ge \frac{TD}{(2r_0 - 2)^\tau} - \frac{1}{2}.$$

Now since by hypothesis $\frac{TD}{(2r_0-2)^\tau} > \frac{1}{2} + n_h$, we get

$$\|\mathfrak{M}_O\| \leq \frac{\sqrt{2}N_f(n_h!)^2}{\pi\left(\frac{TD}{(2r_0-2)^\tau} - \frac{1}{2} - n_h\right)^{1+2n_h}},$$

and this ends the proposition. $\square$

From the bounds of $\|\mathfrak{M}_D^{-1}\|$ and $\|\mathfrak{M}_O\|$ and Lemma 5.6, we can get a bound for $\|M^{-1}\|$. For that, we need bounds of $\|\mathcal{M}_D - \mathfrak{M}_D\|$, $\|M_D - \mathcal{M}_D\|$, $\|\mathcal{M}_O - \mathfrak{M}_O\|$ and $\|M_O - \mathcal{M}_O\|$, which are given in the following lemmas.

Lemma 5.7 *If $[\nu_{min}] > n_h$, where $\nu_{min} = \min\{\nu_1, \dots, \nu_{N_f}\}$ and $[\ ]$ denotes integer part, we have*

$$\|\mathcal{M}_D - \mathfrak{M}_D\| \leq \frac{2(n_h!)^2}{\pi\left(2[\nu_{min}] - n_h\right)^{1+2n_h}}, \qquad \|\mathcal{M}_O - \mathfrak{M}_O\| \leq \frac{2N_f(n_h!)^2}{\pi\left([\nu_{min}] - n_h\right)^{1+2n_h}}$$

Proof: We have

$$\begin{aligned}\|\mathcal{M}_D - \mathfrak{M}_D\| &\leq \max_{i=1\div N_f} \|\mathcal{B}_{i,i} - \mathfrak{B}_{i,i}\| \\ &= \max\left(|\overline{\mathcal{CS}}^{n_h}_{\nu_i}(j_i) - \overline{\mathfrak{cs}}^{n_h}_{\nu_i}(j_i)| + |\widetilde{\mathcal{CS}}^{n_h}_{\nu_i}(j_i) - \widetilde{\mathfrak{cs}}^{n_h}_{\nu_i}(j_i)|\right),\end{aligned}$$

where either $\mathcal{CS} = \mathcal{C}$ and $\mathfrak{cs} = \mathfrak{c}$ or $\mathcal{CS} = \mathcal{S}$ and $\mathfrak{cs} = \mathfrak{s}$. Now, using Lemma 5.5 and the hypothesis, we get the first inequality:

$$\|\mathcal{M}_D - \mathfrak{M}_D\| \leq \max_{i=1\div N_f} \frac{2(n_h!)^2}{\pi(|-\nu_i - j_i| - n_h)^{1+2n_h}} \leq \frac{2(n_h!)^2}{\pi(2[\nu_{min}] - n_h)^{1+2n_h}}.$$

As for the second inequality,

$$\|\mathcal{M}_O - \mathfrak{M}_O\| \leq \max_{i=0\div N_f} \sum_{\substack{l=1 \\ l\neq i}}^{N_f} \left(|\overline{\mathcal{CS}}^{n_h}_{\nu_l}(j_i) - \overline{\mathfrak{cs}}^{n_h}_{\nu_l}(j_i)| + |\widetilde{\mathcal{CS}}^{n_h}_{\nu_l}(j_i) + \widetilde{\mathfrak{cs}}^{n_h}_{\nu_l}(j_i)|\right),$$

where we denote $j_0 = 0$. Using Lemma 5.5 again,

$$\|\mathcal{M}_O - \mathfrak{M}_O\| \leq \max_{i=0\div N_f} \sum_{l=1}^{N_f} \frac{2(n_h!)^2}{\pi\psi_{n_h}(-\nu_l - j_i)} \leq \frac{2N_f(n_h!)^2}{\pi([\nu_{min}] - n_h)^{1+2n_h}}.$$

We lose the factor 2 in front of $[\nu_{min}]$ with respect to the bound of $\|\mathcal{M}_D - \mathfrak{M}_D\|$ because we have to consider the first row ($i = 0$). $\square$

Lemma 5.8 *Assume that $N - T(2r_0 - 2)\|\omega\|_\infty - \frac{1}{2} - n_h > 0$, where r_0 is given by (23). Then*

$$\begin{aligned}\|M_D - \mathcal{M}_D\| &\leq \frac{8(n_h!)^2(1 + \frac{1}{2n_h})}{\pi\left(N - T(2r_0-2)\|\omega\|_\infty - \frac{1}{2} - n_h\right)^{1+2n_h}}, \\ \|M_O - \mathcal{M}_O\| &\leq \frac{8(n_h!)^2 N_f(1 + \frac{1}{2n_h})}{\pi\left(N - T(2r_0-2)\|\omega\|_\infty - \frac{1}{2} - n_h\right)^{1+2n_h}}.\end{aligned}$$

Proof: Using Lemma 5.4,

$$\|M_D - \mathcal{M}_D\| \leq \max_{i=1\div N_f} \|B_{i,i} - \mathcal{B}_{i,i}\| \leq \max_{i=1\div N_f} \frac{8(n_h!)^2\left(1 + \frac{1}{2n_h}\right)}{\pi\left(N - j_i - \nu_i - n_h\right)^{1+2n_h}},$$

and, since by definition $|j_i - \nu_i| < 1/2$ and as $\nu_i = Tk_i\omega$ with $|k_i| \leq r_0 - 1$, we have that $j_i + \nu_i \leq 2\nu_i + 1/2 \leq T(2r_0 - 2)\|\omega\|_\infty + 1/2$, and the first inequality follows immediately. A similar argument proves the second inequality. $\square$

The bound for $\|M^{-1}\|$ that follows from the previous results will be given in Theorem 5.1.

5.1.2 General case

As in the case of known frequencies, we assume in (24) that $j_i > n_h$ for $i = 1 \div N_f$ so the first equation of system (24) is uncoupled with the other ones and $M = Dg(y)$ can be written as

$$M = \begin{pmatrix} 2 & B_{0,1} & \dots & B_{0,N_f} \\ 0 & B_{1,1} & \dots & B_{1,N_f} \\ \vdots & \vdots & \ddots & \vdots \\ 0 & B_{N_f,1} & \dots & B_{N_f,N_f} \end{pmatrix}$$

where $B_{0,l} = v_l$ are 1×3 blocks, being v_l as defined in (19), and $B_{i,l}$, $i, l = 1 \div N_f$, are 3×3 blocks defined as in (19). We split M in its block–diagonal and block–off–diagonal parts,

$$M_D = \begin{pmatrix} 2 & 0 & \dots & 0 \\ 0 & B_{1,1} & \dots & 0 \\ \vdots & \vdots & \ddots & \vdots \\ 0 & 0 & \dots & B_{N_f,N_f} \end{pmatrix}, \quad M_O = \begin{pmatrix} 0 & B_{0,1} & \dots & B_{0,N_f} \\ 0 & 0 & \dots & B_{1,N_f} \\ \vdots & \vdots & \ddots & \vdots \\ 0 & B_{N_f,1} & \dots & 0 \end{pmatrix}.$$

As before, we will obtain bounds for $\|M_D^{-1}\|$ and $\|M_O\|$ and then use them to bound $\|M\|$ through Lemma 5.6.

In order to obtain bounds for $\|M_D\|$, we first state the following

Definition 5.3 *We will denote by $\mathcal{M}$, $\mathcal{M}_D$, $\mathcal{M}_O$ and $\mathcal{B}_{i,l}$ the equivalents of M, M_D, M_O and $B_{i,l}$, respectively, but replacing $\overline{c}_\nu^{n_h}$, $\widetilde{c}_\nu^{n_h}$, etc. by $\overline{C}_\nu^{n_h}$, $\widetilde{C}_\nu^{n_h}$, etc. That is, by replacing the DFT by the TCFT. We will also denote by $\mathfrak{M}$, $\mathfrak{M}_D$, $\mathfrak{M}_O$ and $\mathfrak{B}_{i,l}$ the equivalents of M, M_D, M_O and $B_{i,l}$, respectively, but replacing $\overline{c}_\nu^{n_h}$, $\widetilde{c}_\nu^{n_h}$, etc. by $\overline{\mathfrak{c}}_\nu^{n_h}$, $\widetilde{\mathfrak{c}}_\nu^{n_h}$, etc. For instance,*

$$\mathfrak{B}_{i,i} = \begin{pmatrix} A_i^c \partial\overline{\mathfrak{c}}_{\nu_i,N}^{n_h}(j_i) + A_i^s \partial\widetilde{\mathfrak{c}}_{\nu_i,N}^{n_h}(j_i) & \overline{\mathfrak{c}}_{\nu_i,N}^{n_h}(j_i) & \widetilde{\mathfrak{c}}_{\nu_i,N}^{n_h}(j_i) \\ A_i^c \partial\overline{\mathfrak{s}}_{\nu_i,N}^{n_h}(j_i) + A_i^s \partial\widetilde{\mathfrak{s}}_{\nu_i,N}^{n_h}(j_i) & \overline{\mathfrak{s}}_{\nu_i,N}^{n_h}(j_i) & \widetilde{\mathfrak{s}}_{\nu_i,N}^{n_h}(j_i) \\ A_i^c \partial\overline{\mathfrak{cs}}_{\nu_i,N}^{n_h}(j_i^+) + A_i^s \partial\widetilde{\mathfrak{cs}}_{\nu_i,N}^{n_h}(j_i^+) & \overline{\mathfrak{cs}}_{\nu_i,N}^{n_h}(j_i^+) & \widetilde{\mathfrak{cs}}_{\nu_i,N}^{n_h}(j_i^+) \end{pmatrix},$$

where $\mathfrak{cs}$ denotes either $\mathfrak{c}$ or $\mathfrak{s}$.

In order to invert $\mathfrak{M}_D$, we only have to invert a block $\mathfrak{B}_{i,i}$. The possibility to do that is established by the following

Lemma 5.9 *If $(A_i^s, A_i^c) \neq (0,0)$, $\mathfrak{B}_{i,i}$ is invertible either setting $\mathfrak{cs} = \mathfrak{c}$ or $\mathfrak{cs} = \mathfrak{s}$.*

Proof: Consider the matrix

$$\mathfrak{A} = \begin{pmatrix} \partial\overline{\mathfrak{c}}_{\nu_i}^{n_h}(j_i) & \partial\widetilde{\mathfrak{c}}_{\nu_i}^{n_h}(j_i) & \overline{\mathfrak{c}}_{\nu_i}^{n_h}(j_i) & \widetilde{\mathfrak{c}}_{\nu_i}^{n_h}(j_i) \\ \partial\overline{\mathfrak{s}}_{\nu_i}^{n_h}(j_i) & \partial\widetilde{\mathfrak{s}}_{\nu_i}^{n_h}(j_i) & \overline{\mathfrak{s}}_{\nu_i}^{n_h}(j_i) & \widetilde{\mathfrak{s}}_{\nu_i}^{n_h}(j_i) \\ \partial\overline{\mathfrak{c}}_{\nu_i}^{n_h}(j_i^+) & \partial\widetilde{\mathfrak{c}}_{\nu_i}^{n_h}(j_i^+) & \overline{\mathfrak{c}}_{\nu_i}^{n_h}(j_i^+) & \widetilde{\mathfrak{c}}_{\nu_i}^{n_h}(j_i^+) \\ \partial\overline{\mathfrak{s}}_{\nu_i}^{n_h}(j_i^+) & \partial\widetilde{\mathfrak{s}}_{\nu_i}^{n_h}(j_i^+) & \overline{\mathfrak{s}}_{\nu_i}^{n_h}(j_i^+) & \widetilde{\mathfrak{s}}_{\nu_i}^{n_h}(j_i^+) \end{pmatrix},$$

and denote by $\mathfrak{A}_{l_1,l_2,l_3}^{i_1,i_2,i_3}$ the submatrix of $\mathfrak{A}$ obtained by selecting the rows i_1, i_2, i_3 and the columns l_1, l_2, l_3. Then, the determinant of a block $\mathfrak{B}_{i,i}$ is

$$\det \mathfrak{B}_{i,i} = \begin{cases} A_i^c \det \mathfrak{A}_{1,3,4}^{1,2,3} + A_i^s \det \mathfrak{A}_{2,3,4}^{1,2,3} & \text{if we set } \mathfrak{cs} = \mathfrak{c}, \\ A_i^c \det \mathfrak{A}_{1,3,4}^{1,2,4} + A_i^s \det \mathfrak{A}_{2,3,4}^{1,2,4} & \text{if we set } \mathfrak{cs} = \mathfrak{s}. \end{cases}$$

To see that there exists a choice of $\mathfrak{cs}$ that makes $\det \mathfrak{B}_{i,i} \neq 0$ is equivalent to see that the system

$$\begin{cases} A_i^c \det \mathfrak{A}_{1,3,4}^{1,2,3} + A_i^s \det \mathfrak{A}_{2,3,4}^{1,2,3} = 0 \\ A_i^c \det \mathfrak{A}_{1,3,4}^{1,2,4} + A_i^s \det \mathfrak{A}_{2,3,4}^{1,2,4} = 0 \end{cases},$$

with unknowns A_i^c, A_i^s, has unique solution. That is, that the determinant

$$\det \mathfrak{D} = \begin{vmatrix} \det \mathfrak{A}_{1,3,4}^{1,2,3} & \det \mathfrak{A}_{2,3,4}^{1,2,3} \\ \det \mathfrak{A}_{1,3,4}^{1,2,4} & \det \mathfrak{A}_{2,3,4}^{1,2,4} \end{vmatrix} \tag{31}$$

is different from zero. From Definition 5.1, and since $\nu_i - j_i^+ = \nu_i - j_i - \mathrm{sign}(\nu_i - j_i)$, this determinant only depends on the difference $\varepsilon = \nu_i - j_i$ which, by definition, ranges from $-1/2$ to $1/2$. In order to prove the lemma, we only need to see that the previous determinant is different from zero in this range (see Fig. 6 for the numerical evidence).

In order to simplify the notation, we denote

$$\mathfrak{A} = \begin{pmatrix} a_1 & a_2 & a_3 & a_4 \\ -a_2 & a_1 & -a_4 & a_3 \\ a_5 & a_6 & a_7 & a_8 \\ -a_6 & a_5 & -a_8 & a_7 \end{pmatrix}$$

and

$$A = \mathfrak{A}_{1,3,4}^{1,2,3}, \quad B = \mathfrak{A}_{1,3,4}^{1,2,4}, \quad C = \mathfrak{A}_{2,3,4}^{1,2,3}, \quad D = \mathfrak{A}_{2,3,4}^{1,2,4},$$

so that $\det \mathfrak{D} = \det A \det D - \det B \det C$.

First note that, using $-\big(\varepsilon - \mathrm{sign}(\varepsilon)\big) = -\varepsilon - \mathrm{sign}(-\varepsilon)$ and the fact that $\overline{\mathfrak{c}}_\nu^{n_h}(j)$ and $\widetilde{\mathfrak{c}}_\nu^{n_h}(j)$ are even and odd in ε respectively, we can check that $\det \mathfrak{D}$ is even in ε and therefore we can restrict to $[0, 1/2]$ the range of ε to be considered.

Let $0 < \varepsilon \leq 1/2$ and assume $\det \mathfrak{D} = 0$. We note that $\det A = \det D$ and $\det B = -\det C$, so that $\det \mathfrak{D} = (\det A)^2 + (\det B)^2$ and we have $\det A = \det B = 0$. Expanding through the first column, we get

$$\begin{aligned} \det A &= -a_1(a_3 a_7 + a_4 a_8) + a_2(a_3 a_8 - a_4 a_7) + a_5(a_3^2 + a_4^2) \\ \det B &= a_2(a_3 a_7 + a_4 a_8) + a_1(a_3 a_8 - a_4 a_7) - a_6(a_3^2 + a_4^2) \end{aligned}$$

The $a_3 a_8 - a_4 a_7$ term is readily checked to be zero. We denote $\psi = \psi_{n_h}(\varepsilon)$ and $\psi_m = \psi_{n_h}(\varepsilon - 1)$. We check that $a_3 a_7 + a_4 a_8$ has the same numerator as $a_3^2 + a_4^2$, due to the 1–periodicity in ε of the numerators of $a_1, \ldots, a_8$. The denominators are different: $\psi\psi_m$ for $a_3 a_7 + a_4 a_8$ and ψ^2 for $a_3^2 + a_4^2$. Setting $\det A = \det B = 0$ and simplifying numerators, we get

$$a_1 \psi = a_5 \psi_m, \qquad a_2 \psi = a_6 \psi_m.$$

Now, using the expressions for a_1 and a_5 from Definition 5.1, as well as $a_1\psi = a_5\psi_m$, we obtain $r_{n_h}(\varepsilon) = r_{n_h}(\varepsilon - 1)$, that is $\psi'/\psi = \psi_m'/\psi_m$ (here $'$ denotes derivative), and therefore

$$\frac{d}{d\varepsilon} \frac{\psi_m}{\psi} = \frac{\psi_m' \psi - \psi_m \psi'}{\psi_m^2} = 0. \tag{32}$$

The condition $a_2\psi = a_6\psi_m$ leads to the same conclusion.

But

$$\frac{\psi_m}{\psi} = \frac{\varepsilon - n_h - 1}{\varepsilon + n_h} = 1 - \frac{2n_h + 1}{\varepsilon + n_h},$$

and its derivative with respect to ε is different from zero for $0 < \varepsilon \leq \frac{1}{2}$, which is in contradiction with (32).

For $\varepsilon = 0$, $\det \mathfrak{D}$ is checked to be different from zero using the expressions of Definition 5.1 (it is necessary to compute the limits when $\varepsilon \to 0$). $\square$

Now that we know that a block $\mathfrak{B}_{i,i}$ is invertible, in order to actually invert it we state the following

Definition 5.4 *For $n_h \in \mathbb{N}$, we define G_{n_h} to be an upper bound of*

$$\max_{\substack{\theta \in [0,2\pi] \\ |\nu - j| \leq \frac{1}{2}}} \; \min_{\mathfrak{cs} \in \{\mathfrak{c}, \mathfrak{s}\}} \left\| \begin{pmatrix} (\cos\theta)\partial\overline{\mathfrak{c}}_\nu^{n_h}(j) + (\sin\theta)\partial\widetilde{\mathfrak{c}}_\nu^{n_h}(j) & \overline{\mathfrak{c}}_\nu^{n_h}(j) & \widetilde{\mathfrak{c}}_\nu^{n_h}(j) \\ (\cos\theta)\partial\overline{\mathfrak{s}}_\nu^{n_h}(j) + (\sin\theta)\partial\widetilde{\mathfrak{s}}_\nu^{n_h}(j) & \overline{\mathfrak{s}}_\nu^{n_h}(j) & \widetilde{\mathfrak{s}}_\nu^{n_h}(j) \\ (\cos\theta)\partial\overline{\mathfrak{cs}}_\nu^{n_h}(j^+) + (\sin\theta)\partial\widetilde{\mathfrak{cs}}_\nu^{n_h}(j^+) & \overline{\mathfrak{cs}}_\nu^{n_h}(j^+) & \widetilde{\mathfrak{cs}}_\nu^{n_h}(j^+) \end{pmatrix}^{-1} \right\|.$$

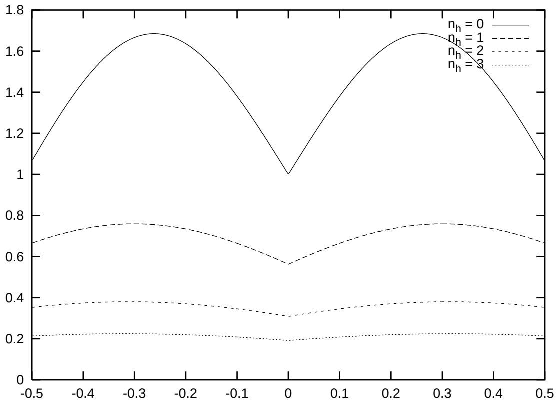

Figure 6: Plot of the determinant (31) for $-1/2 \leq \nu_i - j_i \leq 1/2$ and $n_h = 0, 1, 2, 3$.

n_h	0	1	2	3
G_{n_h}	4.84	8.83	13.3	17.7

Table 1: Some values of the G_{n_h} constants.

In table 1 we give some values of the G_{n_h} constants found numerically. Just for illustration purposes, in figure 7 we display the behavior of

$$\min_{\mathfrak{cs}\in\{\mathfrak{c},\mathfrak{s}\}} \left\| \begin{pmatrix} (\cos\theta)\partial\overline{\mathfrak{c}}_\nu^{n_h}(j) + (\sin\theta)\partial\widetilde{\mathfrak{c}}_\nu^{n_h}(j) & \overline{\mathfrak{c}}_{\nu,N}^{n_h}(j) & \widetilde{\mathfrak{c}}_\nu^{n_h}(j) \\ (\cos\theta)\partial\overline{\mathfrak{s}}_\nu^{n_h}(j) + (\sin\theta)\partial\widetilde{\mathfrak{s}}_\nu^{n_h}(j) & \overline{\mathfrak{s}}_\nu^{n_h}(j) & \widetilde{\mathfrak{s}}_\nu^{n_h}(j) \\ (\cos\theta)\partial\overline{\mathfrak{cs}}_\nu^{n_h}(j^+) + (\sin\theta)\partial\widetilde{\mathfrak{cs}}_\nu^{n_h}(j^+) & \overline{\mathfrak{cs}}_\nu^{n_h}(j^+) & \widetilde{\mathfrak{cs}}_\nu^{n_h}(j^+) \end{pmatrix}^{-1} \right\| \tag{33}$$

in terms of θ and $\nu - j$.

In order to relate the bound of the previous definition to the bound of an actual block $\mathfrak{B}_{i,i}$, we will use the following

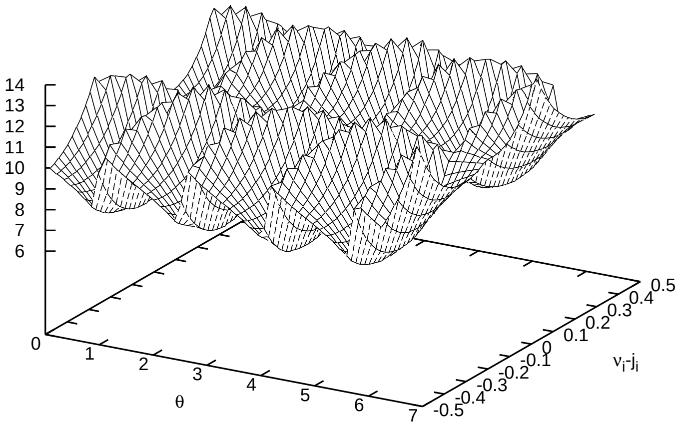

Figure 7: Plot of (33) for $0 \leq \theta \leq 2\pi$, $-1/2 \leq \nu_i - j_i \leq 1/2$ and $n_h = 2$.

Lemma 5.10 *Let K a k–dimensional regular matrix and $\tilde{K}$ the matrix obtained by multiplying the first column of K by a real number $\lambda \neq 0$. Then*

$$||\tilde{K}^{-1}||_\infty \leq \max\{|\lambda|^{-1}, 1\}\, ||K^{-1}||_\infty.$$

Proof: It is enough to remind that $\tilde{K}^{-1}$ is equal to K^{-1} with the first row multiplied by λ^{-1}. $\square$

Let us denote $A_i = \big((A_i^c)^2 + (A_i^s)^2\big)^{1/2}$. Using Definition 5.4 and Lemma 5.10 we have

$$\|(\mathfrak{B}_{i,i})^{-1}\| \leq \max(A_i^{-1}, 1) G_{n_h},$$

and therefore,

$$\|\mathfrak{M}_D^{-1}\| \leq \max(A_{min}^{-1}, 1) G_{n_h},$$

where $A_{min} = \min\{A_1, \ldots, A_{N_f}\}$.

Now we bound the simplified off–diagonal part of M.

Lemma 5.11 *Assume* $\frac{TD}{(2r_0-2)^\tau} > 3 + n_h$. *Then,*

$$\|\mathfrak{M}_O\| \leq \frac{(n_h!)^2\Big[\sqrt{2}(\sum_{l=1}^{N_f} A_l)\Big(\pi + \ln\big(\frac{TD}{(2r_0-2)^\tau} - 1 + n_h\big) - \ln\big(\frac{TD}{(2r_0-2)^\tau} - 2 - n_h\big)\Big) + 2N_f\Big]}{\pi\big(\frac{TD}{(2r_0-2)^\tau} - 1 - n_h\big)^{1+2n_h}}$$

Proof: We first note that, from Lemma 5.3 and Definition 5.1,

$$\begin{aligned} |\overline{\mathfrak{c}}_\nu^{n_h}(j)|, |\widetilde{\mathfrak{c}}_\nu^{n_h}(j)|, |\overline{\mathfrak{s}}_\nu^{n_h}(j)|, |\widetilde{\mathfrak{s}}_\nu^{n_h}(j)| &\leq \frac{(n_h!)^2}{\pi(|\nu-j| - n_h)^{1+2n_h}}, \\ |\partial\overline{\mathfrak{c}}_\nu^{n_h}(j)|, |\partial\widetilde{\mathfrak{c}}_\nu^{n_h}(j)|, |\partial\overline{\mathfrak{s}}_\nu^{n_h}(j)|, |\partial\widetilde{\mathfrak{s}}_\nu^{n_h}(j)| &\leq \\ &\frac{(n_h!)^2\big(\pi + \ln(|\nu-j| + n_h) - \ln(|\nu-j| - n_h - 1)\big)}{\pi(|\nu-j| - n_h)^{1+2n_h}}. \end{aligned}$$

Therefore, using $|A_l^c| + |A_l^s| \leq \sqrt{2}\big((A_l^c)^2 + (A_l^s)^2\big)^{1/2} = \sqrt{2}A_l$,

$$\begin{aligned} \|\mathfrak{B}_{i,l}\| &\leq \max_{\substack{j=j_i, j_i^+ \\ \mathfrak{cs}=\mathfrak{c},\mathfrak{s}}} \Big(|A_i^c||\partial\widetilde{\mathfrak{cs}}_{\nu_i}^{n_h}(j)| + |A_i^s||\partial\widetilde{\mathfrak{cs}}_{\nu_i}^{n_h}(j)| + |\widetilde{\mathfrak{cs}}_{\nu_i}^{n_h}(j)| + |\widetilde{\mathfrak{cs}}_{\nu_i}^{n_h}(j)|\Big) \\ &\leq \max_{j=j_i, j_i^+} \frac{(n_h!)^2\big(\sqrt{2}A_l\big(\pi + \ln(|\nu_l - j| + n_h) - \ln(|\nu_l - j| - n_h - 1)\big) + 2\big)}{\pi(|\nu_l - j| - n_h)^{1+2n_h}}. \end{aligned}$$

Now, for $i, l = 1 \div N_f$ and $j = j_i, j_i^+$ there exists i_j such that $j \in \{[\nu_{i_j}], [\nu_{i_j}] + 1\}$, so $|\nu_{i_j} - j| \leq 1$. As stated at the beginning of this section, we also have that there exists k_{i_j}, with $|k_{i_j}| \leq r_0 - 1$, such that $\nu_{i_j} = Tk_{i_j}\omega$. Then, using the Diophantine condition (21), we obtain

$$\begin{aligned} |\nu_l - j| &\geq |\nu_l - \nu_{i_j}| - |j - \nu_{i_j}| \geq T|(k_l - k_{i_j})\omega| - 1 \geq \frac{TD}{|k_l - k_{i_j}|^\tau} - 1 \\ &\geq \frac{TD}{(2r_0 - 2)^\tau} - 1, \end{aligned}$$

and the lemma follows from

$$\|\mathfrak{M}_O\| \leq \max_{i=0\div N_f} \sum_{l=1}^{N_f} \|\mathfrak{B}_{i,l}\|,$$

where we denote $j_0 = 0$. □

In order to bound $\|M^{-1}\|$ from $\|M_D^{-1}\|$ and $\|M_O^{-1}\|$ by applying Lemma 5.6, we need the bounds of $\|\mathcal{M}_D - \mathfrak{M}_D\|$, $\|M_D - \mathcal{M}_D\|$, $\|\mathcal{M}_O - \mathfrak{M}_O\|$ and $\|M_O - \mathcal{M}_O\|$. We calculate them in the following lemmas.

Lemma 5.12 *Denote* $\nu_{min} = \min\{\nu_1, \ldots, \nu_{N_f}\}$, $A_{max} = \max\{A_0, \ldots, A_{N_f}\}$. *If* $[\nu_{min}] \geq 2 + n_h$, *we have*

$$\begin{aligned} \|\mathfrak{M}_D - \mathcal{M}_D\| &\leq \frac{(n_h!)^2\Big(\sqrt{2}A_{max}\big(\pi + \ln(2[\nu_{min}] + n_h) - \ln(2[\nu_{min}] - n_h - 1)\big) + 2\Big)}{\pi\big(2[\nu_{min}] - n_h\big)^{1+2n_h}}, \\ \|\mathfrak{M}_O - \mathcal{M}_O\| &\leq \frac{(n_h!)^2\Big(\sqrt{2}(\sum_{l=1}^{N_f} A_l)\big(\pi + \ln([\nu_{min}]+n_h) - \ln([\nu_{min}]-n_h-1)\big) + 2N_f\Big)}{\pi\big([\nu_{min}] - n_h\big)^{1+2n_h}}, \end{aligned}$$

Proof: From Definition 5.3 and Lemma 5.5,

$$
\begin{aligned}
\|\mathfrak{B}_{i,l}-\mathcal{B}_{i,l}\| &\leq \max_{j=j_i,j_i^+}\left(\begin{array}{c}|A_l^c||\partial\overline{\mathfrak{cs}}^{n_h}_{\nu_l}(j)-\partial\overline{\mathcal{CS}}^{n_h}_{\nu_l}(j)|+|A_l^s||\partial\widetilde{\mathfrak{cs}}^{n_h}_{\nu_l}(j)-\partial\widetilde{\mathcal{CS}}^{n_h}_{\nu_l}(j)|+\\ |\overline{\mathfrak{cs}}^{n_h}_{\nu_l}(j)-\overline{\mathcal{CS}}^{n_h}_{\nu_l}(j)|+|\widetilde{\mathfrak{cs}}^{n_h}_{\nu_l}(j)-\widetilde{\mathcal{CS}}^{n_h}_{\nu_l}(j)|\end{array}\right)\\
&\leq \frac{(n_h!)^2\Big(\sqrt{2}A_l\big(\ln(|-\nu_l-j|+n_h)-\ln(|-\nu_l-j|-n_h-1)\big)+2\Big)}{\pi(|-\nu_l-j|-n_h)^{1+2n_h}},
\end{aligned}
$$

where either $\mathfrak{cs}=\mathfrak{c}$ and $\mathcal{CS}=\mathcal{C}$ or $\mathfrak{cs}=\mathfrak{s}$ and $\mathcal{CS}=\mathcal{S}$. For the second inequality we have used that

$$|A_l^c|+|A_l^s|\leq\sqrt{2}\big((A_l^c)^2+(A_l^s)^2\big)^{1/2}=\sqrt{2}A_l.$$

Now, the first inequality of the lemma follows from

$$\|\mathfrak{M}_D-\mathcal{M}_D\|\leq\max_{i=1\div N_f}\|\mathfrak{B}_{i,i}-\mathcal{B}_{i,i}\|$$

and the fact that $|-\nu_i-j_i|,|-\nu_i-j_i^+|\geq 2[\nu_{min}]$ for $i=1\div N_f$. The second inequality follows from

$$\|\mathfrak{M}_O-\mathcal{M}_O\|\leq\max_{i=0\div N_f}\sum_{\substack{l=1\\ l\neq i}}^{N_f}\|\mathfrak{B}_{i,l}-\mathcal{B}_{i,l}\|$$

and the fact that $|-\nu_l-j_i|,|-\nu_l-j_i^+|\geq[\nu_{min}]$ for $i=0\div N_f, l=1\div N_f$ (we denote $j_0=j_0^+=0$). $\square$

Lemma 5.13 *Assume* $N-T(2r_0-2)\|\omega\|_\infty>3+n_h$. *Then,*

$$
\begin{aligned}
&\|\mathcal{M}_D-M_D\|\\
&\quad\leq\frac{4(n_h!)^2\Big(\sqrt{2}A_{max}\big(\pi+\ln(N-\Omega+n_h)-\ln(N-\Omega-1-n_h)\big)+2\Big)(1+\frac{1}{2n_h})}{\pi(N-\Omega-n_h)^{1+2n_h}},\\
&\|\mathcal{M}_O-M_O\|\\
&\quad\leq\frac{4(n_h!)^2\Big(\sqrt{2}(\sum_{l=1}^{N_f}A_l)\big(\pi+\ln(N-\Omega+n_h)-\ln(N-\Omega-1-n_h)\big)+2N_f\Big)(1+\frac{1}{2n_h})}{\pi(N-\Omega-n_h)^{1+2n_h}}.
\end{aligned}
$$

being $\Omega=T(2r_0-2)\|\omega\|_\infty+1$.

Proof: For a 3×3 block, we apply Lemma 5.4 and obtain

$$
\begin{aligned}
&\|\mathfrak{B}_{i,l}-\mathcal{B}_{i,l}\|\\
&\quad\leq\max_{j=j_i,j_i^+}\left(\begin{array}{c}|A_i^c||\partial\overline{\mathcal{CS}}^{n_h}_{\nu_l}(j)-\partial\overline{cs}^{n_h}_{\nu_l}(j)|+|A_i^s||\partial\widetilde{\mathcal{CS}}^{n_h}_{\nu_l}(j)-\partial\widetilde{cs}^{n_h}_{\nu_l}(j)|+\\ |\overline{\mathcal{CS}}^{n_h}_{\nu_l}(j)-\overline{cs}^{n_h}_{\nu_l}(j)|+|\widetilde{\mathcal{CS}}^{n_h}_{\nu_l}(j)-\widetilde{cs}^{n_h}_{\nu_l}(j)|,\end{array}\right)\\
&\quad\leq\frac{4(n_h!)^2\Big(\sqrt{2}A_i\big(\pi+\ln(N-j-\nu_l+n_h)-\ln(N-j-\nu_l-n_h-1)\big)+2\Big)(1+\frac{1}{2n_h})}{\pi(N-j-\nu_l-n_h)^{1+2n_h}},
\end{aligned}
$$

where either $\mathcal{CS}=\mathcal{C}$ and $cs=c$ or $\mathcal{CS}=\mathcal{S}$ and $cs=s$. As $j\in\{j_i,j_i^+\}$ and $\nu_l=Tk_l\omega$ with $1\leq|k_l|\leq r_0-1$, we have that $j+\nu_l\leq Tk_i\omega+1+Tk_l\omega\leq T(2r_0-2)\|\omega\|_\infty+1=\Omega$ for some $|k_i|\leq r_0-1$. Using this, the lemma follows from

$$
\begin{aligned}
\|M_D-\mathcal{M}_D\| &\leq \max_{i=1\div N_f}\|B_{i,i}-\mathcal{B}_{i,i}\|,\\
\|M_O-\mathcal{M}_O\| &\leq \max_{i=0\div N_f}\sum_{l=1}^{N_f}\|B_{i,l}-\mathcal{B}_{i,l}\|,
\end{aligned}
$$

where we denote $j_0=j_0^+=0$. $\square$

From these lemmas follows a bound for $\|Dg(y)^{-1}\|$, as will be stated in theorem 5.1.

5.2 Error bounds for $\|\Delta b\|_\infty$

We give first three definitions and one lemma in order to be able to bound finite sums of the type $\sum_{j=r_0}^{r_1} j^\alpha e^{-\delta j}$, with r_1 either finite or infinite.

Definition 5.5 *Given $z \in \mathbb{R}$, we define*

$$\forall x \in \mathbb{R}, \quad [x]_z = \max\{z+n : n \in \mathbb{Z}, z+n \leq x\} = z + [x-z],$$

where [ ] denotes integer part.

Note that, for all $m \in \mathbb{Z}$, we have $[x]_z = [x]_{z+m}$.

In what follows, we will use the incomplete Gamma functions $\gamma(\alpha, x)$ and $\Gamma(\alpha, x)$, which are defined as (see, for instance, [1])

$$\gamma(\alpha, x) = \int_0^x e^{-t} t^{\alpha-1} dt, \qquad \Gamma(\alpha, x) = \int_x^\infty e^{-t} t^{\alpha-1} dt.$$

In order to be able to bound sums by integrals taking into account the intervals of monotonicity is convenient to introduce the following

Definition 5.6 *For $j_1, j_2, \alpha, \delta > 0$ we define the functions*

$$\begin{aligned} G_f(j_1, j_2, \alpha, \delta) \;&=\; \frac{1}{\delta^{\alpha+1}} \chi_{\{j_1 \leq \frac{\alpha}{\delta} - 1\}} \Big(\gamma\big(\alpha+1, \delta \min([\frac{\alpha}{\delta}]_{j_1}, j_2+1)\big) - \gamma\big(\alpha+1, \delta j_1\big)\Big) + \\ &\quad \chi_{\{j_1 \leq \frac{\alpha}{\delta}, j_2 > \frac{\alpha}{\delta} - 1\}} \big([\frac{\alpha}{\delta}]_{j_1}\big)^\alpha e^{-\delta [\frac{\alpha}{\delta}]_{j_1}} + \\ &\quad \chi_{\{j_1 \leq \frac{\alpha}{\delta} + 1, j_2 > \frac{\alpha}{\delta}\}} \big([\frac{\alpha}{\delta}]_{j_1} + 1\big)^\alpha e^{-\delta([\frac{\alpha}{\delta}]_{j_1} + 1)} + \\ &\quad \frac{1}{\delta^{\alpha+1}} \chi_{\{j_2 > \frac{\alpha}{\delta} + 1\}} \Big(\gamma\big(\alpha+1, \delta j_2\big) - \gamma\big(\alpha+1, \delta \max([\frac{\alpha}{\delta}]_{j_1} + 1, j_1 - 1)\big)\Big), \end{aligned}$$

and

$$\begin{aligned} G_\infty(j_1, \alpha, \delta) \;&=\; \frac{1}{\delta^{\alpha+1}} \chi_{\{j_1 \leq \frac{\alpha}{\delta} - 1\}} \Big(\gamma\big(\alpha+1, \delta [\frac{\alpha}{\delta}]_{j_1}\big) - \gamma\big(\alpha+1, \delta j_1\big)\Big) + \\ &\quad \chi_{\{j_1 \leq \frac{\alpha}{\delta}\}} \big([\frac{\alpha}{\delta}]_{j_1}\big)^\alpha e^{-\delta [\frac{\alpha}{\delta}]_{j_1}} + \\ &\quad \chi_{\{j_1 \leq \frac{\alpha}{\delta} + 1\}} \big([\frac{\alpha}{\delta}]_{j_1} + 1\big)^\alpha e^{-\delta([\frac{\alpha}{\delta}]_{j_1} + 1)} + \\ &\quad \frac{1}{\delta^{\alpha+1}} \Gamma\big(\alpha+1, \delta \max([\frac{\alpha}{\delta}]_{j_1} + 1, j_1 - 1)\big). \end{aligned}$$

In the above formulas, $\chi_{\{\text{condition}\}}$ equals 1 if condition is true and 0 otherwise.

Lemma 5.14 *The functions G_f and G_∞ satisfy*

$$\sum_{j=j_1}^{j_2} j^\alpha e^{-\delta j} \leq G_f(j_1, j_2, \alpha, \delta), \qquad \sum_{j=j_1}^{\infty} j^\alpha e^{-\delta j} \leq G_\infty(j_1, \alpha, \delta).$$

Proof: To obtain the expressions for G_f, G_∞ in Definition 5.6 we have bounded the previous sums by integrals. This can be done easily for the subintervals of j of length 1, starting at j_1, for which the function $j^\alpha e^{-\delta j}$ is monotone (see figure 8). Some care must be taken for the intervals around the maximum of the function, which is attained at $j = \frac{\alpha}{\delta}$. This is the reason for the definition 5.5. Both inequalities follow after a careful examination of all the possibilities for the relative position between $[j_1, j_2]$ and the maximum $\frac{\alpha}{\delta}$.

$\square$

We recall from (24) that Δb is defined as,

$$\Delta b = \begin{pmatrix} c^{n_h}_{f-p,T,N}(0) \\ c^{n_h}_{f-p,T,N}(j_i) \\ s^{n_h}_{f-p,T,N}(j_i) \\ cs^{n_h}_{f-p,T,N}(j_i^+) \end{pmatrix},$$

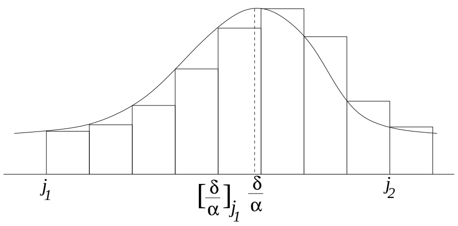

Figure 8: Graphical deduction of G_f and G_∞ (see explanations in the text).

where i ranges from 1 to N_f and cs denotes either c or s. We want to determine the trigonometric approximation $p(t)$ of $f(t)$ using frequencies up to order r_0-1, that is, $\{k\omega : |k| \le r_0-1\}$, so

$$f(t)-p(t) = \sum_{|k|=r_0}^{\infty} a_k e^{i2\pi k\omega t}.$$

Therefore, denoting by J the set of indices $\{0, j_i, j_i^+ : i = 1 \div N_f\}$, we have

$$\begin{aligned} \|\Delta b\| &\le 2\max_{j\in J} |F^{n_h}_{f-p,T,N}(j)| \\ &\le 2\max_{j\in J} \sum_{|k|\ge r_0} |a_k||F^{n_h}_{e^{i2\pi k\omega t},T,N}(j)| \\ &\le 2\max_{j\in J} \sum_{|k|=r_0}^{r_*} |a_k||F^{n_h}_{e^{i2\pi k\omega t},T,N}(j)| + 2\sum_{|k|=r_*+1}^{\infty} |a_k|. \end{aligned} \tag{34}$$

We will keep r_* as an unknown quantity for the moment, and bound the first term of the above sum but replacing the DFT by the TCFT.

Lemma 5.15 *The following inequality is fulfilled:*

$$\#\{k : |k| = j\} \le \frac{2^m}{(m-1)!}\Big(j+\frac{m}{2}\Big)^{m-1}.$$

Proof: See [14], p. 114. □

Lemma 5.16 *If* $\frac{TD}{(r_*+r_0-2)^\tau} > 1+n_h$, *we have*

$$\sum_{|k|=r_0}^{r_*-1} |a_k||\phi^{n_h}_{e^{i2\pi k\omega t},T}(\frac{j}{T})| \le$$

$$\frac{2^m C(n_h!)^2 e^{\delta(r_0-1)} \sum_{l=0}^{m-1} \binom{m-1}{l}\big(\frac{m}{2}-r_0+1\big)^{m-1-l} G_f(2r_0-1, r_*+r_0-2, l+\tau(1+2n_h), \delta)}{E_*(m-1)!\pi(TD)^{1+2n_h}}$$

where

$$E_* = \frac{(z_*-1-n_h)^{1+2n_h}}{z_*^{1+2n_h}}, \quad z_* = \frac{TD}{(r_*+r_0-1)^\tau}.$$

Proof: Using the Cauchy estimates and (9),

$$\begin{aligned} \sum_{|k|=r_0}^{r_*-1} |a_k||\phi^{n_h}_{e^{i2\pi k\omega t},T}(\frac{j}{T})| &\le C\sum_{|k|=r_0}^{r_*-1} e^{-\delta|k|}\frac{(n_h!)^2}{\pi\psi_{n_h}(|Tk\omega-j|)} \\ &\le \frac{C(n_h!)^2}{\pi}\sum_{|k|=r_0}^{r_*-1}\frac{e^{-\delta|k|}}{(|Tk\omega-j|-n_h)^{1+2n_h}} \qquad (35) \\ &\le \frac{C(n_h!)^2}{\pi}\sum_{|k|=r_0}^{r_*-1}\frac{e^{-\delta|k|}}{\big(\frac{TD}{(|k|+r_0-1)^\tau}-1-n_h\big)^{1+2n_h}} \qquad (36) \end{aligned}$$

For the last step we have used that, since $j \in \{j_i, j_i^+\}$ for some $i = 1 \div N_f$, there exists $k_j \in \mathbb{Z}^m$ such that $|j - Tk_j\omega| \le 1$, so

$$
\begin{aligned}
|Tk\omega - j| &\ge |Tk\omega - Tk_j\omega| - |j - Tk_j\omega| \ge T|(k-k_j)\omega| - 1 \ge \frac{TD}{|k-k_j|^\tau} - 1 \\
&\ge \frac{TD}{(|k| + r_0 - 1)^\tau} - 1.
\end{aligned}
$$

In order to be able to sum the above series with the aid of the incomplete Gamma functions, we choose E_* such that $(x - 1 - n_h)^{1+2n_h} \ge E_* x^{1+2n_h}$ for $x \in \{\frac{TD}{(|k|+r_0-1)^\tau}\}_{|k|=1}^{r_*-1}$. This is accomplished setting $E_* = \frac{(z_*-1-n_h)^{1+2n_h}}{z_*^{1+2n_h}}$ with $z_* = \frac{TD}{(r_*+r_0-2)^\tau}$. Therefore,

$$
\begin{aligned}
\Phi := \sum_{|k|=r_0}^{r_*-1} |a_k||\phi^{n_h}_{e^{i2\pi k\omega t},T}(\frac{j}{T})| &\le \frac{C(n_h!)^2}{E_*\pi} \sum_{|k|=r_0}^{r_*-1} \frac{e^{-\delta|k|}}{(\frac{TD}{(|k|+r_0-1)^\tau})^{1+2n_h}} \\
&= \frac{C(n_h!)^2}{E_*\pi(TD)^{1+2n_h}} \sum_{|k|=r_0}^{r_*-1} e^{-\delta|k|}(|k| + r_0 - 1)^{\tau(1+2n_h)}.
\end{aligned}
$$

Now we apply Lemma 5.15,

$$
\Phi \le \frac{C(n_h!)^2}{E_*\pi(TD)^{1+2n_h}} \sum_{j=r_0}^{r_*-1} \frac{2^m}{(m-1)!}\big(j + \frac{m}{2}\big)^{m-1} e^{-\delta j}(j + r_0 - 1)^{\tau(1+2n_h)},
$$

shift the index j,

$$
\Phi \le \frac{2^m C(n_h!)^2}{E_*(m-1)!\pi(TD)^{1+2n_h}} \sum_{j=2r_0-1}^{r_*+r_0-2} \big(j + \frac{m}{2} - r_0 + 1\big)^{m-1} e^{-\delta(j-r_0+1)} j^{\tau(1+2n_h)},
$$

and expand by Netwon's binomial,

$$
\begin{aligned}
\Phi &\le \frac{2^m C(n_h!)^2}{E_*(m-1)!\pi(TD)^{1+2n_h}} \sum_{l=0}^{m-1} \binom{m-1}{l} \big(\frac{m}{2} - r_0 + 1\big)^{m-1-l} \sum_{j=2r_0-1}^{r_*+r_0-2} j^{l+\tau(1+2n_h)} e^{-\delta(j-r_0+1)} \\
&= \frac{2^m C(n_h!)^2 e^{\delta(r_0-1)}}{E_*(m-1)!\pi(TD)^{1+2n_h}} \sum_{l=0}^{m-1} \binom{m-1}{l} \big(\frac{m}{2} - r_0 + 1\big)^{m-1-l} \sum_{j=2r_0-1}^{r_*+r_0-2} j^{l+\tau(1+2n_h)} e^{-\delta j}.
\end{aligned}
$$

Now, to show the lemma, we only have to apply Lemma 5.14. □

In the proof of the previous lemma, we bounded the continuous Fourier transform of a complex exponential term as

$$
|\phi^{n_h}_{e^{i2\pi k\omega t},T}(\frac{j}{T})| \le \frac{(n_h!)^2}{\pi(\frac{TD}{(|k|+r_0-2)^\tau} - 1 - n_h)^{1+2n_h}}.
$$

Therefore, an intrinsic way to choose r_* is to take it equal to the last value of $|k|$ for which the previous bound is < 1. In addition to that, and in order to avoid an excessive amplification of the bound due to the introduction of the E_* constant in the proof of the previous lemma, we will restrict r_* so that $z_* \ge 2(1 + n_h)$ and

$$
E_* \ge \frac{1}{2^{1+2n_h}}. \tag{37}
$$

Therefore,

$$
r_* = \left[\left(\frac{TD}{\max\big((\frac{(n_h!)^2}{\pi})^{\frac{1}{1+2n_h}} + 1 + n_h, 2(1+n_h)\big)}\right)^{\frac{1}{\tau}} - r_0 + 2\right].
$$

Now that we have chosen r_*, we need to bound the error due to the approximation of the discrete Fourier transform by the continuous one. This is done in the two following lemmas.

Lemma 5.17 *If $N - T(r_* + r_0 - 2)\|\omega\|_\infty > 1 + n_h$, then*

$$\Big| \sum_{|k|=r_0}^{r_*-1} a_k F^{n_h}_{e^{i2\pi k\omega t},T,N}(j) - \sum_{|k|=r_0}^{r_*-1} a_k \phi^{n_h}_{e^{i2\pi k\omega t},T}\Big(\frac{j}{T}\Big)\Big| \leq$$
$$\frac{2^{m+1}C(n_h!)^2(1+\frac{1}{2n_h})e^{\delta\frac{m}{2}}G_f(r_0+\frac{m}{2}, r_*-1+\frac{m}{2}, m-1,\delta)}{\pi(m-1)!\big(N-T(r_*+r_0-2)\|\omega\|_\infty - 1 - n_h\big)^{1+2n_h}}$$

Proof: Using Lemma 5.4 and the Cauchy estimates (22),

$$\Big| \sum_{|k|=r_0}^{r_*-1} a_k F^{n_h}_{e^{i2\pi\frac{Tk\omega}{T}t},T,N}(j) - \sum_{|k|=r_0}^{r_*-1} a_k \phi^{n_h}_{e^{i2\pi\frac{Tk\omega}{T}t},T}\Big(\frac{j}{T}\Big)\Big| \leq$$
$$\leq \quad C\sum_{|k|=r_0}^{r_*-1} e^{-\delta|k|}\frac{2(n_h!)^2(1+\frac{1}{2n_h})}{\pi\big(N-T(r_*+r_0-2)\|\omega\|_\infty - 1 - n_h\big)^{1+2n_h}},$$

since, for $|k| = r_0 \div r_* - 1$ and $j \in \{0, j_i, j_i^+ \,:\, i = 1 \div N_f\}$ there exists k_j with $|k_j| \leq r_0 - 1$ and $|Tk_j\omega - j| \leq 1$, and therefore

$$j + |Tk\omega| \leq Tk_j\omega + 1 + T|k\omega| \leq T(|k_j| + |k|)\|\omega\|_\infty + 1 \leq T(r_0 + r_* - 2)\|\omega\|_\infty + 1.$$

Using Lemmas 5.15 and 5.14 and shifting the summation index by $\frac{m}{2}$ units, we get

$$\sum_{|k|=r_0}^{r_*-1} e^{-\delta|k|} \leq \frac{2^m e^{\delta\frac{m}{2}}}{(m-1)!}\sum_{j=r_0+\frac{m}{2}}^{r_*-1+\frac{m}{2}} j^{m-1}e^{-\delta j} \leq \frac{2^m e^{\delta\frac{m}{2}}G_f(r_0+\frac{m}{2}, r_*-1+\frac{m}{2}, m-1,\delta)}{(m-1)!},$$

from which the lemma follows. □

Note that the hypothesis of the previous lemma gives a new constraint for r_*, which is fulfilled if we take

$$r_* = \min\left(\left[\left(\frac{TD}{\max\big((\frac{(n_h!)^2}{\pi})^{\frac{1}{1+2n_h}} + 1 + n_h, 2(1+n_h)\big)}\right)^{\frac{1}{\tau}} - r_0 + 2\right], \left[\frac{N-1-n_h}{T\|\omega\|_\infty} - r_0 + 1\right]\right)$$

Now, in order to complete the bound for $\|\Delta b\|$ we only have to bound the remainder.

Lemma 5.18 *The following inequality holds:*

$$\sum_{|k|=r_*}^{\infty} |a_k| \leq \frac{2^m C e^{\delta\frac{m}{2}}G_\infty(r_*+\frac{m}{2}, m-1,\delta)}{(m-1)!}$$

Proof: It follows from the Cauchy estimates (22), Lemma 5.15 and Definition 5.6. □

From lemmas 5.16, 5.17 and 5.18 follows a bound for $\|\Delta b\|_\infty$ that is stated in Theorem 5.1.
A more explicit description of the behavior of $\sum_{|k|=r_*+1}^{\infty} |a_k|$ is given in proposition 5.2. First we need two lemmas.

Lemma 5.19 *Define $P_l(j) = \#\{k \in \mathbb{Z}^l : |k| = j\}$. Then, for $j \geq 1$ the following recurrence is satisfied:*

$$P_l(j) = 2 + 2\sum_{s=1}^{j-1} P_{l-1}(s) + P_{l-1}(j), \tag{38}$$

with $P_1(j) = 2$. Moreover, $P_l(j)$ is a polynomial in j of degree $l-1$.

Proof: It is obvious that $P_1(j) = 2$. Assume $l \geq 2$. Then every $k \in \mathbb{Z}^l$ can be splitted as $k = (k_1, k_2)$ with $k_1 \in \mathbb{Z}^{l-1}$ and $k_2 \in \mathbb{Z}$. In this way

$$\{k \in \mathbb{Z}^l : |k| = j\} = \{(0, \pm j)\} \cup \left(\bigcup_{s=1}^{j-1}\{(k_1, \pm(j-s)) : |k_1| = s\}\right) \cup \{(k_1, 0) : |k_1| = j\},$$

and (38) follows from the fact that $\#\{(0,\pm j)\} = 2$, $\#\{(k_1,\pm(j-s)) : |k_1| = s\} = 2P_{l-1}(s)$ and $\#\{(k_1,0) : |k_1| = j\} = P_{l-1}(j)$.

We see that $P_l(j)$ has degree $l-1$ in j by induction on l. For $l=0$ it is true by definition. Assume it true for $l-1$, that is

$$P_{l-1}(j) = \sum_{r=0}^{l-2} c_r j^r.$$

Then

$$P_l(j) = 2 + 2\sum_{s=1}^{j-1}\sum_{r=0}^{l-2} c_r s^r + P_{l-1}(j) = 2 + 2\sum_{r=0}^{l-2} c_r \sum_{s=1}^{j-1} s^r + P_{l-1}(j),$$

and the property follows from the fact that

$$\sum_{s=1}^{j-1} s^r = \frac{1}{r+1}\sum_{s=0}^{r}\binom{r+1}{s} B_s j^{r-s+1}$$

(B_s are the Bernoulli numbers, see e.g. [21]) is a polynomial in j of degree $r+1$. □

Lemma 5.20 *(a) For $l, r \in \mathbb{N}$, $x \in \mathbb{C}$, $|x| < 1$ we have*

$$\sum_{j\geq r} j^l x^j = \frac{Q_l(x)}{(1-x)^{l+1}}, \tag{39}$$

where $Q_0(x) = x^r$ and $Q_l(x) = (x-x^2)Q'_{l-1}(x) + lxQ_{l-1}(x)$ for $l \geq 1$.

(b) $Q_l(x)$ is a polynomial in x with minimum degree r and maximum degree $r+l$. Moreover, every coefficient in x is a polynomial in r with maximum degree l.

Proof: For $l=0$, (39) is the sum of a geometric series. Assume (39) true for $l-1$. Then

$$\sum_{j\geq r} j^l x^j = x\sum_{j\geq r} j^l x^{j-1} = x\frac{d}{dx}\sum_{j\geq r} j^{l-1}x^j,$$

and using the induction hypothesis,

$$x\frac{d}{dx}\sum_{j\geq r} j^{l-1}x^j = x\frac{d}{dx}\frac{Q_{l-1}(x)}{(1-x)^l} = \frac{(x-x^2)Q'_{l-1}(x) + lxQ_{l-1}(x)}{(1-x)^{l+1}}.$$

As for (b), $Q_0(x)$ verifies (b) trivially and, assuming that (b) is true for $Q_{l-1}(x)$, it is readily checked that $Q_l(x) = (x-x^2)Q'_{l-1}(x) + lxQ_{l-1}(x)$ also verifies (b). □

Proposition 5.2 *We have*

$$\sum_{|k|=r}^{\infty} |a_k| = O(r^{m-1}e^{-r\delta}) \qquad \text{as } r \to +\infty.$$

Proof: Using the Cauchy estimates (22) and Lemma 5.19,

$$\sum_{|k|=r}^{\infty} |a_k| \leq C\sum_{|k|=r}^{\infty} e^{-\delta|k|} \leq C\sum_{j=r}^{\infty} P_m(j)e^{-\delta j}, \tag{40}$$

where $P_m(j)$ has degree $m-1$ in j. Assume $P_m(j) = \sum_{s=0}^{m-1} c_{m,s} j^s$ and define $x = e^{-\delta}$. Then

$$\begin{aligned} C\sum_{j=r}^{\infty} P_m(j)e^{-\delta j} &= C\sum_{s=0}^{m-1} c_{m,s}\sum_{j=r}^{\infty} j^s x^j = C\sum_{s=0}^{m-1} c_{m,s}\frac{Q_s(x)}{(1-x)^{s+1}} \\ &= C\sum_{s=0}^{m-1}\Big(\frac{c_{m,s}}{(1-x)^{s+1}}\sum_{l=0}^{s} p_{s,l}(r)x^{r+l}\Big), \end{aligned}$$

where, following Lemma 5.20(b), we have expanded $Q_s(x)$ as $\sum_{l=0}^{s} p_{s,l}(r)x^{r+l}$, with $p_{s,l}(r)$ of maximum degree s in r.

To show that this expression is $O(r^{m-1}x^r)$ when $r \to \infty$, it is enough to see that

$$\lim_{r\to\infty} \frac{1}{r^{m-1}x^r} C \sum_{s=0}^{m-1} \Big(\frac{c_{m,s}}{(1-x)^{s+1}} \sum_{l=0}^{s} p_{s,l}(r)x^{r+l} \Big) = \\ C \sum_{s=0}^{m-1} \Big(\frac{c_{m,s}}{(1-x)^{s+1}} \sum_{l=0}^{s} \Big(\lim_{r\to\infty} \frac{p_{s,l}(r)}{r^{m-1}} \Big) x^l \Big)$$

does not depend on r. This is true, since from Lemma 5.20(b) the $p_{s,l}$ polynomials are of degree $\leq s \leq m-1$ and therefore the limit in the right-hand side of the above equation does not depend on r. □

Lemmas 5.19 and 5.20 also allow to improve the bound of Lemma 5.18 for concrete values of m. For instance, if $m = 2$ we have

$$\sum_{\substack{|k|\geq r \\ k\in\mathbb{Z}^2}} |a_k| \leq 4C \frac{re^{-\delta r} + (1-r)e^{-\delta(r+1)}}{(1-e^{-\delta})^2}.$$

5.3 Final results

We end this section by gathering all the previous results in a single theorem that gives the bound for the error in frequencies and amplitudes. We consider both the case of known and the case of unknown frequencies in a single theorem.

Theorem 5.1 *Assume that we perform Fourier analysis of an analytic quasi–periodic function*

$$f(t) = \sum_{k\in\mathbb{Z}^m} a_k e^{i2\pi k\omega t},$$

that satisfies the Cauchy estimates with constants $C, \delta > 0$,

$$|a_k| \leq Ce^{-\delta|k|},$$

and whose frequency vector $\omega = (\omega_1, \ldots, \omega_m)$ satisfies a Diophantine condition of the form

$$|k\omega| > \frac{D}{|k|^\tau},$$

with $D, \tau > 0$. Assume we sample f in N points equally spaced over the interval $[0, T]$, and that we want to determine all the frequencies $Tk\omega$ with $1 \leq |k| \leq r_0 - 1$, $Tk\omega > 0$, and the related amplitudes, from which we have approximations close enough to the actual ones. Assume that we carry out the procedure of section 3.3 with $n_h \geq 1$ and get an approximation of f of the form

$$p(t) = A_0^c + \sum_{l=1}^{N_f} \Big(A_l^c \cos\big(\frac{2\pi\nu_l t}{T}\big) + A_l^s \sin\big(\frac{2\pi\nu_l t}{T}\big) \Big).$$

Assume also that N is such that $N - T(2r_0 - 2)\|\omega\|_\infty > 3 + n_h$, and T is such that $\frac{TD}{(2r_0-2)^\tau} > 3 + n_h$ and $[\nu_{min}] > 2 + n_h$, where $\nu_{min} = \min\{\nu_1, \ldots, \nu_{N_f}\}$. Then, the error in frequencies and amplitudes, which we denote as Δy, can be bounded, in the first order approximation, as

$$\|\Delta y\| \lesssim \|M^{-1}\| \|\Delta b\|, \tag{41}$$

where

$$\|M^{-1}\| \leq \frac{\|M_D^{-1}\|}{1 - \|M_D^{-1}\| \|M_O\|}$$

and

$$\begin{aligned}\|M_O\| &\leq \frac{(n_h!)^2}{\pi}\Bigg(\frac{\sqrt{2}(\sum\limits_{l=1}^{N_f} A_l)\big(\pi+\ln(\frac{TD}{(2r_0-2)^\tau}-1+n_h)-\ln(\frac{TD}{(2r_0-2)^\tau}-2-n_h)\big)+2N_f}{\big(\frac{TD}{(2r_0-2)^\tau}-1-n_h\big)^{1+2n_h}} \\ &+\frac{\sqrt{2}(\sum\limits_{l=1}^{N_f} A_l)\big(\pi+\ln([\nu_{min}]+n_h)-\ln([\nu_{min}]-1-n_h)\big)+2N_f}{\big([\nu_{min}]-n_h\big)^{1+2n_h}} \\ &+\frac{4\Big(\sqrt{2}(\sum\limits_{l=1}^{N_f} A_l)\big(\pi+\ln(N-\Omega_0+n_h)-\ln(N-\Omega_0-1-n_h)\big)+2N_f\Big)(1+\frac{1}{2n_h})}{\big(N-\Omega_0-n_h\big)^{1+2n_h}}\Bigg)\end{aligned}$$

and

$$\|M_D^{-1}\| \leq \frac{\|\mathcal{M}_D^{-1}\|}{1-\|\mathcal{M}_D^{-1}\|\varepsilon_1}, \qquad \|\mathcal{M}_D^{-1}\| \leq \frac{\|\mathfrak{M}_D^{-1}\|}{1-\|\mathfrak{M}_D^{-1}\|\varepsilon_2}, \qquad \|\mathfrak{M}_D^{-1}\| \leq \frac{G_{n_h}}{\min(1,A_{min})},$$

with G_{n_h} as in Definition 5.4, being

$$\begin{aligned}A_{min} &= \min_{l=1\div N_f}\sqrt{(A_l^c)^2+(A_l^s)^2}, \\ A_{max} &= \max_{l=1\div N_f}\sqrt{(A_l^c)^2+(A_l^s)^2}, \\ \varepsilon_1 &= \frac{4(n_h!)^2\Big(\sqrt{2}A_{max}\big(\pi+\ln(N-\Omega_0+n_h)-\ln(N-\Omega_0-1-n_h)\big)+2\Big)(1+\frac{1}{2n_h})}{\pi(N-\Omega_0-n_h)^{1+2n_h}}, \\ \varepsilon_2 &= \frac{(n_h!)^2\Big(\sqrt{2}A_{max}\big(\pi+\ln(2[\nu_{min}]+n_h)-\ln(2[\nu_{min}]-n_h-1)\big)+2\Big)}{\pi\big(2[\nu_{min}]-n_h\big)^{1+2n_h}}, \\ \Omega_0 &= T(2r_0-2)\|\omega\|_\infty+1,\end{aligned}$$

As for $\|\Delta b\|$,

$$\begin{aligned}\|\Delta b\| &\leq \frac{2^{m+1}C}{(m-1)!}\Bigg(\\ &\chi_{\{r_*>r_0\}}\frac{(n_h!)^2e^{\delta(r_0-1)}\sum\limits_{l=0}^{m-1}\binom{m-1}{l}(\frac{m}{2}-r_0+1)^{m-1-l}G_f(2r_0-1,r_0+r_*-2,l+\tau(1+2n_h),\delta)}{E_*\pi(TD)^{1+2n_h}} \\ &+\chi_{\{r_*>r_0\}}\frac{2(n_h!)^2e^{\delta\frac{m}{2}}(1+\frac{1}{2n_h})G_f(r_0+\frac{m}{2},r_*-1+\frac{m}{2},m-1,\delta)}{\pi(N-\Omega-n_h)^{1+2n_h}} \\ &+e^{\delta\frac{m}{2}}G_\infty(r_*+\frac{m}{2},m-1,\delta)\Bigg),\end{aligned} \tag{42}$$

where

$$\begin{aligned}\Omega &= T(r_*+r_0-2)\|\omega\|_\infty+1 \\ r_* &= \max\Bigg(r_0,\min\Bigg(\Bigg[\Bigg(\frac{TD}{\max\big((\frac{(n_h!)^2}{\pi})^{\frac{1}{1+2n_h}}+1+n_h,2(1+n_h)\big)}\Bigg)^{\frac{1}{\tau}}-r_0+2\Bigg], \\ &\qquad\Bigg[\frac{N-1-n_h}{T\|\omega\|_\infty}-r_0+1\Bigg]\Bigg)\Bigg) \\ E_* &= \frac{(z_*-1-n_h)^{1+2n_h}}{z_*^{1+2n_h}}, \\ z_* &= \frac{TD}{(r_*+r_0-2)^\tau},\end{aligned} \tag{43}$$

and the G_f, G_∞ functions are those of Definition 5.6.

If we assume that the frequencies $Tk\omega$ with $1 \le |k| \le r_0 - 1$, $Tk\omega > 0$, are known and want to compute the amplitudes using the procedure described in Section 3.2, formula (41) is still valid, where the bounds for $\|\Delta b\|$ are the same as before and the bounds for $\|M^{-1}\|$ are given by

$$\|M^{-1}\| \le \frac{\|M_D^{-1}\|}{1 - \|M_D^{-1}\| \|M_O\|}$$

being

$$\begin{aligned}\|M_O\| \quad \le \quad & \frac{N_f (n_h!)^2}{\pi} \Bigg(\frac{\sqrt{2}}{\left(\frac{TD}{(2r_0-1)^\tau} - \frac{1}{2} - n_h\right)^{1+2n_h}} + \frac{2}{\left([\nu_{min}] - n_h\right)^{1+2n_h}} \\ & + \frac{8\left(1 + \frac{1}{2n_h}\right)}{\left(N - T(2r_0 - 2)\|\omega\|_\infty - \frac{1}{2} - n_h\right)^{1+2n_h}} \Bigg)\end{aligned}$$

and

$$\|M_D^{-1}\| \le \frac{\|\mathcal{M}_D^{-1}\|}{1 - \|\mathcal{M}_D^{-1}\| \varepsilon_1}, \qquad \|\mathcal{M}_D^{-1}\| \le \frac{\|\mathfrak{M}_D^{-1}\|}{1 - \|\mathfrak{M}_D^{-1}\| \varepsilon_2}, \qquad \|\mathfrak{M}_D^{-1}\| \le \frac{5}{3},$$

being

$$\varepsilon_1 = \frac{8 (n_h!)^2 \left(1 + \frac{1}{2n_h}\right)}{\pi \left(N - T(2r_0 - 2)\|\omega\|_\infty - \frac{1}{2} - n_h\right)^{1+2n_h}}, \qquad \varepsilon_2 = \frac{2 (n_h!)^2}{\pi \left(2[\nu_{min}] - n_h\right)^{1+2n_h}}.$$

Remark 5.1 The above theorem has been stated in order to give a posteriori estimates for the errors in frequencies and amplitudes once the trigonometric approximation of the quasi–periodic function is known. In order to use it to obtain a priori estimates for the T, N parameters providing a prescribed accuracy for $\|\Delta y\|$, we must proceed as follows.

1. Get some empirical estimate of the C, δ constants appearing in the Cauchy estimates.
2. Get estimates for the a posteriori quantities used in the statement of the theorem, namely
   - $\nu_{min} \ge (TD)/(r_0 - 1)^\tau$,
   - $A_{max} \le C$,
   - $A_{min} \ge b_{min}$, where b_{min} is the minimum allowed amplitude for the computed frequencies (see Algorithm 4.1).
3. Choose values of τ and D, so that the measure of the frequency vectors not satisfying this Diophantine condition is small (for instance, $\tau = m - 1/2$, $D = 0.1$).

The values of T, N chosen allow to apply the procedure and obtain approximations of frequencies and amplitudes, which can be used to improve the estimates of the C, δ, D, τ constants and apply the theorem again with a posteriori information.

Remark 5.2 If some frequency of order $\le r_0 - 1$ has an amplitude smaller than the threshold b_{min}, it will not be detected by Algorithm 4.1 and, therefore, we will not have approximations of all the frequencies of order $\le r_0 - 1$, as required in the theorem. The effect of these frequencies can be included in the bound for Δb, by adding all of them to the summation in Lemma 5.16 but bounding their amplitudes by b_{min}.

Remark 5.3 The bound for $\|\Delta y\|$ given by the previous theorem can be improved by replacing the first term in the bound for $\|\Delta b\|$ by any of the intermediate inequalities of the proof of Lemma 5.16. In this case, it may be necessary to modify the definition of r_*. We will give examples in the following section.

Corollary 5.1 *The block Jacobi method as stated in (17), used to obtain the amplitudes from known frequencies, is convergent provided that*

$$\|M_D^{-1}\| \|M_O\| < 1,$$

where for $\|M_D^{-1}\|$ and $\|M_O\|$ we use the bounds given in the previous theorem in the case of known frequencies, but replacing N_f by $N_f - 1$.

Proof: The norm of the iteration matrix of the block Jacobi method (17) is

$$\max_{i=1\div N_f}\left(\|B_{i,i}^{-1}\|\sum_{\substack{l=1\\ l\neq i}}^{N_f}\|B_{i,l}\|\right)<\|M_D^{-1}\|\|M_O\|.$$

The reason for replacing N_f by N_f-1 in the bounds of the previous theorem is that we apply the block Jacobi method to system (13) without its first equation. □

6 A few numerical illustrations

In this section we illustrate the procedures described in two different contexts. The first one serves to test the accuracy of the methods. A data set is synthesized from a known function and we check the accuracy of the experimental results against the theoretical values. The effect of random errors in the data is also considered, to check the robustness of the procedures.

The second one is related to the application of the Fourier analysis to decide whether some dynamics can be considered as regular or chaotic. It is known that frequency analysis gives, as a byproduct, a criterion to recognize if a dynamics is periodic or quasi–periodic (i.e., the frequencies are constants of the motion), as it happens in a generic regular orbit of a Hamiltonian system, if the frequencies change slowly with time or simply they do not exist. We have applied this to the dynamics of a simple area preserving map.

6.1 Recovering the frequencies of a known function. The effect of noise

The first example is intended to show the performance of the procedures described and to test the error bounds obtained. We have analyzed a family of quasi–periodic functions from which the Fourier coefficients can be explicitly calculated. The functions are

$$f_\mu(t)=\frac{\sin(2\pi\omega_1 t+\varphi_1)}{1-\mu\cos(2\pi\omega_1 t+\varphi_1)}\cdot\frac{\sin(2\pi\omega_2 t+\varphi_2)}{1-\mu\cos(2\pi\omega_2 t+\varphi_2)},\qquad \mu\in[0,1).$$

They verify $f_\mu(t)=\sum_{k\in\mathbb{Z}^2}a_k^{\mu,\varphi}e^{2\pi i(\omega,k)t}$ with

$$a_k^{\mu,\varphi}=\begin{cases}\frac{-\operatorname{sign}(k_1k_2)}{\mu^2}c_2^{|k|}e^{i(k,\varphi)} & \text{if } k_1,k_2\neq 0\\ 0 & \text{if } k_1=0 \text{ or } k_2=0\end{cases}\tag{44}$$

being

$$\omega=(\omega_1,\omega_2),\quad \varphi=(\varphi_1,\varphi_2)\quad\text{and}\quad c_2=\frac{1-\sqrt{1-\mu^2}}{\mu}$$

The parameter μ is directly related to the parameter δ in the Cauchy estimates (22), namely

$$\delta=\operatorname{Im}\arccos\frac{1}{\mu}=-\log c.$$

It is clear that the phases φ_1 and φ_2 do not play any other role than to introduce a mild source of errors in the computations.

We have applied the algorithm described in 4.1 to the f_μ functions for $\omega=(1,\sqrt{2})$, $\varphi=(\sqrt{0.2},\sqrt{0.3})$, $n_h=2$ and several values of μ, T and N. As ω_2/ω_1 is a quadratic irrational, the exponent τ in the Diophantine condition (21) can be taken equal to 1. The value of D in (21) is $2\sqrt{2}-2\approx 0.82842712$ and it is attained for $k_1=-1$, $k_2=1$. However, from the continuous fraction expansion of $\sqrt{2}$, it is inmediate that the lim inf of $|k\omega|\cdot|k|$ is $D_\infty=(2+\sqrt{2})/4\approx 0.85355339$. The values of $|k\omega|\cdot|k|$ are below D_∞ only when $-k_1/k_2$ are best approximants to $\sqrt{2}$ which are less than $\sqrt{2}$, i.e., 1/1, 7/5, 41/29, etc. We have stopped the procedure when all the frequencies (with nonzero amplitudes) of order $|k|\leq 5$ have been refined. The error of the Fourier approximation as well as the corresponding bound, as given by theorem 5.1, are shown in Fig. 9.

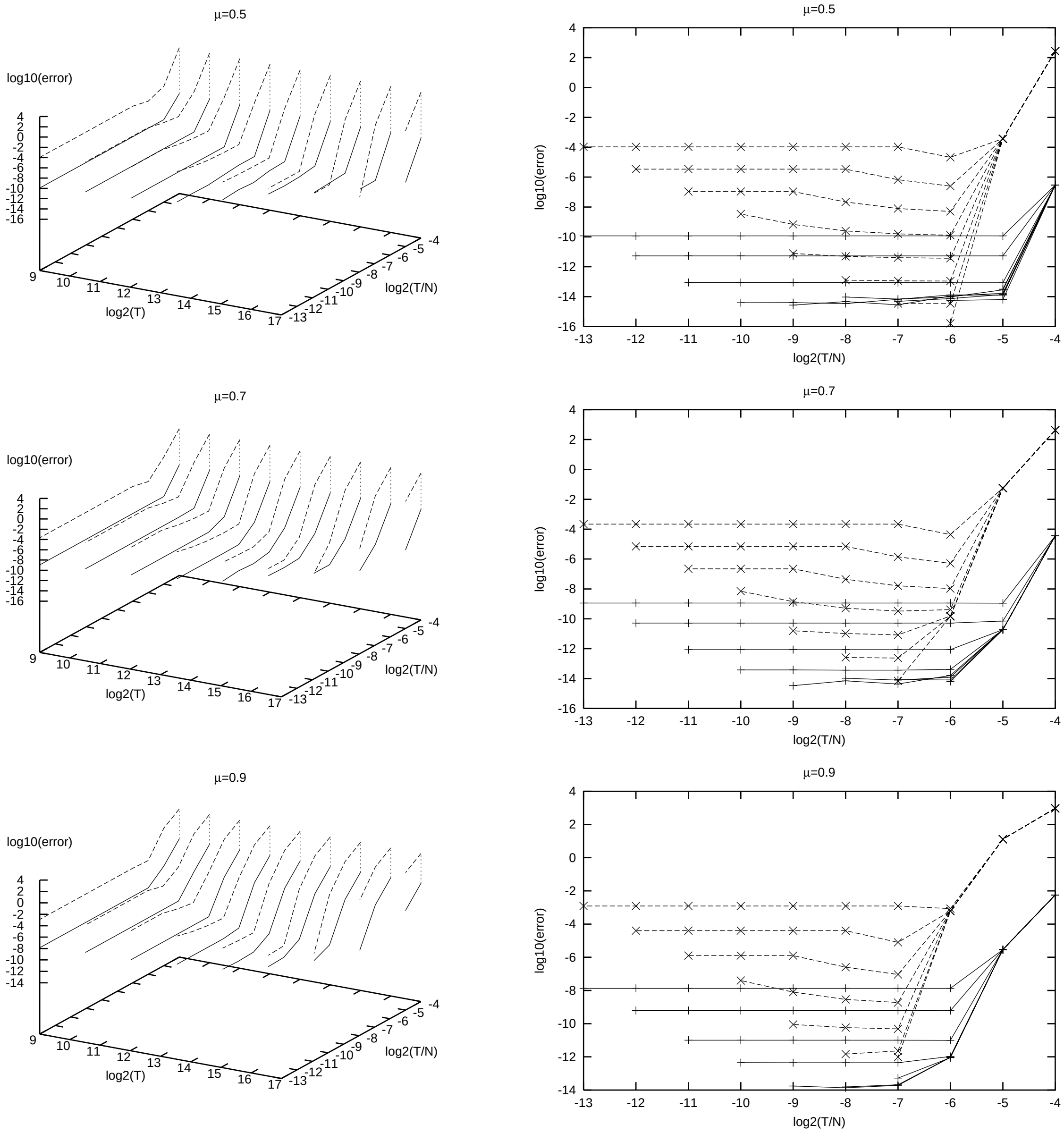

Figure 9: Fourier analysis of the f_μ functions for $\mu = 0.5, 0.7, 0.9$ and several values of T and N. Points corresponding to analysis with the same value of T have been joined by lines. The solid lines represent the error in frequencies and amplitudes of the corresponding Fourier analysis. This means that we have represented the maximum value between the error in the frequencies and the error in the amplitudes. The points joined by dashed lines correspond to the bound given by theorem 5.1. The right–hand figures are the (y, z) projection of the left–hand side ones.

It must be noted that the error in frequencies and amplitudes is much smaller than the difference between the analyzed function f and its computed quasi–periodic approximation Q_f. For instance, in the case of $\mu = 0.9$, from (44) the maximum amplitude of the frequencies not determined is $c_2{}^6/\mu^2 = 0.0749$, whereas we reach errors as small as 10^{-14} for some values of T and N. This is due to the fact that the truncation error of our procedure is not introduced by the difference $f - Q_f$ but by its DFT, as is seen in Section 5.

We observe that, for every value of T, as N increases the error decreases and becomes constant after a value of N. We also note that the minimum error for each value of T decreases as we increase T. This behavior of the error in terms of the parameters T, N, can be explained in terms of the bound (34).

Let r_1 be such that $2C\sum_{|k|=r_1}^{\infty} e^{-\delta|k|}|F^{n_h}_{e^{i2\pi k\omega t},T,N}(Tk\omega - j)|$ is small (this might be different from the order r_* of Section 5, which is "the order up to which the TCFT helps"). Then the frequencies of order greater than r_1 can be considered irrelevant and we can focus in frequencies of orders from r_0 to $r_1 - 1$. If N is large enough, we can replace the DFT by the TCFT in (34), that is

$$\|\Delta b\| \lesssim \max_{j\in\{0,j_i,j_i^+\}_{i=1}^{N_f}} 2C\sum_{|k|=r_0}^{r_1-1} e^{-\delta|k|}\left|\phi^{n_h}_{e^{i2\pi k\omega t},T}\left(\frac{Tk\omega - j}{T}\right)\right|.$$

In order to normalize, we note that $|\phi^{n_h}_{e^{i2\pi k\omega t},T}(\frac{Tk\omega-j}{T})| \le |g^{n_h}(Tk\omega - j)| = |\widetilde{g}^{n_h}(Tk\omega - j)|$, being

$$g^{n_h}(\alpha) = \frac{(-1)^{n_h}(n_h!)^2(e^{i2\pi\alpha} - 1)}{2\pi i\psi_{n_h}(\alpha)}, \qquad \widetilde{g}^{n_h}(\alpha) = \frac{(-1)^{n_h}(n_h!)^2}{\pi i\psi_{n_h}(\alpha)}.$$

The moduli of these functions are plotted in Fig. 10. As T increases, the differences $|Tk\omega - j|$ become larger and, since $|\widetilde{g}^{n_h}(\alpha)|$ decreases with $|\alpha|$, this explains why, for sufficiently large N, the error decreases as T increases.

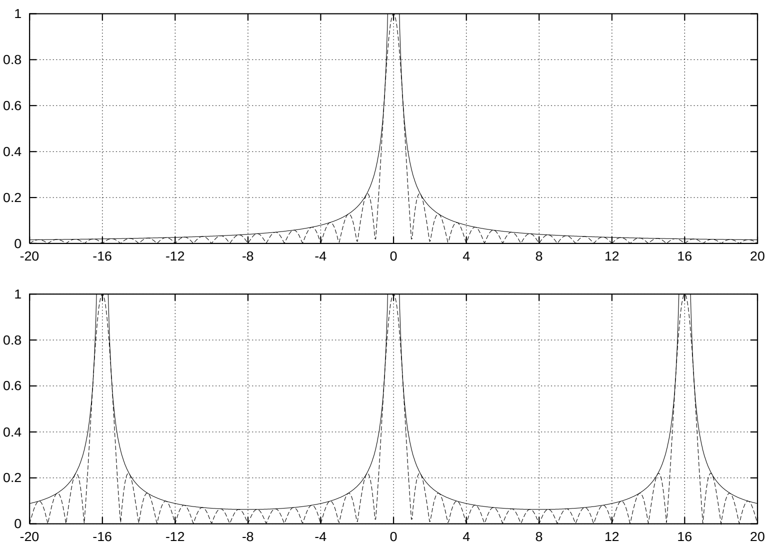

Figure 10: Top: graph of the functions $|g^{n_h}(\alpha)|$ (dashed line) and $|\widetilde{g}^{n_h}(\alpha)|$ (solid line) for $n_h = 0$. Bottom: graph of the functions $|h^{n_h}_N(\alpha)|$ (dashed line) and $|\widetilde{h}^{n_h}_N(\alpha)|$ (solid line) for $n_h = 0$ and $N = 16$.

In order to consider the case in which N is not large, we note $|F^{n_h}_{e^{i2\pi k\omega t,T,N},T,N}(j)| = |h^{n_h}_N(Tk\omega - j)| \le |\widetilde{h}^{n_h}_N(Tk\omega - j)|$, being

$$\begin{aligned}
h^0_N(\alpha) &= \frac{1 - e^{i2\pi\alpha}}{N(1 - e^{i2\pi\alpha/N})}, & h^{n_h}_N(\alpha) &= \frac{q_{n_h}}{2^{n_h}}\sum_{l=-n_h}^{n_h}(-1)^l\binom{2n_h}{n_h + l}h^0_N(\alpha + l),\\
\widetilde{h}^0_N(\alpha) &= \frac{2}{N(1 - e^{i2\pi\alpha/N})}, & \widetilde{h}^{n_h}_N(\alpha) &= \frac{q_{n_h}}{2^{n_h}}\sum_{l=-n_h}^{n_h}(-1)^l\binom{2n_h}{n_h + l}\widetilde{h}^0_N(\alpha + l).
\end{aligned}$$

The moduli of these functions are plotted in Fig. 10. Now, if N is not large enough, it may happen that one of the $|Tk\omega - j|$ approaches N and raises the bound (34). This explains the fact that, for a fixed value of T, as we decrease N the error ends up increasing.

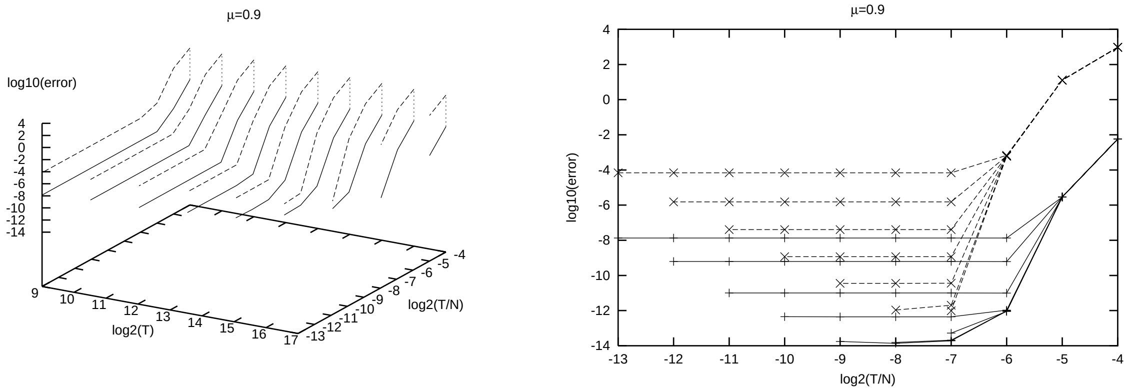

Figure 11: This is the same exploration as the one of Fig. 9, except that the dashed lines represent the bound obtained replacing the first term in (42) by (36). For shortness, only the worst case $\mu = 0.9$ is displayed.

The qualitative behaviour of the bound given by theorem 5.1 is not the same as the one of the real error. For each value of T, as N increases, the bound given by theorem 5.1 decreases up to a minimum value, then increases slightly and becomes constant. This increasing is due to the introduction of the E_* constant in the proof of the Lemma 5.16, which can enlarge the bound by a factor $1/E_*$ (at most 32 for $n_h = 2$, see (37)). In Fig. 11, we evaluate the bound for $\|\Delta y\|$ replacing the first term in (42) by (36), which is the last bound in the proof of 5.16 before the introduction of E_*. We see how the increasing of the bound after the minimum of Fig 9 disappears.

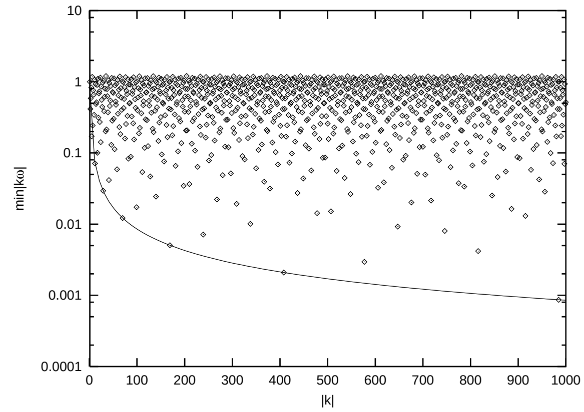

Figure 12: Illustration of the non–optimality of the Diophantine condition. The points represent the values of $\min_{|k|=j} |k\omega|$ for $j = 1 \div 1000$. The curve represents the Diophantine condition $D_\infty/|k|$. The only points that are approximately on the curve correspond to the values $|k|$=1, 2, 5, 12, 29, 70, 169, 408, 985.

The drawback of this approach is that the sum in (36) runs over multiindices $|k| = r_0 \div r_* - 1$ instead of their orders $j = r_0 \div r_* - 1$, and its evaluation can be prohibitive in terms of computing time, especially if the number of basic frequencies m is large. An alternative could be to lower r_* in (43) in order to raise the minimum value of E_*. For instance, if we set r_* equal to

$$\begin{aligned} r_* &= \max\Big(r_0, \min\Big(\Big[\Big(\frac{TD}{\max\big((\frac{(n_h!)^2}{\pi})^{\frac{1}{1+2n_h}} + 1 + n_h, \frac{1+n_h}{1-(1/2)^{1/(1+2n_h)}}\big)}\Big)^{1/\tau} - r_0 + 2\Big], \\ &\qquad \Big[\frac{N-1-n_h}{T\|\omega\|_\infty} - r_0 + 1\Big]\Big)\Big), \end{aligned}$$

then the minimum allowed value of E_* is 1/2. But this can lead to a worse global bound if the Fourier coefficients $|a_k|$ decrease slowly, as we illustrate in table 2. A different alternative is to take as value of

$\max 1/E_*$	μ	T	N	r_*	actual $1/E_*$	bound
32	0.9	1024	262144	61	3.53332	4.53023E–06
32	0.9	1024	524288	121	16.4812	2.08997E–05
32	0.9	1024	1048576	141	31.2714	3.96552E–05
2	0.9	1024	262144	33	1.97207	1.32447E–02
2	0.9	1024	524288	33	1.97207	1.32447E–02
2	0.9	1024	1048576	33	1.97207	1.32447E–02

Table 2: Computation of the bound given by theorem 5.1 using two different maximum allowed values for $1/E_*$. We see how, by lowering the maximum value of $1/E_*$, the bound can increase drastically.

r_* the one that minimizes the bound given by theorem 5.1. The results in this case are given in Fig. 13. Of course, they are worse that the ones of Fig. 11.

In Fig. 11, the bound is still several orders of magnitude larger than the actual error. This is due to the Diophantine condition, which give only a lower bound for the difference between frequencies. As mentioned, this difference approaches the exact Diophantine condition in very few cases, as shown in Fig. 12. In Fig. 14 we evaluate the bound of theorem 5.1 by replacing the first term of the bound of $\|\Delta b\|$ by (35). We see that in this case there is a very good agreement between the error predicted and the actual error.

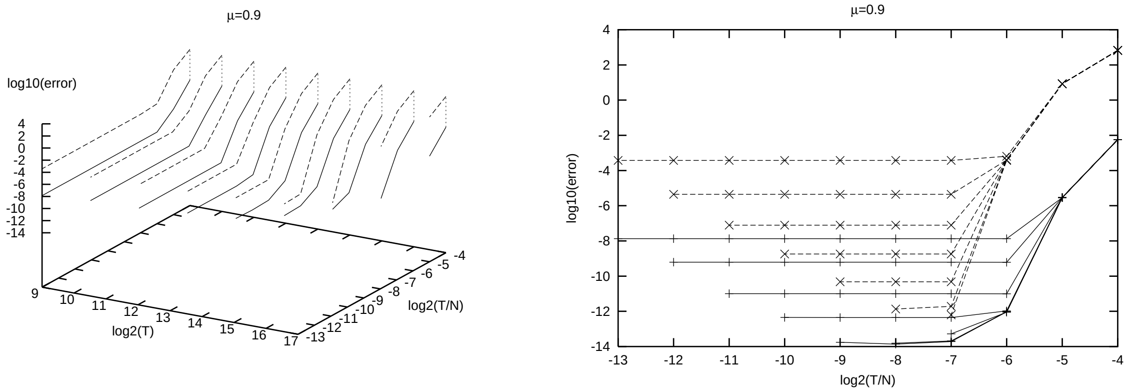

Figure 13: Same exploration as the one of Fig. 9. Dashed lines represent now the error bound obtained by minimizing $\|\Delta b\|$ with respect to r_* in theorem 5.1, instead of using (43). Only the case $\mu = 0.9$ is displayed.

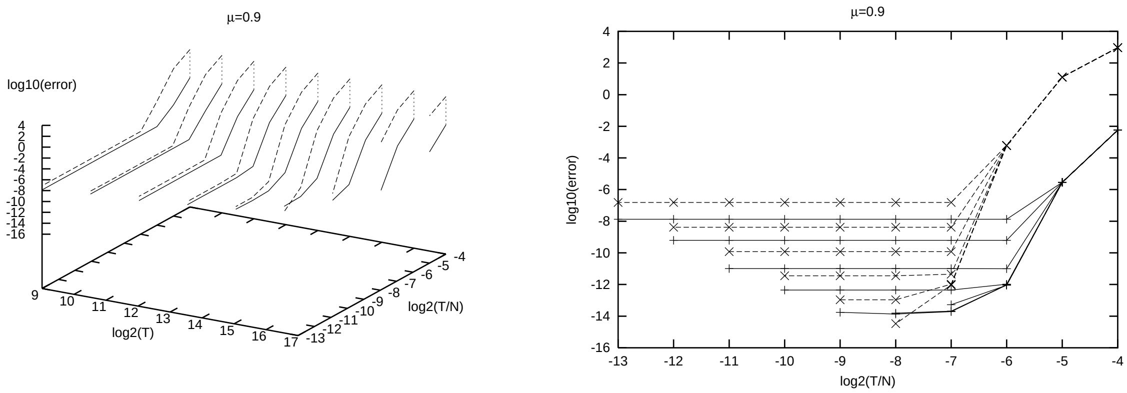

Figure 14: Same exploration as the one of Fig. 9. Dashed lines represent now the error bound obtained by replacing the first term of (42) by (35). Only the case $\mu = 0.9$ is displayed.

In Fig. 15, we have represented the results of the Fourier analysis of the f_μ functions ($\mu = 0.7$) after adding a uniform noise to its samples. The amplitude Δ of this noise has been varied between 0.1 and 10^{-10}. The computations have been done for different values of the number of samples N. The results

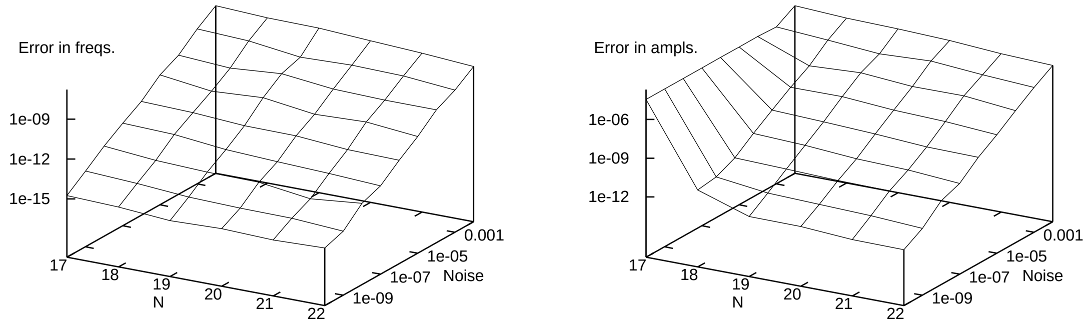

Figure 15: Fourier analysis of the f_μ functions, $\mu = 0.7$, with uniform noise of amplitude Noise=Δ. To each sample of f_μ, we have added a uniform deviate in the interval $[-\Delta, \Delta]$.

show an almost linear behaviour (in logarithmic scale) for the error with respect to Δ, with slope 10^{-5} for the frequencies and 10^{-2} for the amplitudes, at least for large values of N. As a consequence of these tests, we can ensure the robustness of the proposed procedure. The results using a Gaussian noise with mean 0 and standard deviation $\Delta/2$ are essentially identical.

6.2 A dynamical application: detection of regular and chaotic motion

The analysis of frequencies is a very popular tool to study dynamical systems (see, e.g., [15],[16]). The basic idea is: consider a dynamical system in dimension d, either continuous ($x(t) = \varphi(t, x(0))$) or discrete ($x(n) = T^n(x(0))$). Take different initial conditions $x(0)$, along some line or submanifold for instance, and compute the orbits of them for some time interval or for some number of iterates. In the continuous case we sample the points of the orbits at times of the form $t_j = j\Delta t$, $j = 0, 1, 2, \ldots$, for a selected Δt. We consider an observable of the states of the system (i.e., a smooth function f of x) and take $\{f(x(t_j))\}$ or $\{f(x(j))\}$ for $j = 0, 1, \ldots, N-1$, as the sample to be analyzed. We can compute the main frequencies of the sample, or decide that the sample is not periodic nor quasi–periodic. If the orbit lives in a compact set, the lack of periodicity can be interpreted as the existence of some amount of chaos. If the sample displays a periodic or quasi–periodic behaviour, then we can take another sample along the orbit (after an eventual transient) and carry out the frequency analysis again. If the motion is regular the frequencies should be constant. Hence, we can set up a threshold for the admissible variation of the computed frequencies, and consider the motion as regular if the variation is less than the threshold.

In the present illustration we have considered a discrete system of the standard–like kind in dimension 2. More concretely, we study the family

$$T_{\varepsilon,\mu,\varphi}\begin{pmatrix} x \\ y \end{pmatrix} = \begin{pmatrix} \bar{x} \\ \bar{y} \end{pmatrix} = \begin{pmatrix} x + \varepsilon\bar{y} \\ y + \varepsilon f_{\mu,\varphi}(x) \end{pmatrix}, \tag{45}$$

where $f_{\mu,\varphi}$ is a 2π-periodic function with zero average. We shall take

$$f_{\mu,\varphi}(x) = g_{\mu,\varphi}(x) - \bar{g} \quad \text{with} \quad g_{\mu,\varphi}(x) = \frac{\sin(x+\varphi)}{1 - \mu\cos(x)} \tag{46}$$

where $\bar{g}$ denotes the average of g, which is equal to $\sin(\varphi)\dfrac{\mu}{1 - \mu^2 + \sqrt{1-\mu^2}}$. We can take $\mu \in [0, 1)$ and $\varphi \in [0, 2\pi)$. There are several reasons to consider maps of the form (45) with f as in (46) .

- If $\mu = 0$, $\varphi = 0$ we recover the classical Taylor–Chirikov standard map.
- Some of the inconvenients of the classical standard map are that f is an *entire* function and that the effect of higher order harmonics is "too well averaged". This is avoided by taking $\mu > 0$ which implies that f has harmonics of all orders.
- The introduction of φ destroys the symmetry of f.

The map (45) is also $2\pi/\varepsilon$-periodic in y. We can convert it to a 2π-periodic in y by using the alternative version

$$\bar{x} = x + \bar{y} \bmod 2\pi, \quad \bar{y} = y + \varepsilon^2 f_{\mu,\varphi} \bmod 2\pi. \tag{47}$$

The form (47) will be used in the sequel. Then the map becomes a discrete dynamical system in the two-dimensional torus $\mathbb{T}^2$. We shall also fix $\mu = 0.5$, $\varphi = 1$ and, hence, we shall skip the dependence of f and T on μ and φ in (46). Fig. 16 displays a few phase portraits. From left to right (increasing ε) they show an increasing amount of stochasticity. We would like to have a compact representation of the full evolution for ε in a suitable range. We have used $\varepsilon \in [0, 1]$. It is clear that for $\varepsilon = 0$ (47) is integrable, all points being in invariant curves with rotation number going from 0 to 1 when y_0 ranges from 0 to 2π. Furthermore, it is clear using (45) that when $\varepsilon \to 0$ the phase portrait looks like a (distorted) pendulum.

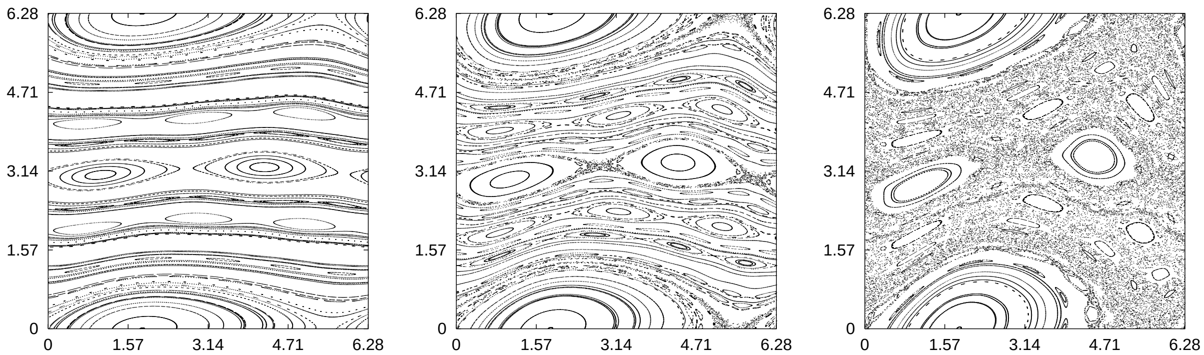

Figure 16: Phase portraits of the map (47). The horizontal (vertical) variable is x (y). From left to right we have used $\varepsilon = 0.4$, 0.6 and 0.8, respectively. In each plot we have taken $x, y \in \{2\pi j/10, j = 0, \ldots, 9\}$ and we have displayed the first 500 iterates.

6.2.1 The numerical experiment

For ε small it is enough to look at orbits with $x_0 = 0$ to describe essentially all the dynamics in $\mathbb{T}^2$. When ε increases, fixing $x_0 = 0$ implies that we shall miss several "islands", as can be seen in Fig. 16, but we still have a clear understanding of the full dynamics if we confine x_0 to a fixed value. This is what we have done using values of ε of the form $j/1000$, $j = 1, \ldots, 1000$ and values of y_0 of the form $j2\pi/1000$, $j = 0, \ldots, 999$. For each one of these 10^6 cases we have analyzed the corresponding orbit using the procedure described in this paper.

We have used values of N of the form 2^k. Then $3 \times N$ additional iterates of T_ε have been done and we have analyzed again the last N. The selected observable is $\sin(x)$ (however see later for an additional observable). In principle we have studied the dominant frequency, that is, the one with the largest amplitude. An a priori value of the threshold has been taken equal to 10^{-12}. We start with $k = 14$. If the orbit can be considered as regular the indices of the points are recorded as well as the frequency and the observed difference of the dominant frequencies in the two analysis. Otherwise k is increased up to a maximum of $k = 18$. If this value is reached then the dominant frequency and the difference of frequencies are written. In any case we have set up a maximal range for the values of y_j, which are considered in $\mathbb{R}$ without taking modulus 2π, in contrast with Fig. 16. If some iterate has y_j outside this range, then the orbit is considered as chaotic. A typical such range is $[-2\pi, 4\pi]$.

Two problems remain at this point. The first one is that the method is only able to determine frequencies in $(0, 1/2)$. Hence we are not able, for instance, to decide that an orbit lies in the main island around the elliptic fixed point or in the islands around the period 2 elliptic points (see Fig. 16). The second one is the ultimate selection of a threshold to decide about the regular or chaotic character of the orbits.

To solve the first problem a simple device is to consider the map (47) in a slightly modified form which does not affect the dynamics. To this end we have considered the modified map $\hat{T}_\varepsilon$ given by

$$(\bar{x}, \bar{y}) = \hat{T}_\varepsilon(x, y), \quad \text{with} \quad \bar{x} = x + \bar{y} + 2\pi \bmod 10\pi, \quad \bar{y} = y + \varepsilon^2 f_{\mu,\varphi} \tag{48}$$

and as selected observable we have taken $\sin(x/5)$. In this way an initial frequency ω is transformed to $\hat{\omega} = (\omega+1)/5$. As we obtain values $\hat{\omega} \in (0, 1/2)$ we can recover the full range $\omega \in [0:1]$. Furthermore, we use not only the dominant frequency in each run, but also the other frequencies obtained by the procedure (we have selected to detect, at least, the frequencies having the largest 10 amplitudes). From these frequencies we can compute basic frequencies such that all the remaining ones can be expressed as linear combinations of them. Hence, inside an island of a given period, it is possible to detect the rotation number of an invariant curve located in this island, or the periods of the islands which are satellites of a given island (either primary or secondary, etc, satellites).

The second problem was the ultimate selection of the threshold. To this end we have made tests against different indicators of the dynamics. We refer to the *Lyapunov indicators*. They give a measure of the hyperbolicity in the vicinity of an orbit. The most classical is the *Lyapunov exponent*. Let $\{z_j, j = 0, 1, \ldots\}$ be an orbit of a discrete system, with $z_j = F^j(z_0)$. Let us take a random initial vector ξ on the tangent space at the point z_0 to the manifold $\mathcal{M}$ where F acts. Let $\xi_j = DF^j(z_0)\xi$ the vector obtained by the action of the differential on the tangent space. If $\mathcal{M}$ is Riemannian, for instance, we can measure the lengths on the tangent spaces. In our case this is trivial, the tangent spaces being $\mathbb{R}^2$. Assume $||\xi|| = 1$, where $||\ \ ||$ denotes any Riemannian metric. The Lyapunov exponent associated to the vector ξ along the orbit of z_0 is defined as

$$\lim_{j\to\infty} \frac{1}{j} \log(||\xi_j||). \tag{49}$$

The limit exists almost for all ξ and z_0 and it converges to the *maximal Lyapunov exponent* almost for all ξ and z_0. Note that the maximal Lyapunov exponent depends on z_0.

From (49) is it clear that a difficulty appears concerning the passage to the limit. Typically (i.e., except in systems which high instability) the behavior of the quotients in (49) is quite erratic. This is easy to understand if an orbit of a system like (47) is mildly chaotic: the iterates of a point can remain until a large value of j close to a nearby chain of islands, to migrate then quickly to the vicinity of another chain of islands and remain there for a while. Furthermore this means that we are measuring an average of the hyperbolicity and not the *behavior of the dynamics near* z_0. This can be solved by taking final values of j not too large. They are a good measure of the *local properties* of the dynamics. It is also not necessary to compute the quotient nor the log in (49) if we are only interested in deciding whether the motion can be considered as chaotic or regular. Just to fix a maximal number of iterates J and a value L and decide that the orbit is chaotic if $||\xi_j|| > L$ for some $j \le J$ or regular otherwise. Of course, depending on the selected values of J and L we shall consider as regular some orbits that are chaotic and vice versa. But this is unavoidable with finite computations and with finite accuracy. We refer to [8], [9] and references therein for an introduction to these ideas and examples. Alternative methods based on suitable filtering and weighting of data and on a deeper use of the dynamics can be found in [7] and [22].

Assuming we have selected J and L and decided about the character of a subset of the orbits analyzed by the Fourier procedure, we can find the more convenient threshold that minimizes the number of orbits which have been identified in a different way by both methods. This is the threshold that we shall use.

6.2.2 The results

We proceed, as described above, using values $J = 10^6$ and $L = 10^{24}$ to set up the threshold. Smaller values can be used, but we wanted to be almost sure that the character decided by the Lyapunov indicator was correct. Using, say, $J = 10^4$ and $L = 10^6$ the fraction of wrong identifications is around 0.005, while with the selected values seems to be largely below 0.0001 . With these values the character of the different orbits has been compared to the one assigned by the Fourier procedure, which depends on the value of the threshold. Optimal results are produced for a threshold of 7×10^{-12}. Then the fraction of points with a lack of agreement is around 0.0018 .

Fig. 17 shows a graphical representation of the results. The scanning has been done using $x_0 = 0$. In the horizontal axis we represent $y_0/2\pi$ and in the vertical one the value of ε. On the left plot the grey domain means that a chaotic behavior has been found. Otherwise the orbits are regular. The black domains represent dynamics around the elliptic fixed point (domains to the left and right of the plot) or around the period 2 elliptic periodic orbit (central black part). The white pixels correspond to regular orbits, either on invariant curves or in islands of period greater than 2. On the right plot all the domains of regular motion in an island (periods have been limited to 100) are shown.

From Fig. 17 one can guess bifurcations and a fairly good idea of the full dynamics. This would change with the selected value of x_0, specially in what concerns the concrete location of the different islands, but this is not so relevant.

Running the analysis for the full 10^6 orbits lasted for 7 hours on HIDRA, an array of 42 dual PC (mostly Pentium II at 500 MHz). This can be drastically reduced if the maximal number of points in each Fourier analysis is reduced to 2^{14} instead to 2^{18}, at the price of a larger number of wrong identifications. But this reduced test still gives a very good feeling of the dynamics and the resonances.

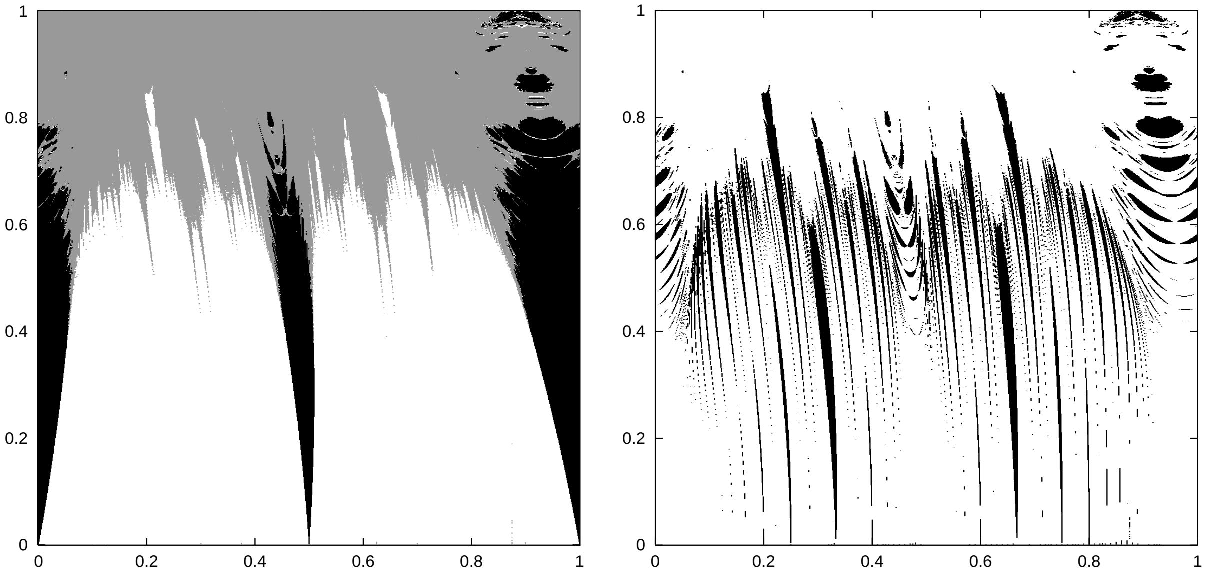

Figure 17: Results of the analysis of (47). Left: the domain of chaotic behavior is shown in grey. All other pixels represent regular motion. In black the regular data having main frequency 0 or 1/2. Right: Domains of regular motion in an island. See the text for additional explanation.

6.2.3 Additional comments

The frequency analysis allows, not only to determine the character of the different orbits, but also to know the relevant frequencies and to locate and determine the resonances. If we are only interested in the character of the orbits and the location of the resonances, without a knowledge of the involved frequencies, then a Lyapunov indicator is faster. A method recently developed (see [6], [23]) allows an accurate and fast determination of the character of the motion. Fig. 18 shows a detail, using this new method, of the regular domain for ε and $y_0/2\pi$ in $[0.8, 1]$, computed with step size 10^{-4} in both variables and using 8 minutes of CPU time in HIDRA. It seems that a good strategy to learn about the properties of a dynamical system is to use a combination of Lyapunov indicators and frequency analysis. The additional use of other indicators, which take into account the dynamics, and continuation of relevant objects and their bifurcations, seems to be the optimal strategy (see [3], [23]).

Finally we would like to explain the main reasons of the observed disagreement between the Fourier and Lyapunov results, which affects roughly 1800 pixels among the 10^6. This number can be decreased if the size of the samples in the Fourier analysis is increased. To decide about the reasons, we have examined visually (with successive magnifications when required, with magnifying factors over 10^6 in some cases) around 500 different cases. In all of them visual inspection agrees with the character of the orbit assigned by the Lyapunov indicator.

A first source of disagreement relies in the *robustness* of the Fourier analysis mentioned at the end of Section 6.1. Indeed, a small chaotic zone near a chain of tiny islands of width below 10^{-6} can be not detected by the Fourier methods with the maximal sample size used. Another source of errors are invariant curves passing extremely close to a hyperbolic periodic orbit. Looking in a rough way at a significant number of iterates, it can seem that we are in a periodic orbit. Finally there are motions on invariant curves (either rotational, i.e., projecting on the full x-axis, or librational, i.e., with several

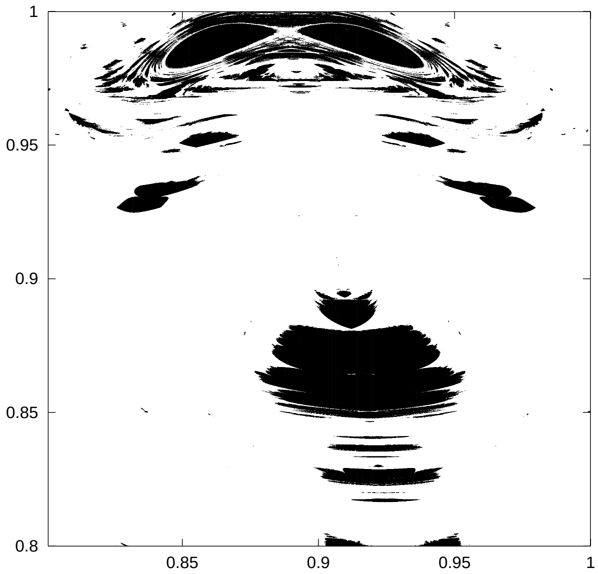

Figure 18: A magnification of the regular domain in Fig. 17 near the upper right corner.

components around an elliptic periodic orbit) which look only as arcs of a curve if the number of iterates is small. The rotation number is too close to a rational.

6.3 Other applications

A different application of the proposed procedures, and where the methods are used with the full power, is the analytical construction of quasi–periodic models. Assume that a differential equation has a periodic or quasi–periodic (in time) external excitation but the form of the equations is rather cumbersome. An example of this situation is the motion of a spacecraft in a vicinity of the Earth-Moon system. The motion of both Earth and Moon and the effects of Sun (main perturbing body) but also the effects of other planets, can be assumed to be quasi–periodic for moderate time intervals (the chaotic behavior of the bodies in the solar system only becomes relevant after several million years, see [15]). Expanding the Hamiltonian of the problem around the Earth or the Moon, or around one of the instantaneous libration points, we obtain a Taylor series whose coefficients are quasi–periodic in time through the ephemeris of the bodies of the solar system. The expressions of the coefficients, as functions of the coordinates of the bodies, are known (see [11]). Using this refined Fourier analysis, analytic models are constructed. They reproduce in a faithful way the true equations of motion and are useful both for theoretical and massive numerical studies at a cheaper price than by using the current ephemeris. Work in this direction can be found in [13].

7 Conclusions

Refined Fourier analysis, to obtain in a very accurate way the frequencies and amplitudes of a quasi–periodic function, has been studied in detail. In the paper we proceeded with the theoretical background, the detailed procedures and a full theoretical and practical analysis of the errors. Some examples illustrate the properties and the applicability of this analysis.

8 Acknowledgements

The research has been supported by DGICYT grants PB94-0215 and BFM2000-805 (Spain). Partial support of the Catalan grants CIRIT 1998S0GR-00042 and 2000 SGR-27 is also acknowledged. An extensive use of HIDRA has been made. We are grateful to CIRIT, DGICYT and the University of Barcelona who are providing funds for this array of processors. J. M. M. wishes also to acknowledge the support of the doctoral research grant 1997FI00136PG from the Generalitat de Catalunya.

References

[1] M. Abramowitz and I. A. Stegun. *Handbook of Mathematical Functions.* Dover Publications, 1965.

[2] A. S. Besicovitch. *Almost Periodic Functions.* Cambridge University Press, 1932.

[3] H.W. Broer, I. Hoveijn, M. van Noort, C. Simó, and G. Vegter The parametrically forced pendulum: a case study in $1+\frac{1}{2}$ degrees of freedom. Preprint, 2001.

[4] W. L. Briggs and V. E. Henson. *The DFT: an owner's manual for the Discrete Fourier Transform.* SIAM, 1995.

[5] E. O. Brigham. *The Fast Fourier Transform and its Applications.* Prentice–Hall, 1988.

[6] P. M. Cincotta, C. M. Giordano, and C. Simó. Phase space structure of multidimensional systems by means of the Mean Exponential Growth factor of Nearby Orbits. In preparation.

[7] P. M. Cincotta and C. Simó. Simple tools to study global dynamics in non–axisymmetric galactic potentials – I. *Astronomy & Astrophysics Supp.*, 147:205–228, 2000.

[8] C. Froeschlé, E. Lega, and R. Gonczi. Fast Lyapunov Indicators. Application to asteroidal motion. *Celest. Mech. and Dynam. Astron*, 67:41, 1997.

[9] C. Froeschlé, M. Guzzo, and E. Lega. The Fast Lyapunov Indicator. In B. Steves and A. Maciejewski, editors, *The Restless Universe*, pages 327–338. IOP Publishing, 2001.

[10] G. Gómez, A. Jorba, J. Masdemont, and C. Simó. *Dynamics and Mission Design Near Libration Point Orbits – Volume 4: Advanced Methods for Triangular Points.* Reprinted from ESA Report *Study on Orbits near the Triangular Libraion Points in the Perturbed Restricted Three–Body Problem, 1993.* World Scientific, 2001.

[11] G. Gómez, J. Llibre, R. Martínez, and C. Simó. *Dynamics and Mission Design Near Libration Point Orbits – Volume 1: Fundamentals: The Case of Collinear Libration Points.* Reprinted from ESA Report *Station Keeping of Libration Point Orbits, 1985.* World Scientific, 2001.

[12] G. Gómez, J. Llibre, R. Martínez, and C. Simó. *Dynamics and Mission Design Near Libration Point Orbits – Volume 2: Fundamentals: The Case of Triangular Libration Points.* Reprinted from ESA Report *Study of Poincaré Maps for Orbits near Lagrangian Points, 1987.* World Scientific, 2001.

[13] G. Gómez, J. J. Masdemont, and J. M. Mondelo. Solar system models with a selected set of frequencies. Preprint, 2001.

[14] À. Jorba and C. Simó. On the reducibility of linear differential equations with quasiperiodic coefficients. *Journal of Differential Equations*, 98(1):111–124, 1992.

[15] J. Laskar. The chaotic motion of the solar system. a numerical estimate of the size of the chaotic zones. *Icarus*, 88:266–291, 1990.

[16] J. Laskar. Introduction to frequency map analysis. In C. Simó, editor, *Hamiltonian Systems With Three or More Degrees of Freedom*, pages 134–150. Kluwer Academic Pub., 1999.

[17] J. Laskar, C. Froeschlé, and A. Celletti. A measure of chaos by the numerical analysis of the fundamental frequencies. Application to the standard mapping. *Physica D*, 56:253–269, 1992.

[18] B. M. Levitan and V. V. Zhikov. *Almost Periodic Functions and Differential Equations.* Cambridge University Press, 1982.

[19] J. M. Mondelo. *Contribution to the Study of Fourier Methods for Quasi–Periodic Functions and the Vicinity of the Collinear Librations Points.* PhD thesis, Universitat de Barcelona, 2001.

[20] W. H. Press, B. P. Flannery, S. A. Teukolsky, and W. T. Vetterling. *Numerical Recipes. The Art of Scientific Computing.* Cambridge University Press, 1987.

[21] A. P. Prudnikov, Y. A. Brychkov, and O. I. Marichev. *Integrals and Series*, volume 1. Gordon and Breach Science Publishers, 1988.

[22] C. Simó. Global Dynamics and Fast Indicators. In H. Broer et al., editors *Global Analysys of Dynamical Systems*, IOP Publishing, pages 263–289, 2001.

[23] C. Simó. Numerical indicators of the dynamics. Applications to diffusion. In preparation.

[24] J. Stoer and R. Bulirsch. *Introduction to Numerical Analysis.* Springer Verlag, second edition, 1993.

[25] E. T. Whittaker and G. N. Watson. *A course of modern analysis.* Cambridge University Press, 1940.